Doctoral Dissertation

Design of Novel Targeted Co-delivery System for Combined Chemotherapy and Gene Therapy of Hepatocellular Carcinoma

(肝細胞癌に対する化学療法と遺伝子治療の新規併用療法の確立)

Mahmoud AbuBakr Ahmed Younis

Laboratory for Molecular Design of Pharmaceutics

Biomedical and Pharmaceutical Science Course

Graduate School of Life Science, Hokkaido University, Japan

September 2020

Abstract

ABSTRACT

Hepatocellular carcinoma (HCC), is the 5th most common cancer worldwide and the third most common cause of cancer-related deaths. Treating advanced stages of HCC is difficult and the response rate to most chemotherapeutics is still low (10-15%) mainly due to the emergence of multidrug resistance (MDR). These drawbacks necessitate looking for novel approaches such as gene therapy that can effectively cure the disease by targeting its primary cause at the molecular level.

Sorafenib (SOR) is a multiple kinase inhibitor designated by FDA as the drug of choice for resistant HCC. However, it remains the last therapeutic approach and there are no effective solutions if the tumor develops resistance to it. In addition, its systemic administration is restricted by numerous toxicities and side effects. Meanwhile, Midkine (MK) is a growth cytokine overexpressed in HCC with anti-apoptotic, mitogenic, angiogenic and chemoresistant roles.

In the current study, we propose that combining SOR with anti-Midkine nucleic acid therapy (MK-siRNA) would exert a synergistic therapeutic activity against HCC. Furthermore, we developed novel lipid nanoparticles (LNPs) for the co-delivery of such payload to HCC with high efficiency and selectivity. The selected main lipid was YSK05, a novel pH-sensitive lipid designed in our laboratory. LNPs were modified with a novel highly-selective HCC-targeting peptide, SP94.

In the first part of this study, we tested our hypothesis *in vitro*. We optimized various aspects regarding the formulation and composition of

these LNPs to control their efficiency and selectivity. Our results revealed significant uptake in human and murine HCC (HepG2 and Hepa 1-6, respectively) compared to other cancerous cells (HeLa) or normal hepatocytes (FL83B) Evaluation of the cytotoxicity and MK gene knockdown activity confirmed the same pattern of selectivity. In addition, we showed the first evidence that MK-siRNA increases the sensitivity of HCC cells to SOR as suggested from its effect on SOR dose-response curve which significantly differed when MK-siRNA was replaced by a control siRNA (siCntrl).

The promising *in vitro* results triggered us to extend the applicability of our system to the *in vivo* level. Preliminary *in vivo* evaluation of the system after intravenous administration to HCC-bearing mice indicated that it could not accumulate in the tumor or exert MK knockdown activity there which reflected the challenges of the *in vivo* delivery to HCC. To overcome this, we designed a step-wise optimization process considering the possible challenges restricting the delivery of LNPs to the tumor; the pharmacokinetic performance, the stroma-rich tumor microenvironment hindering the penetration of LNPs to HCC cells, and the inadequate endosomal escape capability upon shifting from the *in vitro* to the *in vivo* situation.

Controlling PEG-SP94 density in the LNPs dramatically affected their pharmacokinetic performance which lead to improvement in MK knockdown activity in the tumor, but the selectivity remained poor as indicated upon comparing the activity in the tumor versus the healthy liver. We applied a microfluidic device (iLiNP) and optimized diverse

factors related to the operation or lipid composition to tune the particle size. Interestingly, reducing the particle size to 70 nm dramatically improved the gene knockdown activity and increased the selectivity to the tumor indicating successful penetration through the stroma barrier. However, further reduction in the particle size by increasing YSK05 ratio above 50 mol% sensitized Apolipoprotein E (ApoE) transporter in the serum to redirect the LNPs to the healthy liver, therefore LNPs with 70 nm size (50 mol% YSK05) were considered to be the optimum. To avoid significant effect on the healthy liver, we attempted masking ApoE recognition of our LNPs by filling the interspaces in their surface by additional DSPE-PEG_{2K}-MA. Surprisingly, at 3 mol% ratio, the LNPs showed strong knockdown activity in the tumor compared to limited activity in the healthy liver. Moreover, the particle size of the new LNPs was reduced to 60 nm by the effect of the additional PEG. Eventually, we screened various helper lipids to maximize the endosomal escape performance which revealed the superiority of DOPE. The optimized system was referred to as ultra-small lipid nanoparticles (usLNPs).

We evaluated the therapeutic activity of these usLNPs for the treatment of HCC-bearing mice. SOR and siRNA doses were adjusted to 2.5 mg/Kg and 0.5 mg/Kg, respectively. Treatment was given on days 7,10,13,16,19,22 and 25 post tumor inoculation and the mice were terminated on the 28^{th} day. Surprisingly, SOR+MK-siRNA combination showed ~85% eradication of the tumor compared with SOR+siCntrl (~40%) or MK-siRNA (~18%) which suggested the synergism between SOR and MK-siRNA. The treatment did not result in significant body weight loss commonly seen with ordinary chemotherapeutics suggesting

the biosafety of our usLNPs. Furthermore, treatment with SOR+MK-siRNA combination resulted in 3-fold down regulation of the characteristic HCC marker, Alpha fetoprotein (AFP), and 4-fold down regulation of Osteopontin (OSP) and vascular endothelial growth factor-1 (VEGF-1).

We raised the challenge and attempted the treatment of SOR-resistant tumor. *In vitro* results suggested the ability of MK-siRNA to reverse the resistance to SOR in established SOR-resistant HepG2 cells. The upregulation of MK gene by 3-folds in the resistant cell line suggested the role of MK pathway in acquiring the resistance to SOR. Surprisingly, SOR+MK-siRNA combination could eradicate SOR-resistant tumor in mice by ~70% which was almost insensitive to SOR+siCntrl at the same dose.

In conclusion, we designed LNPs for efficient and selective co-delivery of SOR and MK-siRNA to HCC both *in vitro* and *in vivo*. We reported the synergism between SOR and MK-siRNA for the first time. According to our knowledge, our system is the most efficient for siRNA delivery to HCC so far (ED_{50}=0.1 mg/Kg). We could eradicate HCC in mice using the lowest dose of SOR so far (2.5 mg/Kg). We challenged SOR-resistant HCC for the first time. We believe that our system holds a great promise for potential clinical application in HCC treatment.

Contents

CONTENTS

Page

LIST OF ABBREVIATIONS

HCC	Hepatocellular carcinoma
SOR	Sorafenib
MK	Midkine
RNAi	RNA interference
RISC	RNA-induced silencing complex
siRNA	Small interfering RNA
shRNA	Small hairpin RNA
miRNA	MicroRNA
ASO	Antisense oligonucleotide
pDNA	Plasmid DNA
mRNA	Messenger RNA
ASO	Antisense oligonucleotide
TALENs	Transcription activator-like effector nucleases
ZFNs	Zinc finger nucleases
CRISPR-Cas	Clustered regularly interspaced short palindromic repeats/CRISPR-associated systems
MDR	Multidrug resistance
LNPs	Lipid nanoparticles
PNPs	Protein nanoparticles
InNPs	Inorganic nanoparticles
STR-R8	Stearylated octaarginine
CPP	Cell-penetrating peptide

NPs	Nanoparticles
PEI	Polyethylene imine
DOPE	1,2-dioleoyl-sn-glycero-3-phosphoethanolamine
POPE	1-Palmitoyl-2-oleoyl-sn-glycero-3-phosphoethanolamine
EPC	egg L-α-phosphatidylcholine
DOPC	1,2-dioleoyl-sn-glycero-3-phosphocholine
DSPC	1,2-distearoyl-sn-glycero-3-phosphocholine
PEG	Polyethylene glycol
DSPE-PEG$_{2K}$-MA	1,2-distearoyl-sn-glycero-3-phosphoethanolamine-N-[maleimide (polyethylene glycol)-2000]
DOTAP	N- [1- (2,3- dioleoyloxy) propyl] - N, N, N-trimethylammonium chloride
MTT	3-(4,5-Dimethylthiazol-2-yl)-2,5-Diphenyltetrazolium Bromide
DiD	1,1'-Dioctadecyl-3,3,3',3'-Tetramethylindodicarbocyanine 4-Chlorobenzenesulfonate Salt
TFA	Trifluoroacetic acid
EE	Encapsulation efficiency
GAPDH	Glyceraldehyde 3-phosphate dehydrogenase
FACS	Fluorescence-activated cell sorting
CLSM	Confocal laser scanning microscopy
qRT-PCR	Quantitative real time polymerase chain reaction
MALDI-TOF-MS	Matrix-assisted laser desorption ionization time-of-flight mass spectrometry
TEM	Transmission electron microscopy
PDI	Polydispersity index
EE	Encapsulation efficiency

IC_{50}	Half-maximal inhibitory concentration
EC_{50}	Half-maximal effective gene silencing concentration
iLiNP	Invasive lipid nanoparticle production device
IVIS	*In vivo* imaging system
usLNPs	Ultra-small lipid nanoparticles
ApoE	Apolipoprotein E
AFP	Alpha fetoprotein
OSP	Osteopontin
VEGF-1	Vascular engothelial growth factor-1
CC-3	Cleaved caspase-3
CD31	Cluster of differentiation 31
Ki-67	Cell proliferation protein
AUC	Area under the curve
MRT	Mean residence time
AUMC	Area under moment curve
$t_{1/2}$	Biological half-life
CL	Clearance
SI	Stability index
AST	Aspartate aminotransferase
ALT	Alanine aminotransferase
ALP	Alkaline phosphatase
LDH	Lactate dehydrogenase
CK	Creatine kinase
ChE	Cholinesterase

LIP	Lipase
GLU	Glucose
T-CHO	Total cholesterol
TG	Triglycerides
NEFA	Non-esterified fatty acids
TP	Total protein
ALB	Albumin
BUN	Blood urea nitrogen
CRE	Creatinine
IP	Inorganic phosphorus
T-Bil	Total bilirubin
ED_{50}	Half-maximal effective gene silencing dose

LIST OF FIGURES

LIST OF TABLES

LIST OF EQUATIONS

INTRODUCTION

Gene Therapy for Hepatocellular Carcinoma; Highlighting The Journey from Theory to Clinical Applications

INTRODUCTION

1. OVERVIEW

Hepatocellular carcinoma (HCC), Hepatoma, is the 5th most common cancer worldwide with 841,080 new cases recorded in 2018 and the incidence rate is expected to reach 1,361,836 in 2040.[1] It is considered to be the third most common cause of cancer-related deaths.[2] Epidemiological studies have shown that the highest incidence rates of HCC occur in areas with endemic hepatitis B virus (HBV) and/or hepatitis C virus (HCV) infections [3] as well as environmental exposure including dietary aflatoxins produced by Aspergillus molds that infect stored grains [4] and agricultural exposures to insecticides and herbicides.[5] These collective factors make HCC a national challenge in several developing countries with an increasing load on health care budgets. The currently available treatment strategies for HCC include surgical intervention (liver resection and liver transplantation) and local radiotherapy which are beneficial only for early-stage patients with localized small liver tumors who show a good response to the treatment and have a good survival rate.[6] On the other hand, treating advanced stages of HCC is much more difficult and the survival rate has not significantly improved in the past three decades.[7] A number of chemotherapeutic agents, including doxorubicin (DOX) and sorafenib (SOR) have been used but the response rate is still low, ranging between 10% and 15% mainly due to the emergence of multidrug resistance (MDR).[7]

Other therapeutic strategies, such as anti-angiogenic therapy targeting vascular endothelial growth factor (VEGF) (e.g. bevacizumab) [8]

and the mammalian target of rapamycin (mTOR) (e.g. everolimus) [9] have been evaluated to inhibit tumor growth. Although these therapies showed some success in reducing tumor growth and metastasis, the systemic administration of VEGF inhibitors was found to develop adverse effects including hypertension.[10]

The drawbacks associated with conventional therapeutic strategies necessitate looking for novel approaches that can effectively cure the disease by targeting its primary cause at the molecular level to shut down the pathological circulation. Gene therapy involves several approaches including the introduction of a specific gene into certain cells where the endogenous gene is missing or under-expressed, the introduction of a specific gene that expresses a therapeutic protein, knocking down an over-expressed or pathogenic gene or modulating certain immune responses through DNA vaccines. Since the discovery and development of gene therapy in the 1990s, it has been extensively studied in the treatment of various diseases including cancers, genetic diseases and virologic diseases.[11-12] After more than two decades of academic research, gene therapy has now become a clinical reality with the approval of the first gene therapy against cancer, Kymriah®, which involves genetically-engineered immune cells (chimeric antigen receptor T cells, CAR T-cells) in 2017 by the US Food and Drug Administration (FDA),[13] followed by the approval of Luxturna® for the treatment of a rare genetically-inherited form of blindness in the same year [14] and Onpattro (Patisiran)® for the treatment of polyneuropathy caused by hereditary transthyretin-mediated amyloidosis (hATTR) in 2018.[15] The approval of these medicines has triggered a revolution, with widespread investigations of gene therapy for the treatment of more complicated diseases that have been considered uncurable for many decades.

As a result of the increased global interest in gene therapy, the number of researchers and laboratories entering the stream is continuously growing. We believe that successful scientific research should stand on the shoulders of previous scientists. Therefore, a deep literature review is crucial before designing a novel therapeutic strategy to understand the existing challenges, the progress of research and past and current achievements. However, the currently available reviews deal with HCC gene therapy as a part of other general topics (liver diseases, gene therapy, nanomedicine, …etc). As a result, there continues to be a great need for a detailed review that focuses exclusively on the gene therapy of HCC.

In the current review of literature, we summarize the treatment modalities used in HCC gene therapy as a key point to understand the different approaches that have been adopted for such therapy. We then discuss the gene targets involved in HCC therapy with a special focus on the molecular signaling pathways that have a particular contribution to HCC progression and we highligh the recent studies that attempted their targeting. The special challenges facing HCC gene delivery and the trials adopted to overcome them, the methods recruited for HCC targeting, and the diverse delivery systems that are in use are discussed, with a particular focus on the novel biomaterials designed for selective gene delivery to HCC. In addition, we review some novel combinational strategies in which gene therapy is merged with other techniques for the integrative treatment of HCC. Moreover, we highlight and compare some of the experimental animal models used in studies of HCC gene therapies. For a correlation between the bench and the market, we list clinical trials involving HCC gene therapies until the moment. Eventually, we discuss

future perspectives of these strategies and the scope for future HCC gene therapies.

2. TREATMENT MODALITIES USED IN HCC GENE THERAPY

Common treatment modalities or genetic payloads recruited in gene therapy have been extensively discussed in other general reviews. To maintain the specific focus of the current review on HCC gene therapy, we provide a brief summary of these modalities to facilitate the reader's understanding of the approaches described in subsequent sections without distorting the main purpose of this article. **Fig. 1** provides a schematic illustration for the modalities that are commonly used in HCC gene therapy.

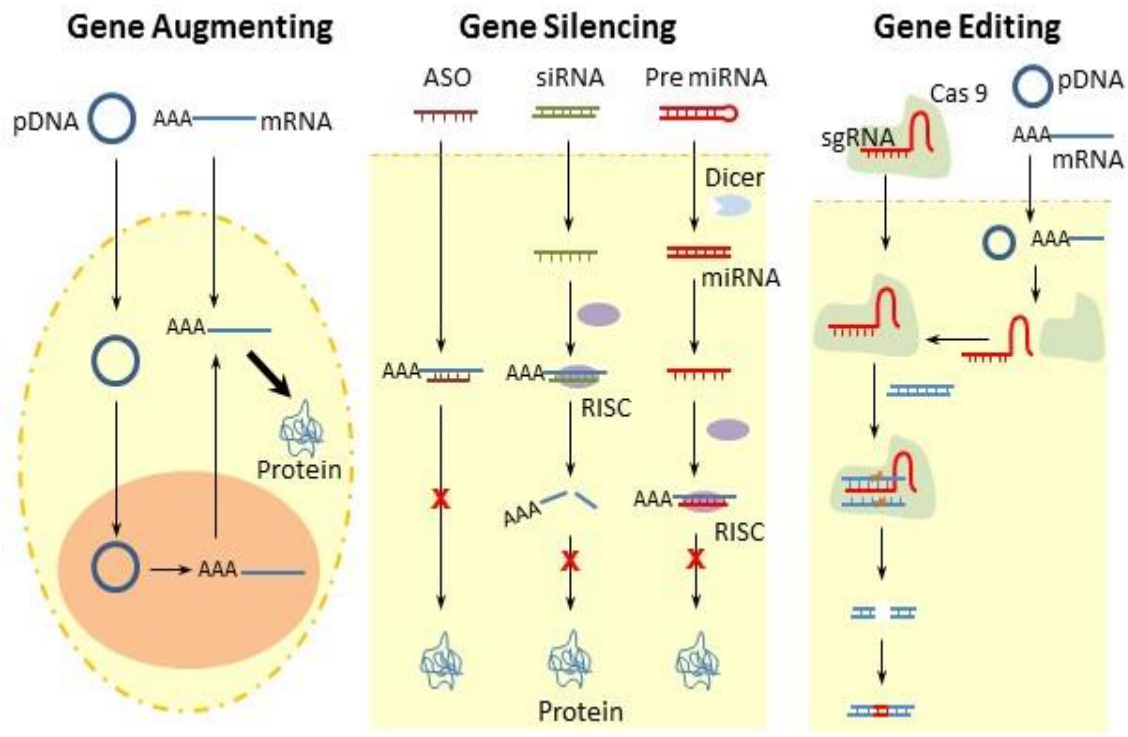

Figure 1. Schematic illustration for the different modalities used in HCC gene therapy. In gene augmentation, a therapeutic pDNA is introduced into the cell and is localized in the nucleus where it is transcribed into the corresponding mRNA that is transferred back to the cytosol. mRNA is then translated into the corresponding protein that exerts the therapeutic function. Therapeutic mRNA can also be directly introduced into the cytosol to function in a similar manner. In gene silencing, ASO is introduced into the cytosol to bind to the mRNA of the target gene, preventing its translation into the corresponding pathogenic protein. The siRNA molecule is introduced into the cytosol to be incorporated with other proteins forming the RISC that cleaves the target mRNA. miRNA is produced via the action of dicer on the precursor, pre miRNA. The formed miRNA can also form RISC to cleave the target mRNA. In gene editing, Cas 9 enzyme and its associated sgRNA are either introduced directly into the cell or in the form of pDNA or mRNA that produces them inside the cell. The Cas 9 editing system can induce a specific double-stranded DNA break at the desired sequence in the target genome allowing the existing genes to be edited in different ways. Abbreviations: pDNA, plasmid DNA; mRNA, messenger RNA; ASO, anti-sense oligonucleotide; siRNA, small interfering RNA; RISC, RNA-induced silencing complex; Pre miRNA, precursor micro RNA; miRNA, micro RNA; Cas 9, CRISPR associated system 9; sgRNA, single-guide RNA.

2.1. Gene augmentation

In the gene augmentation approach, the cell is induced to produce a beneficial protein which is malfunctioning or missing in the disease state. This can be manipulated by the introduction of a plasmid DNA (pDNA) that encodes the desired gene or a messenger RNA (mRNA) that encodes the desired protein.

The discovery of recombinant DNA technology allowed the widespread use of plasmids as cloning vectors in biotechnology and gene therapy.[16] The recombinant plasmid can be either introduced into bacterial cells (a process called transformation) that can produce millions of copies of it, thus allowing the large-scale production of proteins (e.g. insulin) [17] or introduced into human or animal cells (a process called transfection) to express a functional or therapeutic protein.[18] pDNA delivery is challenging due to the large size of the molecule and the necessity for it to be localized in the target nucleus, where it is transcribed into the corresponding mRNA.[19]

The breakthrough in mRNA delivery technology has led to its wide use as a replacement to the traditional pDNA. mRNAs can be easily *in vitro* transcribed from the corresponding pDNAs using commercially available kits. Moreover, the intracellular delivery of mRNA is much easier than pDNA due to its lower molecular size and its ability to function in the cytosol, which eliminates the need for the challenging nuclear delivery. In addition, mRNA does not integrate into the host genome, thus reducing the risk for mutagenicity.[20] In the past, intracellular delivery of mRNA was challenging due to its high instability and immunogenicity, but the evolution of chemically-modified mRNAs

as well as advancements in mRNA delivery systems have significantly overcome these challenges.[21]

2.2. Gene silencing

In opposite to gene augmentation, the ultimate goal of gene silencing is to stop the translation of a pathogenic or overexpressed gene into its protein product.

Antisense Oligonucleotide (ASO) is one of the modalities that can be used for gene silencing. It is a single strand of 18-21 deoxyribonucleotides having a sequence that is complementary to the messenger RNA (mRNA) of the target gene. After binding to the target mRNA, it inhibits mRNA translation into the corresponding protein via steric hindrance with ribosomes and the induction of RNase H endonuclease activity to cleave the target mRNA.[22]

RNA interference (RNAi) is a technique in which a small RNA molecule (small interfering RNA; siRNA, small hairpin RNA; shRNA or microRNA; miRNA) is introduced into cells where it assembles with certain proteins in the cytosol forming RNA-induced silencing complex (RISC) that binds specifically to the target mRNA and induces its cleavage to prevent its translation into the corresponding protein; thus, resulting in gene silencing.[23] RNAi has achieved a breakthrough in gene therapy due to its lower molecular size (19-29 bp), ease of preparation and the ability to exert the silencing action directly in the cytosol allowing the easier delivery.[24]

2.3. Genome editing

Genome editing is now one of the most intense approaches in the field of gene therapy. It depends on the use of designer nucleases, which are engineered bacterial or mammalian enzymes with a high affinity for

binding to a specific sequence in the target genome where they can induce a double-stranded cleavage. Genome editing has been investigated in the treatment of some diseases including viral hepatitis and acquired immune deficiency syndrome (AIDS).[25-27] Agents that are used in genome editing include Zinc finger nucleases (ZFNs), transcription activator-like effector nucleases (TALENs) and clustered regularly interspaced short palindromic repeats (CRISPR) with CRISPR-associated systems (Cas).[25-27]

3. GENE TARGETS INVOLVED IN THE TREATMENT OF HCC

Molecular studies of HCC have resulted in the discovery of several genes and associated proteins that control critical pathways that are involved in the development, growth, survival or resistance of HCC and they therefore offer potential targets for therapeutic treatment. We summarize some molecular signaling pathways with special importance in HCC progression in **Fig. 2.** Additional targets are schemed in **Fig. 3**.

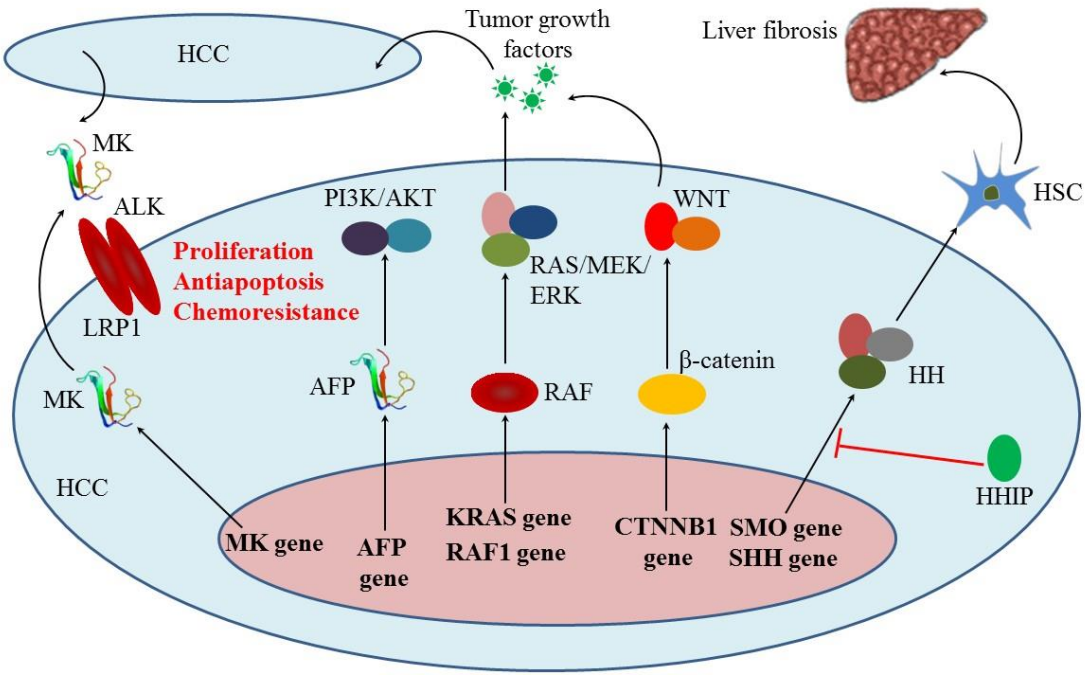

Figure 2. Summary of some molecular signaling pathways with special importance in HCC progression. Details are discussed in the relevant text. Abbreviations: MK, Midkine; ALK, anaplastic lymphoma kinase; LRP1, LDL-receptor-related protein 1; AFP, Alfa fetoprotein; PI3K/AKT, phosphatidylinositol-3 kinase; Raf, rapidly accelerated fibrosarcoma tyrosine kinase effector; CTNNB1, Catenin Beta 1; WNT, Wingless/Int-1; SMO, Smoothened homolog; SHH, Sonic Hedgehog Signaling Molecule; HHIP, Hedgehog Interacting Protein ; HH, Hedgehog; HSC, Hepatic stellate cell.

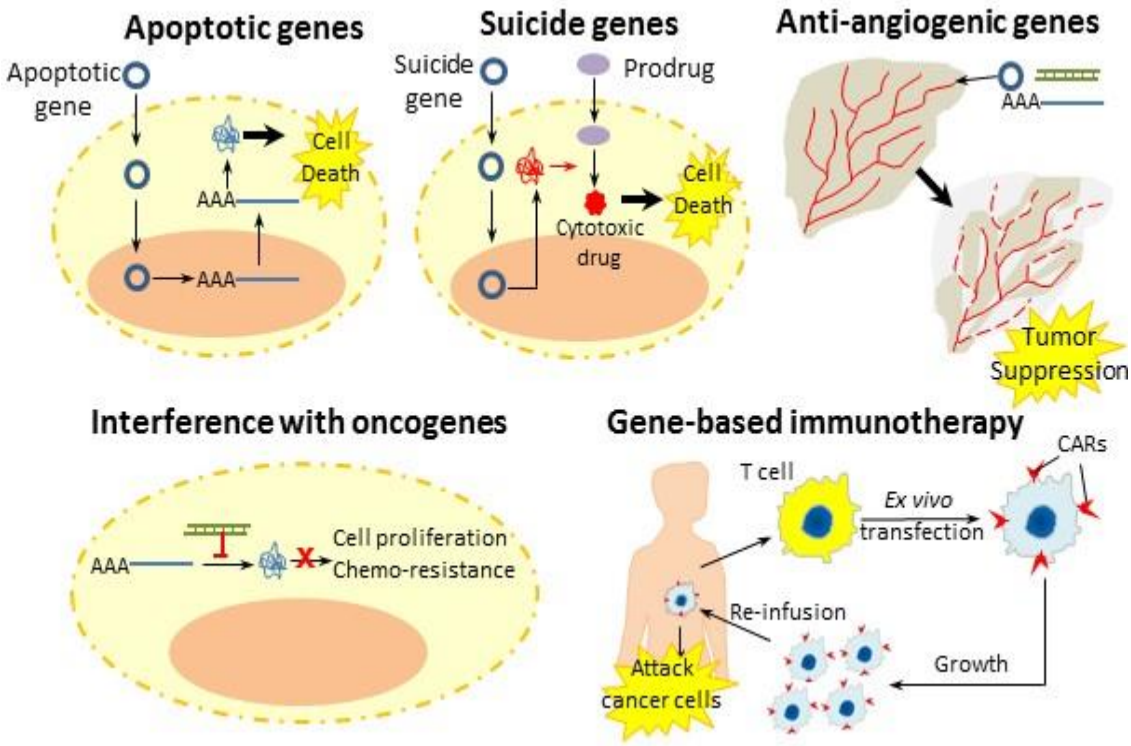

Figure 3. Schematic illustration of additional gene targets and approaches adopted for HCC gene therapy. Apoptotic genes are introduced into HCC cells to be transcribed and translated into apoptotic proteins, leading to cell death. A non-toxic prodrug together with a suicide gene encoding a certain enzyme are introduced into HCC cells where the suicide gene is translated into the corresponding enzyme that activates the prodrug *in situ* into cytotoxic form, thus leading to specific cell death. Anti-angiogenic genes are translated into their protein products that inhibit the formation of new blood vessels in the tumor leading to diminished blood and nutrition supply with consequent shrinkage of the tumor. In interference with oncogenes approach, RNA interference is utilized to knockdown the oncogene inhibiting their translation into oncoproteins responsible for cell proliferation, metastasis or chemoresistance. In gene-based immunotherapy, autologous T-cells are drained from the patient, *ex-vivo* transfected with genes expressing chimeric antigen receptors that recognize specific HCC antigens, and re-introduced into the patient to attack the tumor. Abbreviations: CARs, chimeric antigen receptors.

3.1. Molecular signaling pathways with special importance in HCC progression

3.1.1. Wingless/Int-1 (WNT) pathway

WNT is considered one of the top well-characterized pathways in HCC progression.[28] It is associated with the differentiation of epithelial cells with prominent effect on hepatocytes. Mutations in exon 3 region of Catenin Beta 1 (CTNNB1) gene lead to overactivation of WNT signaling with consequent loss of inhibitory signal controlling cell division after the completion of epithelial sheet formation.[29] A meta-analysis conducted by Hoshida and co-workers on 603 HCC patients revealed the correlation between WNT de-regulation and clinical progression of HCC and suggested its mediation via the overexpression of Transforming growth factor beta (TGF-β) influencing the subcellular localization of CTNNB1. The results suggested co-targeting of both TGF-β and CTNNB1 as a potential therapy for HCC.[30]

Tao *et al.*, studied the WNT signaling in specimens retrieved from human patients with different types of liver cancer including 104 with hepatocellular carcinoma (HCC), 62 with intrahepatic cholangiocarcinoma (ICC), and 94 with hepatoblastoma. Their investigation revealed the overexpression of CTNNB1 in most samples as concluded from immunohistostaining. The authors reported that silencing CTNNB1 gene by siRNA resulted in dramatic inhibition of the cellular proliferation of 6 different human HCC cell lines; HuH6, HepG2, HepT1, HC-AFW1, HepG2, and HC-AFW1. Moreover, they demonstrated that co-silencing of CTNNB1 and Yes Associated Protein 1 (YAP-1) genes synergistically inhibited the tumor growth suggesting potential interaction between the two aforementioned genes in WNT

signaling. The study was extrapolated to the *in vivo* level recruiting orthotopic liver cancer model. *In vivo* examination revealed the contribution of the overactivated WNT signaling in increasing the tumor aggressivity and lethality.[31]

3.1.2. Hedgehog (HH) pathway

HH signaling is associated with the invasion and migration of HCC cells. In addition, it plays a key role in the activation of Hepatic Stellate Cells (HSCs) to accumulate collagen with subsequent initiation and exaggeration of liver fibrosis in advanced HCC. A recent study investigated the remodeling of HH pathway by the selective delivery of the small molecular inhibitor, Vismodegib, to HCS using liposomes modified with the cRGDyK peptide targeting integrin receptors in HSCs. The results demonstrated attenuation of advanced liver fibrosis model in mice.[32] In addition to small molecular inhibitors, genetic studies confirmed the activation of HH pathway via the overexpression of smoothened homolog (SMO) and Sonic Hedgehog Signaling Molecule (SHH) genes or the underexpression of the gene encoding Hedgehog Interacting Protein (HHIP).[28] The former genes offer potential candidates for gene therapy.

Huang *et al.*, demonstrated that the repression of SMO gene by microRNA, miR-338-3p, inhibits the invasion of HCC cell line, SMMC-7721.[33] Additional evidence was provided by other studies which revealed the correlation between miR-338-3p or SMO levels and the progression of HCC.[34]

3.1.3. RAS/RAF/MEK/ERK signaling

This complex pathway involves multiple signaling molecules that activate numerous protein kinases responsible for the regulation of cell cycle progression, mitosis and apoptosis including RAF serine-threonine kinases and mitogen-activated protein kinases.[35] Upregulation of K-Ras gene (KRAS) or downregulation Ribosomal Protein S6 Kinase A3 (RPS6KA3) gene correlate with the uncontrolled activation of such pathway.[36-37] Currently, multiple kinase inhibitors such as Sorafenib, Cabozantinib, Lenvatinib and Regorafenib are widely used to affect RAS/RAF/MEK/ERK signaling in clinical management of non-resectable HCC. However, the clinical output is still poor with numerous side effects precipitated.[38] Gene therapy by knocking out KRAS or knocking in RPS6KA3 is a suggested therapeutic strategy.

In a recent study by Ghousein *et al.*, RAF1 protein was upregulated in 59.3% of samples collected from HCC patients. A microRNA, miR-4510, suppressed HCC growth both *in vitro* and *in vivo* via its inhibitory effect on RAF1 mRNA leading to down regulation of RAS/RAF/MEK/ERK signaling.[39] In another recent study, Liu and co-workers reported that the siRNA-mediated silencing of BRAF gene associated with RAS/RAF/MEK/ERK signaling inhibits the growth of murine HCC cell line, Hepa 1-6, and synergizes with the photothermal therapy.[40]

3.1.4. Alfa fetoprotein (AFP)

AFP is a cell growth regulator promoting the pluripotency of hepatocytes during fetal life and its levels are diminished after birth. Molecular studies revealed that AFP is overexpressed during hepatocarcinogenesis where it activates phosphatidylinositol-3 kinase

(PI3K)/AKT pathway leading to induction of cell cycle progression, survival and migration.[41] High serum levels of AFP are currently used as a key clinical diagnostic marker for human HCC.[42]

Ohkawa *et al.*, demonstrated that targeting AFP with a specific antibody reactivated phosphatase and tensin homolog (PTEN) in human HCC cells, FLC7, with consequent inhibition of PI3K/AKT signaling. The outcome was significant inhibition of cell proliferation.[43] In terms of gene therapy, genetic reprogramming of autologous T-cells retrieved from human patients to target AFP was investigated and one therapy is currently undergoing Phase I clinical trials.[44] The latter approach is highlighted in a relevant section of this review article discussing the gene-based immunotherapy of HCC. In another study, Zhu *et al.*, found that AFP antagonizes the apoptotic action of paclitaxel on HCC cells. The transfection of paclitaxel-resistant HCC cell line, Bel 7402, with siRNA against AFP gene increased their sensitivity to paclitaxel treatment as shown by the increased levels of the apoptosis marker, cleaved caspase-3 (CC-3), and the decreased levels of cell growth markers, CD44 and CD133.[45]

3.1.5. Midkine (MK)

MK is a heparin-binding growth cytokine highly expressed in the middle trimester of fetal life, from which it received its nomenclature, Mid-Kine.[46] The gene expression of MK significantly diminishes in healthy subjects after labor, but it is upregulated in HCC patients where MK demonstrates diversity of functions including the promotion of cell proliferation and angiogenesis, the resistance to apoptosis, and the decreased efficiency of chemotherapeutics.[47-48]

Zhong *et al.*, reported that silencing MK gene by siRNA inhibits the proliferation of HCC cells *in vitro*. [49] In a recent study, we demonstrated for the first time that siRNA targeting the MK gene (MK-siRNA) increases the sensitivity of HCC cells to the cytotoxic drug, Sorafenib (SOR). Our results suggested potential synergism between SOR and MK gene silencing therapy allowing the improvement of SOR therapeutic effect at low doses with potential avoidance of the side effects associated with SOR treatment.[50]

3.2. Apoptotic genes

Apoptotic genes are normally expressed as a self-defense mechanism in most living cells, where they induce the programmed death of malfunctioning or cancerous cells. However, these genes are mostly downregulated or missing in HCC. The re-introduction of these genes into HCC cells offers an interesting approach for fighting a tumor.

P53 is an endogenous gene that has a tumor suppressor function. It either induces DNA repair systems to correct minor damage or induces apoptosis if the damage is irreparable.[51] It has been reported that the *in vitro* transfection of some HCC cell lines with p53 gene induce apoptosis.[52] Furthermore, *in vivo* studies in both ectopic and orthotopic HCC mice models showed that p53 gene transfer reduced tumor growth making it a promising gene therapeutic approach for HCC.[53-54]

TRAIL is a type II transmembrane protein that exists in two forms; a membrane-bound and a soluble form. Both forms can selectively induce apoptosis in most tumors and have a minimal effect on normal tissues. Ma *et al.* concluded that the oral or intra-peritoneal administration of adeno-associated viral (AAV) vector encoding TRAIL resulted in the

efficient inhibition of HCC growth in mice without detectable toxicity to normal hepatocytes.[55]

3.3. Suicide genes

Suicide genes are genes that encode enzymes that activate non-toxic prodrugs and convert them into toxic forms. The specific delivery of these genes into target cells facilitates the *in situ* activation of prodrugs with the selective induction of cytotoxicity. A famous example is Herpes Simplex Virus Thymidine kinase (HSV/Tk) enzyme. Co-delivery of the prodrug, ganciclovir (GCV) and the pDNA expressing HSV/Tk to HCC mediates the *in situ* phosphorylation of GCV which is then incorporated into the DNA of HCC cells leading to the inhibition of DNA replication and apoptosis.[56]

3.4. Anti-angiogenic genes

HCC is a tumor characterized with excessive angiogenesis. The inhibition of angiogenesis leads to a reduction in tumor blood supply, growth and invasion.

Kang *et al*. reported on the inhibition of the growth of HCC in mice using antisense cDNA against mRNA of vascular endothelial growth factor (VEGF), which is responsible for promoting angiogenesis.[57] Schmitz *et al*. investigated the treatment of colorectal carcinoma (CRC) and HCC by the transfer of genes encoding the anti-angiogenic factors; endostatin and angiostatin. Their results showed the inhibition of tumor growth in mice with angiostatin being superior to endostatin.[58] Similar results were reported by Xu and co-workers using an angiostatin-expressing vector.[59] Furthermore, trials involving the use of pDNA expressing the recently-discovered, most powerful, endogenous

anti-angiogenic factor, pigment epithelium-derived factor (PEDF), succeeded in inhibiting tumor growth in HCC bearing mice.[60]

3.5. Interference with oncogenes

There are two types of malignant genes that have value in HCC gene therapy; oncogenes that are uniquely expressed in HCC cells and associated with carcinogenesis and tumor invasiveness and those genes that are normally expressed in healthy cells, but are upregulated in HCC leading to uncontrolled cell proliferation. We list some of these genes from both types in **Table 1**. RNAi, mostly by siRNA, is the favorite choice for knocking down these genes which usually results in inhibited cell proliferation, the induction of apoptosis and inhibited tumor growth or metastasis.

An example of oncogenes is the Decoy receptor 3 (DCR3) which acts as an agonist for several cancer cells associated with tumor growth and metastasis.[61] Another example is Gankyrin ($p28^{GANK}$) that was found to be overexpressed in 97% of HCC cells. Its protein product, Gankyrin, accelerates cell cycle progression via the phosphorylation of pRB and the inhibition of $p16^{INK4a}$ activity.[62] The polo-like kinase (PLK1) gene is an example of the second type. It is a regulatory protein that plays multiple roles in cell cycle progression, mostly through the regulation of the spindle checkpoint at the M-phase. It is overexpressed in several tumors where it is associated with uncontrolled cell proliferation by overcoming mitotic checkpoints. The Arbutus Biopharma company is currently performing phase I/II clinical trials on its product, ARB 1467®, for the treatment of HCC by the delivery of siRNA against PLK1. Promising results have been published with 51% of subjects showing a stable

disease status, 22% showing partial response and a reduction in tumor density of 59% was achieved.[63]

Table 1. Some common gene targets used for HCC gene therapy.

Gene target	Function(s)	Therapeutic tool	Outcomes	References
Vimentin	maintaining cellular integrity, tumor invasion	siRNA	inhibited HCC growth in mice	[64]
PLK1	Uncontrolled cell proliferation	siRNA	Inhibited HCC growth *in vitro* and *in vivo*	[65]
MK	anti-apoptotic, mitogenic, angiogenic and chemo-resistant	siRNA	Inhibited HCC proliferation *in vitro*	[49]
DCR 3	Tumor growth, metastasis	shRNA	inhibited growth and invasiveness of $HepG_2$ cells	[66]
DBC-1	Regulation of cellular apoptosis, RNA splicing and metabolism	shRNA	Inhibited HCC proliferation *in vitro*	[67]
EpCAM	Cell-cell adhesion, proliferation, metastasis and chemo-resistance	siRNA	Inhibited Huh-7 cell proliferation Increased sensitivity to chemotherapy *in vitro*	[68-69]
Bmi-1	Cell proliferation and chemo-resistance	siRNA	Inhibited HCC proliferation and increased sensitivity to 5-FU	[70]

Gene target	Function(s)	Therapeutic tool	Outcomes	References
Transcription factor E_2F_1	Promotes cell proliferation through enhancement of G_1/S phase transition	siRNA	Decreased HCC proliferation with G_1/G_0 phase-cells accumulation	[71]
$KNTC_2$	Chromosome segregation during M phase of mitosis	siRNA	Inhibited tumor growth in mice	[72]
JNK	Anti-apoptotic	siRNA	Enhanced CD95-mediated apoptosis and induced G_2/M Cell Cycle arrest in $HepG_2$ cells	[73]
Mcl-1	Anti-apoptotic	siRNA	Increased HCC sensitivity to chemotherapy and TRAIL	[74]
$p28^{GANK}$	Accelerates cell cycle progression	siRNA	Inhibition of HCC growth *in vitro* and *in vivo*	[62]
LPA/ATX	Inflammation-related HCC through TNFα/$NF_{\kappa B}$	shRNA targeting LPA receptor (LPAR6)	impaired HCC tumorigenesis in mice	[75]
Chk_2	Chromosomal instability and promotion of tumorigenesis	siRNA	reduced the mitotic index in HCC cells *in vitro*	[76]

Gene target	Function(s)	Therapeutic tool	Outcomes	References
Serine protease inhibitor (Serpin)	Promotion of cellular proliferation and epithelial-mesenchymal transition associated with metastasis	siRNA	Inhibited HeG2 cell proliferation	[77]

Abbreviations: PLK1, Polo-like kinase 1; MK, Midkine; DCR3, Decoy receptor 3; DBC1, Deleted in bladder cancer protein-1; EpCAM, Epithelial cell adhesion molecule; Bmi-1, B cell-specific Moloney murine leukemia virus integration site 1; 5-FU, 5-Fluorouracil; $KNTC_2$, Kinetochore-associated protein-2; JNK, c-Jun-N-terminal-kinase; Mcl-1, Myeloid cell leukemia-1; $p28^{GANK}$, Gankyrin; LPA/ATX, Lysophosphatidic acid/autotaxin pathway; Chk_2, Checkpoint kinase 2; $TNF\alpha/NF_{\kappa B}$, tumor necrosis factor alpha-nuclear factor kappa pathway.

3.6. Gene-based immunotherapy

Cancer immunotherapy has recently witnessed a breakthrough. Modulating the human immune system to recognize and attack cancer cells is a promising approach that has been crowned by the approval of Opdivo® (nivolumab) that can overcome the PD-1-based immune cell evasion responsible for cancer cells to escape from human immunity.[78] The discoverer, Tasuku Honjo, was awarded the Nobel prize for Medicine in 2018.[79] In the current section, we focus on gene-based immunotherapy for HCC.

Genetically-engineered T-cells are a good example of the applicability of gene therapy in cancer immunotherapy. In this approach, human cytotoxic T-cells are transfected ex-vivo with genes expressing specific receptors that recognize specific tumor surface antigens (T-cells receptors, TCRs, or chimeric antigen receptors, CARs). These modified

T-cells are then transferred to the patient, where they efficiently attacks the target tumor.[80] The first genetically-modified T-cells (CAR T-cells) were approved by the FDA in 2017 under the commercial name of Kymriah® for the treatment of lymphoblastic leukemia and large B-cell lymphoma.[13] This approach is, however, not limited to these tumors, and can be extended to HCC as well. In a recent study, Zhu *et al.*, modified clusters of differentiation 8 (CD8)-positive T-cells to recognize the human HCC antigen, the alpha fetoprotein (AFP), with the consequent efficient eradication of HCC in mice.[81] In another study, Spear *et al.*, engineered T-cells to recognize the Hepatitis C virus antigen, the HCV NS3:1406-1415 epitope, and this treatment showed a high efficiency in established HCC and an HCV mouse model.[82] Gao and co-workers, developed CAR T-cells recognizing the HCC antigen, glypican 3 (GPC-3), which resulted in the efficient eradication of HCC in mice with prolonged survival rates.[83] Furthermore, genetically-modified T-cells targeting AFP are currently undergoing a Phase I clinical trial,[44] while CAR T-cells targeting EpCAM are in phase II clinical trials.[84]

4. TARGETING HEPATOCELLULAR CARCINOMA

After selecting the suitable genetic payload, tumor tissue-specific targeting is critical for efficient gene therapy to ensure maximal accumulation at tumor tissue and minimal effects on normal adjacent tissues.

4.1. Challenges associated with the gene delivery to HCC via systemic administration

Although systemic gene delivery via intravenous administration is challenged by multiple obstacles, it remains the most reliable method to ensure uniform and reproducible delivery.[85] Following intravenous

administration, the integrative escape from various biological barriers should be accomplished. First, sufficient retention time of the vector in the blood circulation is needed to facilitate reaching the tumor site without being eliminated by the liver and spleen, the common fate for injected xenobiotics. Second, the delivery system should extravasate from the tumor vasculature to access the tumor cells. Due to the need for excessive blood supply and nutrients to permit rapid growth, tumors are characterized by a vasculature that is different from normal tissues. They possess a leaky vasculature with large-gap junctions ranging from 100 nm to 2 μm. Furthermore, tumors have been found to show a decreased lymphatic drainage. Therefore, these unique characteristics have led to the approach of passive targeting via the Enhanced Penetration and Retention (EPR) effect by exploiting the small size of nanoparticles that can penetrate through this leaky vasculature and ultimately accumulate in tumor tissues.[86] Since the first report by Matsumura and Maeda in 1986, the EPR effect was extensively adopted for cancer drug delivery.[87] However, the use of EPR-based targeting is now controversial due to heterogeneity of the EPR effect in different tumors and animal models and clinical data regarding its benefits in humans are limited.[88] In addition, HCC is characterized by a stroma-rich microenvironment, comprised mainly of collagen and fibroblasts, which represents a great obstacle facing HCC delivery.[89] This problem is worse in the case of gene delivery because the hydrophilic, metabolically-labile genetic materials cannot diffuse and reach the tumor cells without their delivery vehicle, unlike small molecular weight drugs that are commonly used in chemotherapy. An approach to fight this challenge is modulating the tumor microenvironment via the action of anti-stroma agents. One example involved the use of monoclonal antibodies against fibroblast activation protein (FAP).[90] The extension of these approaches to gene

therapy is, however, limited by the complexity of the delivery system and the effectiveness of such approaches remains controversial. After penetration through the stroma barrier, the delivery vehicle should recognize and selectively-accumulate in HCC cells to facilitate sufficient therapeutic efficacy and minimize the harm to other adjacent or healthy tissues. A scheme outlining the aforementioned challenges is shown in **Fig. 4.**

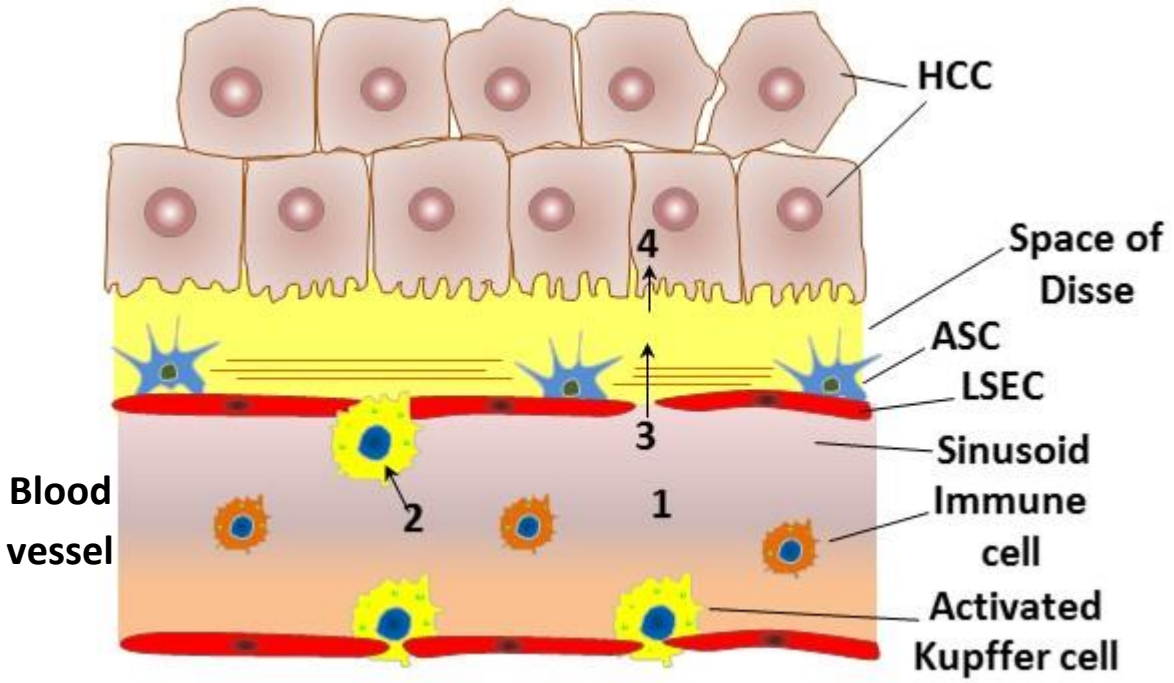

Figure 4. Schematic illustration for the challenges facing gene delivery to HCC via systemic intravenous administration. The tumor microenvironment and the space of Disse are enriched with collagen fibers, activated stellate cells and immune cells. The sinusoids are enriched with activated macrophages and several types of immune cells. (1) The ideal delivery system should have a long blood circulation time to facilitate sufficient extravasation and accumulation at the tumor site. (2) The delivery system should escape from being recognized by the reticulo-endothelial system, e.g. Kupffer cells, to avoid phagocytosis and degradation. (3) The delivery system should have enough penetration through the collagen stroma barrier to access the tumor cells. (4) The delivery system should possess significant uptake into HCC cells and endosomal escape capability to release its payload into the cytosol. Abbreviations: HCC, hepatocellular carcinoma cells; ASC, activated stellate cell; LSEC, liver sinusoidal endothelial cell.

4.2. Active targeting of HCC

The EPR-dependent gene delivery, known as passive targeting, mostly requires extensive PEGylation of the nanocarrier to prolong its circulation time which interferes with its cellular uptake and endosomal escape capabilities, the phenomenon known as PEG dilemma.[91] The increasing drawbacks of passive targeting lead to the introduction of the

active targeting concept in which the nanocarrier is functionalized with targeting moieties recognizing certain receptors that are uniquely-expressed or particularly-overexpressed on cancer cells or alternatively, exploiting certain unique conditions in the tumor microenvironment.[92]

4.2.1. Differential targeting

With the aid of molecular cellular biology studies, scientists have discovered several receptors that are differentially-overexpressed in HCC. Thus, this differential distribution is being invested to increase the chance of the delivery vehicle accumulating in HCC cells to a greater extent than other healthy cells. Here, we list some of these receptors and their associated targeting ligands.

Asialoglycoprotein receptors (ASGPRs) are normally expressed in hepatocytes, but are particularly overexpressed in HCC . This differential distribution of ASGPRs was exploited in targeting HCC with several ligands including galactose and its derivatives,[93] lactose,[94] lactoferrin [95] and lactobionic acid.[96]

Transferrin (Tf), an iron-binding protein involved in iron homeostasis, has two types of receptors; TfR1 and TfR2 that are particularly abundant in hepatocytes.[97] Transferrin receptors are overexpressed in several tumors including HCC to fulfill the increased demand for iron. Nanoparticles modified with transferrin were used for the targeted chemotherapy of HCC.[98] In addition, antibodies against transferrin receptors were developed to aid in HCC targeting.[99]

Folic acid, vitamin B9, a member of the vitamin B family, has important roles in cellular metabolism. Folic acid receptors are upregulated in several malignancies and therefore, have been exploited in active targeting. Zhang *et al.* designed folate-targeted micelles containing

superparamagnetic iron oxide nanoparticles (SPIONs) and sorafenib to target $HepG_2$ cells.[100] Xia *et al*. used Folate-targeted selenium nanoparticles to deliver siRNA to HCC.[101]

Glycyrrhetinic acid (GA) is a natural product that results from hydrolysis of glycyrrhizic acid extracted from the licorice root. GARs are abundantly expressed on the surfaces of hepatocytes and HCC. Zhu *et al*. decorated polymeric micelles with GA for the targeted delivery of etoposide (ETO) to HCC.[102]

4.2.2. Targeting tumor-specific antigens

Glypican-3 (GPC3), a heparan sulfate proteoglycan, is abundantly-expressed in HCC, but not in normal hepatocytes. It functions as a co-receptor for some ligands that promote neoplasia and has been considered to be a diagnostic element for HCC.[103] Wang *et al*. used a specific antibody against GPC3 for the targeted delivery of siRNA to HCC.[104]

AF-20 is a glycoprotein tumor antigen that is highly expressed in HCC and colon cancer.[105] Mohr *et al.* used monoclonal antibodies (mAbs) against the AF-20 antigen for the targeted delivery of pDNA or oligonucleotides to HCC.[106]

Somatostatin, a peptide hormone, is responsible for the regulation of cell proliferation and growth through interaction with G protein-coupled somatostatin receptors (SSTRs) inhibiting the release of growth hormone (GH) and multiple other secondary messengers.[107] Reynaert *et al*. reported that SSTRs are expressed in cirrhotic livers and HCC, but they did not find it in normal hepatocytes which makes these receptors a potential target for therapeutics against HCC.[108] Octreotide is a synthetic analogue of somatostatin and can function as agonist for SSTRs. Sun *et al*. used Octreotide as a targeting ligand for SSTRs to deliver

doxorubicin to a human HCC cell line, SMMC-7721 and other cancerous cells.[109]

4.2.3. Targeting tumor endothelial cells

Integrin receptors are transmembrane receptors that are responsible for the adhesion of cells to the extracellular matrix . They mediate various intracellular functions such as the regulation of the cell cycle, organization of the intracellular cytoskeleton and the movement of new receptors to the cell membrane.[110] Among the integrin receptors, there are two types that are abundant in the angiogenic endothelium of several malignant tumors, namely αvβ3 and αvβ5.[111] RGD is a tripeptide composed of Arginine-Glycine-Aspartic acid and is known to serve as a ligand for integrin receptors in both of its forms; linear and cyclic with the cyclic form (cRGD) having the highest affinity.[112] Chen *et al*. used RGD-modified liposomes to target paclitaxel (PTX) towards HCC both *in vitro* and *in vivo.*[113]

4.2.4. Towards absolute targeting

Phage display is an innovative technique that has been first described by George P. Smith in 1985. It depends on inserting a gene coding a certain protein or peptide into a bacteriophage and then using the virus to express this protein on its surface, which permits studies of its interaction with cellular membranes and other proteins. Thanks to this technique, huge libraries of peptides can be generated and evaluated for their affinity towards certain cells or receptors.[114] Smith was awarded Nobel prize in chemistry in 2018 for his efforts.[115] Using phage display technology, Lo *et al.* discovered SP94, a twelve amino acid-peptide that showed absolute specificity towards HCC.[116] Li *et al*. utilized a SP94 peptide for the specific *in vivo* imaging and radiotherapy of HCC.[117]

In 1990, Tuerk and Ellington designed a strategy to discover highly-specific targeting ligands based on the use of oligonucleotides, which they called the Systematic Evolution of Ligands by Exponential Enrichment (SELEX). This strategy depends on the synthesis of massive libraries of oligonucleotides, called aptamers, and screening their ability to bind to certain types of cells or molecules.[118-119] In a recent study, Kaur reported on an aptamer called SL2-B which binds specifically to the VEGF165 protein in HCC cells, HepG2. The aptamer was further conjugated to semiconducting crystals (quantum dots) to facilitate the imaging of its cellular uptake in HepG2 cells.[120] In another study, Zhou and co-workers developed fast-off and slow-off aptamers targeting the dickkopf-1 (DKK1) protein in HCC and proposed that they could be used in the diagnosis of early stage HCC.[121] For application in gene therapy, Xiao *et al.*, conjugated an aptamer targeting EpCAM in HepG2 cells to a recombinant adenovirus for the targeted delivery of the tumor suppressor gene, Phosphatase and the tensin homolog (PTEN). The results revealed that HCC could be efficiently treated both *in vitro* and *in vivo.*[122] Liu *et al.*, functionalized the cell-penetrating peptide, H_3R_5, with an aptamer ST21 to target PEG nanoparticles to HCC for the co-delivery of the microRNA, miRNA-195 (miR195), as anti-VEGF gene therapy and the antiangiogenic drug, fasudil. A high cellular uptake and therapeutic efficiency were confirmed *in vitro* and *in vivo.*[123]

4.3. Biomaterials for HCC-targeted gene therapy

Although active targeting has been extensively reported in the literature and is still very efficient, it is challenged by several demerits that subtract from its value. Delivery systems decorated with targeting ligands are complex and their stability *in vivo* is controversial due to the probability of detachment of the ligand from the delivery system after

administration. In addition, it is difficult to guarantee the degree of perfectness of ligand-receptor interactions.[124-125] Therefore, interest has been directed towards the development of smart biomaterials that have an intrinsic affinity to target a certain tissue or organ. Furthermore, through the appropriate study of structure-activity relationship (SAR), the chemical structures of these materials can be modulated to allow them to acquire desirable properties like biodegradability, stability, efficiency and selectivity.[124-125]

Siegwart and co-workers[126] synthesized a library of 1,500 dendrimers with modular degradability via the introduction of ester bonds and molecular diversity at each expansion step. Using this approach, they identified a promising candidate, 5A2-SC8, with a high tolerability, that could deliver siRNA against the coagulation factor (FVII) gene in hepatocytes of mice bearing aggressive HCC tumors with a high efficiency (half-maximal effective dose, ED_{50} < 0.02 mg siRNA/kg). Moreover, it could also efficiently deliver the tumor suppressor microRNA (miRNA), *let-7g*, to HCC cells leading to a significant inhibition of tumor growth and the subsequent prolongation of survival rate.

Zamboni *et al.*, prepared nanoparticles based on biodegradable Poly(Beta-Amino Ester) (PBAE) to specifically deliver a reporter pDNA, pEGFP-N1 (eGFP), to HCC. Selective gene transfer was confirmed *in vitro* in eight HCC cell lines compared to normal hepatocytes. A high selectivity and transfection efficiency was also confirmed *in vivo* using a subcutaneous HCC mouse model.[127]

4.4. Gene delivery to HCC via alternative routes of administration

Although the application of systemic intravenous administration is predominant in literature, there are alternatives routes of administration which have been investigated. We attempted to highlight these routes below.

4.4.1. Intrahepatic/intratumoral administration

Local intrahepatic/intratumoral administration of HCC gene therapies can be adopted to ensure selectivity, efficiency and rapid effect while bypassing several complicated challenges and barriers associated with the systemic administration.[128-129] Yet, such procedure is aggressive, requires highly-skilled medical personnel, and needs to be done under anesthesia which complicate the procedure. In addition, the risks of liver injury and bleeding as well as the little benefits in case of disseminated multi-nodular or metastatic tumors limit its applicability. Furthermore, the risk of disseminating the tumor to other distant parts of the liver during such procedure cannot be avoided.[130-131]

In a recent study, Song and co-workers used a multi-functional perfusion-thermal Radio Frequency electrode for the intratumoral infusion of the genetically-modified oncolytic virus, T-VEC, to rats bearing intrahepatic tumors. They reported that the hyperthermia resulted from the used radiofrequency electrode enhanced the direct oncolytic effect of the virotherapy.[132] Intratumoral administration has been investigated in a clinical trial involving CAR T-cells targeting GPC3. In another clinical trial, adenovirus encoding the suicide gene, HSV/Tk, was administered similarly.[133]

4.4.2. Transarterial administration

Administration of HCC gene therapies via the hepatic artery may be beneficial to escape from the harsh barriers that obstacle systemic administration while coping with the limitations of the direct intratumoral administration. Such route of administration is widely-used in the transarterial chemoembolization (TACE) approach for the clinical management of HCC. [134]

Transarterial administration of Doxorubicin and Cisplatin showed benefit in patients with advanced HCC as reported by Ma *et al.*[135] Anderson *et al.*, used intra-arterial administration to deliver a recombinant adenovirus expressing the tumor suppressor gene, P53, to rats bearing HCC.[54] Some clinical trials recruited transcatheter arterial infusion for the administration of CAR T-cells targeting GPC3 or CD147 HCC antigens or the human adenovirus 5 expressing P53.[133]

5. VECTORS FOR HCC GENE THERAPY

Delivering nucleic acids to a target is not any easy matter. It is challenged by multiple biological barriers including being degraded by serum or intracellular nucleases, immunogenicity, a short biological half-life which is insufficient to induce a therapeutic response and poor cellular uptake and endosomal escape due to their hydrophilicity, high negative charge and high molecular weight.[11-12, 136] Therefore, proper selection of the gene delivery vector is critical to ensure the delivery of the desired cargo to the target cells in an amount sufficient to induce the desired therapeutic effect.

5.1. Viral vectors

Delivering nucleic acids by exploiting viral machinery capable of infecting eukaryotic cells and overcoming the existing biological barriers was the first trial to be investigated. Retrovirus, lentivirus, adenovirus, adeno-associated virus, Herpes simplex virus and hybrids derived from them have been examined.[136] The first two FDA-approved gene therapies utilized viral vectors; namely lentivirus in the case of Kymriah® [137] and adeno-associated virus serotype 2 (AAV2) in the case of Luxturna®.[138] However, viral vectors have several drawbacks due to their immunogenicity, mutagenicity and difficulties in scale-up.[136] Therefore, interest has been directed to non-viral vectors which comprise diverse nanocarriers such as lipid-based nanosystems, polymer-based nanosystems, protein nanoparticles and inorganic nanoparticles.

5.2. Non-viral vectors

5.2.1. Lipid-based nanosystems

Lipid-based nanosystems were the first non-viral vectors developed to simulate the viral machinery in human cell transfection while overcoming the drawbacks associated with the use of viruses. Two types of lipids can be used; cationic lipids with persistent positive charge, and pH-sensitive lipids with ionizable groups that are responsive to the pH microenvironment at the site of action (e.g. tumor) or the endosome upon cellular internalization. The latter type is superior to avoid problems associated with the high cationic charge including toxicity, immunogenicity, non-specific interactions with biological membranes, low transfection efficiency resulting from the large particle size, poor endosomal escape and rapid elimination from the circulation.[139-141] Lipid-based nucleic acid delivery has made great advances and was crowned by

the FDA approval of the first siRNA therapy, Onpattro (Patisiran)®, which utilizes lipid nanoparticles for delivering siRNA to the liver.[15]

Lipid-based nanocarriers have high applicability as gene delivery vectors to HCC. An interesting example was developed by Liu and co-workers who designed multifunctional nanoparticles called liposome-calcium phosphate-protamine (LCPP) for the delivery of TRAIL-expressing pDNA to the livers of HCC-bearing mice. First, pDNA was complexed with calcium phosphate, protamine and the anionic lipid, 1,2-dioleoyl-sn-glycero-3-phosphate (DOPA) to form a core. Then the negatively-charged core was further coated with the cationic lipid 1,2-dioleoyl-3-trimethylammonium-propane (DOTAP), cholesterol and a PEG-lipid moiety functionalized with HCC-selective SP94 peptide. Protamine functions as a nuclear localization signal (NLS) to improve the nuclear delivery of pDNA, one of the critical rate-limiting steps determining the efficiency of gene transfer. Meanwhile, calcium phosphate functions as endosomal escape device. These nanoparticles had an average particle diameter of 100 nm and could accumulate efficiently in livers with HCC following intravenous administration and significantly eradicated HCC tumor upon concomitant administration with the anticancer drug, sorafenib (SOR).[142]

5.2.2. Polymer-based nanosystems

Polymer-based nanosystems are colloidal macromolecules with diverse structures and characteristics. They possess several advantages including feasibility of controlling their design so as to acquire the desired characteristics, diversity, tolerability, biodegradability and physiological stability. Polymeric nanocarriers are sub-classified into

many categories including polyplexes, micelles, dendrimers, polymersomes, nanogels and block copolymers.[143]

Polymer-based nanosystems have been extensively studied for gene delivery. Xue and colleagues prepared polymeric nanoparticles based on carboxymethyl chitosan with dual-targeting functionalities, namely galactose for asialoglycoprotein receptors and iron oxide to acquire magnetic properties. Nanoparticles were loaded with pDNA encoding the tumor suppressor gene, RASSF1A. Following intravenous administration in HCC-bearing mice, these small nanoparticles (~40 nm) highly accumulated in HCC tumor, particularly upon application of external magnetic field, with the final outcome of reduced tumor volume and increased apoptosis rate as shown by terminal deoxynucleotidyl transferase-mediated dUTP nick end labeling (TUNEL) assay.[144]

5.2.3. Protein nanoparticles (PNPs)

Protein-based nanocarriers share common merits including ease of preparation by self-assembly, biosafety, biodegradability, high loading capacity, feasibility of chemical modifications and versatility of applications.[145]

Ashley and co-workers designed Virus-like Particles (VLPs) based on MS2 bacteriophage coat protein, functionalized with SP94 peptide, for the selective delivery of versatile payloads to human HCC cell line, Hep3B. The payloads included quantum dots, ricin toxin A-chain (RTA) protein, cytotoxic drugs such as doxorubicin, cisplatin and 5-fluorouracil, and siRNA cocktails. The MS2-VLPs demonstrated 10^4-fold higher affinity for HCC cells than for other normal cells such as hepatocytes, endothelial cells, monocytes, or lymphocytes. The encapsulated siRNAs targeted cyclin family genes in HCC and induced apoptosis at siRNA

doses less than 150 pM.[146] Similarly, Wang *et al.* prepared MS2-based PNPs for the delivery of microRNA-122 (miR-122) to three different HCC cell lines; namely Hep3B, HepG2, and Huh7 cells. The PNPs were cross-linked to the cell-penetrating peptide, TAT, derived from HIV virus to enhance the cellular uptake and endosomal escape capabilities. The proposed system showed high cytotoxicity *in vitro* and resulted in efficient tumor suppression *in vivo* in Hep3B animal models.[147] Tian *et al.*, used PNPs based on TAT-modified tobacco mosaic plant virus (TMV) for the delivery of a reporter siRNA against the green fluorescent protein (GFP) to a highly-metastatic, GFP-expressing HCC mice model. About 80% reduction in GFP signal was obtained following 10-day treatment schedule.[148]

5.2.4. Inorganic nanoparticles (InNPs)

The recruitment of inorganic nanoparticles based on metals for the gene delivery to HCC has been also emerged. These nanoparticles have several advantages including small particle size facilitating high tumor penetration, good biotolerability, and compatibility with most nucleic acids. In addition, they can possess optical properties facilitating the tumor imaging or photothermal therapy.[149]

In a recent study, Xia *et al.* designed selenium nanoparticles (SeNPs) for the delivery of siRNA against Hairy and enhancer of split 5 (HES5) transcription factor to human HCC cells, HepG2, or to grafted HCC tumor in mice. The nanoparticles were modified with the tumor-targeting polypeptide, RGDfC. The authors demonstrated that the aforementioned nanoparticles are uptaken via Clathrin-mediated endocytosis (CME) and induced significant inhibition of the cell growth compared to the commercially-available transfection reagent,

Lipofectamine 2000. SeNPs were biosafe upon systemic administration to mice and could accumulate efficiently in the tumor tissue with significant anticancer effect.[150] In another study, Qin and co-workers prepared gold nanorods (Au NRs) for the delivery of siRNA against human telomerase reverse transcriptase (hTERT) gene to HepG2 cells. siRNA was loaded onto ZnGa2O4:Cr (ZGOC) nanofibers to facilitate photo-responsive enhancement of cellular uptake and endosomal escape.[151] Wang *et al.*, utilized gold nanocages (AuNCs) for the delivery of microRNA 21 inhibitor, anti-miR-21, to Doxorubicin-resistant HCC cells, HepG2/ADR. This strategy significantly inhibited the overexpression of p-glycoprotein (p-gp) in the resistant cells and increased their sensitivity to Doxorubicin.[152]

In **Table 2**, we summarize some non-viral vectors based on nanoparticles that are used for gene delivery to HCC.

Table 2. Some non-viral vectors used for the gene therapy of HCC.

Category	Name of system/ composition	Targeting method	Cargo	Key outcomes	References
LNPs	ARB 1467	Undisclosed	siRNA against PLK1	Phase I/II clinical trial: 51% stable status, 22% partial response, 59% tumor reduction	[63]
	WO2016021683 /DPPC/Chol /DSG-PEG_{2000}	Passive	siRNA against $KNTC_2$	Inhibited tumor growth in mice	[72]
	Liposome-calcium phosphate-protamine (LCPP)	SP94 peptide	TRAIL pDNA	Attenuated HCC progression and liver fibrosis	[142]
	LNP-DP1	Passive	miR-122	50% growth reduction of HCC in mice within 30 days	[153]
	RL01-17(5)	Passive	Anti-miR-17	Inhibited HCC growth *in vitro* and *in vivo*.	[154]
Polymer-based	PHEA-DETA-PEG-GAL	Galactose	siRNA against E_2F_1	Inhibited HCC growth *in vitro*	[71]

Category	Name of system/ composition	Targeting method	Cargo	Key outcomes	References
Polymer-based	MixNCH	-	siRNA against MK	Inhibited HCC growth and decreased cell viability *in vitro*	[49]
	LA-PAEP	Lactobionic acid	Luc-pDNA	High transfection efficiency *in vitro* and *in vivo*	[155]
	NP-siLuc-GPC3	GPC3 MAB	siRNA against Luc gene	Efficient *in vivo* gene silencing and tumor targeting	[104]
	Gal-CMCS-Fe_3O_4-NPs	Galactose	RASSF1A pDNA	Reduced tumor size in HCC bearing mice.	[144]
	Pectinate NPs (Ca,Mg or Mn pectinate)	-	pDNA encoding EGFP	Enhanced *in vitro* transfection in Huh7 cells.	[156]
PNPs	MS2-VLPs (Nanoparticles based on MS2 coat protein)	SP94 peptide	siRNAs targeting cyclin family genes	Inhibition of Hep3B cell growth *in vitro*	[146]

Category	Name of system/ composition	Targeting method	Cargo	Key outcomes	References
PNPs	TAT-TMV (TAT-modified tobacco mosaic plant virus)	Passive	siRNA against GFP	80% reduction in GFP in HCC-bearing mice	[148]
InNPs	SeNPs (Selenium nanoparticles modified with RGDfC polypeptide)	RGDfC peptide	siRNA against HES5	Inhibited HCC growth *in vitro* and *in vivo*	[150]
	AuNCs (gold nanocages)	-	anti-miR-21	Reversal of resistance in DOX-resistant HCC *in vitro*	[152]

LNPs, Lipid nanoparticles; PNPs, protein nanoparticles; InNPs, inorganic nanoparticles; Chol, cholesterol; WO2016021683, patented cationic lipid chemically-named as 3-((5-(dimethylamino)pentanoyl)oxy) −2,2-bis (((3-pentyloctanoyl)oxy)methyl)propyl 3-pentyloctanoate; DPPC, 1,2-dipalmitoyl-sn-glycero-3-phosphocholine; DSG-PEG_{2000}, 1,2-Distearoyl -rac-glycero-3-methylpolyoxyethylene; DOTAP, 1,2-dioleoyloxy-3-(trimethylammonium) propane; DSPE-PEG, 1,2-distearoyl-*sn*-glycero-3-phosphoethanolamine-N-[carboxy(polyethylene glycol)-2000]; DOPA, 1,2-dioleoyl-sn-glycero-3-phosphate; DODMA, dioleyloxy-N,N-dimethyl-3-aminopropane; EPC, egg phosphatidylcholine; DSPC, 1,2-Distearoyl-sn-glycero-3-phosphatidylcholine; DMPE-PEG2000, 1,2-dimyristoyl-*sn*-glycero-3-phosphoethanolamine-N-[methoxy (PEG)-2000]; PHEA, α, β-poly-(N-2-hydroxyethyl)-D,L-aspartamide; DETA, diethylene triamine; GAL, galactose; LA, lactobionic acid; PAPE, Poly(2-(2-aminoethyoxy)ethoxy)phosphazene; NP, nanoparticle; Luc, luciferase; PEI, polyethylene imine; CMC, carboxymethyl chitosan; MAB, Monoclonal antibody; EGFP, Enhanced green fluorescent protein; VLPs, Virus-like particles; GFP, green fluorescent protein; HES5, Hairy and enhancer of split 5; miR, microRNA; RASSF1A, tumor suppressor gene; Luc, luciferase; DOX, Doxorubicin.

6. GENE THERAPY COMBINATIONS FOR TREATMENT OF HCC

Due to the promising advantages of gene therapy, efforts have been exerted to involve it in integrated therapeutic regimens, by combining one type of gene therapy with another type of gene therapy or other approaches such as chemotherapy or immunotherapy. This would be beneficial in terms of imparting a synergistic effect that can maximize therapeutic benefits and minimize side effects. Here, we discuss some approaches for combinational therapy that have been investigated for treatment of HCC involving gene therapy.

6.1. Multiple gene therapy

The goal of multiple gene therapy is to simultaneously deliver two or more types of gene therapy targeting different genes. Ren *et al*. designed a co-delivery system in the form of polymeric nanoparticles based on pullulan for the simultaneous delivery of two pDNAs coding two tumor suppressors, p53 and MEG3. The prepared system showed a higher efficiency over systems containing individual p53 or MEG3, both *in vitro* and *in viv*o, with overall tumor suppression.[157] Li *et al.* proved a similar concept by investigating multi-target siRNAs against three genes in HCC; NET-1, EMS1 and VEGF. The results showed more inhibitory effects on cellular proliferation and growth and induced more apoptosis in HCC cells than what was obtained using single target siRNAs.[158]

6.2. Chemotherapy/gene therapy combinations

The concept of combining chemotherapy with gene therapy has received recent interest regarding increasing the sensitivity of cancer cells to chemotherapy and overcoming drug resistance by knocking down its

correlated genes. Zhu *et al*. prepared N-succinyl chitosan nanoparticles conjugated to human low-density lipoprotein (LDL) for the co-delivery of DOX and siRNA targeting the multidrug resistance (MDR) gene expressing the p-glycoprotein (P-gp), the major protein responsible for multi-drug resistance by facilitating the efflux of drug molecules outside cancer cells. The results revealed an increased sensitivity of HCC cells and their *in vivo* tumor models to DOX.[159] Oh *et al*. designed galactose-targeted liposome for the co-delivery of DOX and siRNA against the vimentin gene and confirmed their synergistic anti-tumor activity both *in vitro* and *in vivo.* [64] Shen *et al*. prepared nanocomplexes composed of Pluronic P85 (P85)/Polyethyleneimine (PEI)/D-α-tocopheryl polyethylene glycol 1000 succinate (TPGS) for the co-delivery of SOR and shRNA against the Survivin anti-apoptotic and chemo-resistant gene and showed increased efficiency and the reversal of MDR in resistant HCC.[160] Devulapally *et al.* prepared polymeric nanoparticles composed of PEGylated poly(lactide)-co-glycolide (PEG-PLGA) encapsulating gemcitabine and antisense-miRNA-21 against microRNA 21 (MiR-21) that promotes HCC cell proliferation, angiogenesis, invasion and apoptosis-resistance and obtained synergistic anti-tumor effect.[161]

6.3. gene therapy/thermal therapy combinations

This approach merges suicide gene therapy and magnetic-induced hyperthermia therapy. Simply, a prodrug and pDNA encoding the enzyme required for the activation of the prodrug (suicide gene) are co-loaded into a delivery system with magnetic properties. Upon the application of an external magnetic field, targeted delivery of the system can be achieved to its site of action where the suicide pDNA expresses the activating enzyme for the *in situ* conversion of the non-toxic prodrug

into cytotoxic compound [162] while the system itself is induced in response to the external magnetic field to produce excessive heat [163] leading to cell death by a combination of cytotoxicity and hyperthermia.

Wang *et al.*, [164] prepared magnetic mesoporous silica nanoparticles (MSNs) for the co-delivery of the prodrug, ganciclovir (GCV), and pDNA bearing herpesvirus thymidine kinase (HSV/Tk) gene to HCC. Following intravenous administration in HCC-bearing mice, the tumor was subjected to an external magnetic field to direct the nanoparticles to the tumor. Upon cellular internalization, the *in situ* produced HSV/Tk mediates the phosphorylation of GCV which is incorporated into the DNA of HCC cells leading to the inhibition of DNA replication and apoptosis. The magnetic MSNs mediated hyperthermia which augmented cell death. The outcome of this combination was an effective treatment of HCC with limited systemic toxicity. In addition, the researchers found that the shape of these nanoparticles affected their performance with rod-like MSNs being superior to sphere-like MSNs.

7. ANIMAL MODELS USED FOR THE EVALUATION OF HCC GENE THERAPIES

Successful translation of the proposed gene therapies against HCC into clinically-beneficial products requires accurately-relevant animal models for use in pre-clinical studies. Although non-human primates remain the ideal choice for human similarity, mice are preferred as animal models being easy to handle, economic, simple and rapidly-developed.[165] Animal tumor models can be roughly-classified according to the origin of cancerous tissues into syngeneic models, in which the cancerous tissues/cells are derived from the same species (e.g. using murine cancerous cells to induce tumors in mice), and xenograft models, in

which the cancerous tissues/cells are derived from different species (e.g. human cells). Although xenograft models are easy to establish, they require immunocompromised mice (e.g. athymic nude mice or severe combined immunodeficiency, SCID, mice) to avoid the rejection of the implanted cells, and therefore, they are not suitable for studying immunotherapies or interactions of the tumor with the immune system. According to other classifications based on the site of tumor induction, tumor models can be classified into orthotopic models, in which the tumor is induced into its original site (e.g. HCC induced in liver), and ectopic models, in which the tumor is induced outside its original site, mostly subcutaneously. Ectopic models are easy to induce and follow-up due to their superficial nature, but they do not reflect the actual tumor environment.[166-167] According to these characteristics, the most relevant models are syngeneic-orthotopic models. In **Table 3** we highlight the most common methods used to create syngeneic-orthotopic mice HCC models.

Genetically-engineered mice (GEM) offer the best choice because they spontaneously develop HCC, thus facilitating appropriate studies of genetic factors related to HCC development. They are mostly developed through the genetic deletion of the tumor suppressor gene, p53 by CRISPR/Cas 9 in mice embryos or through the introduction of oncogenes (e.g. c-Myc) with liver-specifc promotors to facilitate specific tumorigenesis in the liver. Yet, these models are too expensive and lack some of the features associated with human HCC like fibrosis.[168] Implantation models based on cultured cells are the most popular among researchers due to the feasibility of creation in laboratories, however, they are criticized for the differences between cells cultured *in vitro* for numerous generations and the tumor cells existing in reality. Other

applied methods including hydrodynamic cell transfer or chemo-toxic induction are controversial and criticized for the high mortality rates during formation. Although syngeneic models allow the study to be conducted in immunocompetent mice, some criticisms have arisen based on differences between murine and human tumors.[169] Patient-derived xenografts (PDX) appeared to approach the opposing points of view. In these models, tumor cells from actual human patients are used to replace the cultured cell lines that are commonly used for the establishment of xenografts in mice. Thanks to this technique, a human tumor microenvironment can be maintained with a wide window for personalized therapy case by case.[170]

Table 3: Summary of some of the common methods used to create syngeneic-orthotopic mice models of HCC.

	Genetically-engineered mice (GEM)	Implantation	Hydrodynamic cell delivery	Chemo-toxic agents
Procedure	Genetic deletion of tumor suppressor gene (e.g. p53) or activation of oncogene	Injection of murine HCC cells intra-hepatically intra-portally or intra-spleenically	Injection of murine HCC cells intra-venously rapidly in large volume	Oral or IP treatment with carcinogens (e.g. DEN and DMBA)
Time to develop HCC	4-14 months	7-14 days	2-3 weeks	Variable, >11 weeks
Merits	Simple, suitable to study genetic basis of oncogenesis	100% incidence rate, rapid development	100% incidence rate, rapid development	Simple, suitable to study chemical carcinogenesis
Demerits	Expensive, may take long time to develop into HCC	Technical difficulties, mostly involve surgical procedures	Aggressive procedure leads to high mortality rate	Slow, involves several stages before the development, needs infant-age mice
References	[171]	[172]	[173]	[174]

IP, intraperitoneal; DEN, diethylenetriamine; DMBA, 9,10-dimethyl-1,2-benzanthracene; CCl_4, Carbon tetrachloride.

8. CLINICAL TRIALS INVOLVING HCC GENE THERAPIES

Although no gene therapies have yet been approved for the treatment of HCC, there are several therapies undergoing clinical trials which we highlight in **Table 4**. Upon screening the announced clinical trials on human HCC patients available at the website of National Institute of Health (NIH) as of May 2020, we found a total of 1,882 trials.[133] The vast majority of clinical trials involve chemotherapy, surgical procedures or a combination of them. There were only 47 instances of studies involving gene therapy, representing 2.5% of the total studies. This low ratio may be attributed to the challenges facing HCC gene delivery as alluded to above. However, scientists are now breaking the ice and taking steps forward. Among these trials, genetically-modified T-cells as CAR T-cells or TCR-cells recognizing characteristic HCC antigens like GPC3, AFP, DR5 or EGFR VIII were the most recruited (~68%). T-cells with multiple targets were also introduced by Shenzhen BinDeBio Ltd., which developed T-cells that simultaneously recognize 10 targets of different human tumors, namely; CD19 and CD22 for B cell leukemia and lymphoma, CD33 for myeloid leukemia, B-cell maturation antigen (BCMA) and CD38 for multiple myeloma, Cancer/testis antigen 1 (NY-ESO-1) for multiple myeloma, esophagus cancer, lung cancer, melanoma and synovial sarcoma, death receptor 5 (DR5) for HCC, C-met for HCC, colorectal cancer, ovarian cancer and renal carcinoma, EGFR VIII for HCC, lung cancer and glioma, and Mesothelin for gastric cancer, pancreatic cancer and mesothelioma. Despite great promise hold by T-cells therapies, they are limited by several pitfalls including the risk of immune side effects-called cytokine release syndrome- manifested by headache, nausea, vomiting, muscle pain and lowered blood pressure.[175]

Another interesting approach was the genetically-engineered oncolytic virus, OBP-301, developed by Oncolys BioPharma Inc which was modified with the human telomerase reverse transcriptase (hTERT) promotor to selectively replicate in cancer cells only and is currently undergoing Phase I trials.[133]

Genetic vaccines based on pDNA or mRNA encoding neoantigens have also appeared in some trials. Moreover, Geneos Therapeutics and the National Cancer Institute (NCI) are developing personalized genetic vaccines based on the elevated levels of neoantigens in each patient case.[133]

The recruitment of nucleic acid therapies in clinical trials for HCC treatment is still minimal (~21%) probably, due to challenges facing their efficient delivery. Arbutus Biopharma and Mina Alpha Ltd. are performing clinical trials involving siRNAs.[133] Aegera Therapeutics has developed chemically-modified ASO targeting X-linked inhibitor of apoptosis gene (XIAP) in the liver and it has entered phase I clinical trials.[133]

In most clinical trials, the use of viral delivery vectors was dominant with the recruitment of non-viral vectors, mainly LNPs, being limited. The global dependence on viral vectors can be understood in terms of their exclusive delivery efficiency. However, we believe that the future holds great promise for nanoparticulate delivery systems which are improving very fast with their superiority in terms of biosafety, cost-effectiveness and scalability.[176]

Table 4. HCC gene therapies undergoing clinical trials (as of May 2020).[133]

Name	Nature/ payload	Vector	Phase	Sponsor	NIH identifier
TKM 080301	siRNA against PLK1	LNPs	Phase I/II	Arbutus Biopharma	NCT02191878
MTL-CEBPA	siRNA against CEBPA	LNPs	Phase I	Mina Alpha Ltd.	NCT02716012
AEG35156	ASO targeting XIAP mRNA in the liver	Self (chemically -modified ASO)	Phase I	Aegera Therap., Chinese Univ. of Hong Kong	NCT00882869
NCI-4650	mRNA-based Personalized Cancer Vaccine	undisclosed	Phase I/II	National Cancer Institute (NCI)	NCT03480152
ADV-TK	HSV Thymidine kinase gene	Adenovirus	Phase II	Beijing Chao Yang Hosp., Tongji Univ.	NCT00300521
ADV-TK			Phase III	Huazhong University of Science and Technology	NCT03313596
TK99UN			Phase I	Clinica Universidad de Navarra	NCT00844623

Name	Nature/ payload	Vector	Phase	Sponsor	NIH identifier
p53MVA vaccine	p53 gene	Modified Vaccinia Virus Ankara	Phase I	City of Hope Medical Center	NCT02432963
Ad5CMV-p53		Adenovirus	Phase I	National Cancer Institute (NCI)	NCT00003147
rAd-p53		Adenovirus	Phase II	Shenzhen SiBiono GeneTech Co.Ltd	NCT02509169
rhAd5	E1B gene deleted adenovirus	Adenovirus	Phase III	Sun Yat-sen Univ.	NCT01869088
INO-1400	pDNA vaccine encoding hTERT	Electroporat-ion	Phase I	Inovio Pharm.	NCT02960594
INO-9012	pDNA vaccine encoding IL-12				
CEA RNA-pulsed DC cancer vaccine	Autologous dendritic cells pulsed with CEA RNA	N/A	Phase I	Duke Univ.	NCT00004604
TEGAR T cells	Genetically-modified T-Cells Targeting GPC3 and expressing IL-21 and IL-15	N/A	Phase I	Baylor College of Medicine	NCT04093648

Name	Nature/ payload	Vector	Phase	Sponsor	NIH identifier
CD147-CART	CAR T-cells targeting CD147	N/A	Phase I	Xijing Hosp.	NCT03993743
CARTEPC	CAR T-Cells Targeting EpCAM	N/A	Phase I/II	First Affiliated Hosp.of Chengdu Med. College	NCT03013712
AFP^{c332}T	Genetically-modified T-cells targeting AFP	N/A	Phase I	Adapt-immune	NCT03132792
C-TCR055			Phase I	Cellular Biomed. Gr. Ltd.	NCT03971747
ET 140202 - T			Phase I	First Affiliated Hosp. Xi'an Jiaotong Univ.	NCT03965546
ET1402L1-CART			Phase I	Aeon Therap. Co. Ltd., Eureka Therap. Inc.	NCT03349255
ET1402L1-ARTEMIS™			Phase I	First Affiliated Hosp. Xi'an Jiaotong University	NCT03888859

Name	Nature/ payload	Vector	Phase	Sponsor	NIH identifier
Anti-NY ESO-1 mTCR PBL	Genetically-modified T-cells targeting ESO-1	N/A	Phase II	NCI	NCT01967823
CAR-GPC3 T	Genetically-modified T-cells targeting GPC3	N/A	N/A	Carsen Therap. Ltd	NCT03146234
GLYCAR T			Phase I	Baylor College of Medicine	NCT02905188
GPC3 CAR T			Phase I	Xinqiao Hosp. of Chongqing	NCT03084380
CAR-GPC3 T			Phase I	Carsgen Therap. Ltd.	NCT03884751
CAR-T cell immuno-therapy			Phase I	Nanjing Drum Tower Hosp.	NCT04121273
4G CAR-GPC3			Phase I	Carsgen Therap. Ltd.	NCT03980288
GPC3/CAR-T Cell			Phase I/II	Fuda Cancer Hosp.	NCT02723942
Anti-GPC3 CAR T			Phase I	RenJi Hosp.	NCT02395250
CAR-GPC3 T			N/A	Kang YU	NCT03302403

Name	Nature/ payload	Vector	Phase	Sponsor	NIH identifier
GPC3-T2	Genetically-modified T-Cells Targeting GPC3 and soluble TGFβ	N/A	Phase I	Second Affiliated Hosp. of Guangzhou Medical Univ.	NCT03198546
HBV/TCR T	Genetically-modified T-cells targeting HBV antigen	N/A	Phase I	Lion TCR Pte. Ltd, Agency for Sci. Tech. Res.	NCT02719782
LioCyx			Phase I/II		NCT03634683
TCR-Redirected T Cells			Phase I	Beijing 302 Hosp.	NCT03899415
VSV-hIFN-b	Recombinant Virus expressing IFN-β	Vesicular Stomatitis Virus (VSV)	Phase I	Mayo Clinic, NCI	NCT01628640
GNOS-PV02+INO-9012	personalized neoantigen DNA vaccine+ IL-12 pDNA	CELLECTRA®2000 EP Device	Phase I/II	Geneos Therap.	NCT04251117
anti-MUC1 CAR T	CAR T-cells targeting MUC 1	N/A	Phase I/II	PersonGen BioTherap. (Suzhou) Co., Ltd.	NCT02587689
anti-MUC1 CAR-pNK			Phase I/II		NCT02839954

Name	Nature/ payload	Vector	Phase	Sponsor	NIH identifier
c-Met/PD-L1 CAR-T	CAR T-cells targeting c-Met and PD-L1	N/A	Phase I	Second Hosp. of Nanjing Medical Univ.	NCT03672305
JX-594	recombinant vaccinia virus modified with GM-CSF	Vaccinia virus	Phase II	Jennerex Biotherap.	NCT01387555
Pexa-Vec			Phase II		NCT01171651
CAR-T/TCR-T cells immuno-therapy	Genetically-modified T-cells targeting DR5 and EGFR VIII	N/A	Phase I/II	Shenzhen BinDeBio Ltd.	NCT03941626 NCT03638206
DNA vaccine therapy	AFP pDNA+ sargramostim GM-CSF pDNA+ boosting AFP-adenovirus	Adenovirus	Phase I/II	Jonsson Compr. Cancer Center	NCT00093548
AFP + GM-CSF + AdVhAFP immunization			Phase I	Lisa H. Butterfield, NCI	NCT00669136
OBP-301	oncolytic adenovirus modified with hTERT promotor	Adenovirus	Phase I	Oncolys BioPharma Inc.	NCT02293850

PLK1, Polo-like kinase; CEBPA, CCAAT/enhancer-binding protein alpha; XIAP, X-linked inhibitor of apoptosis; HSV, Herpes Simplex virus; AFP, Alpha fetoprotein; N/A, Not applicable; CEA, Carcinoembryonic antigen; hTERT, Human telomerase reverse

transcriptase; IL, Interleukin; GPC3, Glypican-3; TGFβ, Tumor growth factor β; CAR, Chimeric antigen receptor; CD, Cluster of differentiation; EpCAM, Epithelial cell adhesion molecule; HBV, Hepatitis B virus; IFN-β, Interferon β; MUC 1, Mucin 1; c-Met, Hepatocyte growth factor; PD-L1, Programmed death-ligand 1; GM-CSF, Granulocyte-macrophage colony-stimulating factor; ESO-1, Cancer/testis antigen 1; DR, death receptor; EGFR, Epidermal growth factor receptor.

9. CONCLUSIONS

Gene therapy holds a promise to compensate for the demerits of current conventional anticancer strategies based on chemotherapy, radiotherapy or surgery. In the current review, we tried to provide a comprehensive overview on the concept of gene therapy for HCC highlighting diverse treatment modalities, gene targets, challenges associated with gene delivery to HCC, delivery strategies and the vectors designed to cope with the aforementioned challenges. The ideal delivery system should possess the following characteristics: controlled physico-chemical properties allowing immune system evasion, long life span in the blood circulation following sytemic administration, selective and high accumulation in the tumor site, sufficient penetration through the stroma barrier shielding HCC cells, efficient uptake into HCC cells with successful bypass from lysosomal degradation, sufficient release of the genetic cargo into the cytosol and the biosafety of the delivey vehicle upon acute or chronic administration. In addition, the proposed therapies and their delivery vectors should be evaluated in properly-selected animal models that reflect close evironment to human HCC. In response to the complexity of HCC, gene therapy can be combined with other strategies such as chemotherapy, immunotherapy or thermal therapy to fulfill integrated therapeutic approach. Gene therapy still represents only 2.5% of the ongoing clinical trials for the treatment of HCC and the vast

majority of clinical trials recruit viral vectors or gene-based immunotherapies. However, the continuous development in nucleic acid therapies and their non-viral nanovectors can change such situation in the near future.

10. FUTURE PERSPECTIVES

The approval of gene therapies for several diseases will trigger a rapid competition and continuous improvement to bring the current research to clinical applications. In addition, global competition between brand drug makers in this virgin field will stimulate more funding to enhance and develop ongoing research. The proper selection of gene targets and therapeutic modalities, the design of smart delivery systems that can deliver their payload efficiently and specifically to tumor site with minimal effects on healthy tissues, the biocompatibility and safety of the used systems as well as the development of representative animal models are key factors that will determine the clinical potential of any developed therapy.

From our point of view, we conclude that more focus on the development of delivery vectors based on nanoparticles would be desirable. Despite their lower efficiency compared to viral vectors, they are the most promising candidates that can be tailored to overcome the challenging barriers facing HCC delivery, the most biosafe and the most realistic for industrial scale-up. Tweaking the structures and characteristics of these nanoparticles can affect their fate and *in vivo* performance. Deep-study of the interaction of these carriers with the *in vivo* biological environment is needed to facilitate the control of their physico-chemical properties, pharmacokinetics and escape from the immune system, with consequent enhancement of their tumor

accumulation, the most critical drawback facing the clinical translation of non-viral gene delivery vectors.

The ongoing development in bioinspired materials simulating viral capsids can be considered a promising approach to learning from nature. The introduction of deep learning and artificial intelligence in the development of these biomaterials can save both time and costs, thus facilitating the rational design of experiments. Eventually, there remains much to accomplish before HCC gene therapies become a reality in the market, but we believe it will become a fact soon based on the current progress rate in the gene delivery research and associated funding.

Scope of work

SCOPE OF WORK

It has recently been concluded that cancer is not a simple single disease, but actually includes a group of diseases and abnormalities. Therefore, the concept of combinational therapy comes to the forefront, which involves the use of two or more different strategies such as chemotherapy, gene therapy and immunotherapy in order to maximize therapeutic benefits, overcome resistance mechanisms and reduce side effects.[177-178]

Sorafenib (SOR) is a multiple kinase inhibitor that has been approved by the FDA as the drug of choice for the treatment of resistant non-resectable HCC. It acts by dual mechanisms, either by blocking the production of Fms-like tyrosine kinase-3 and Raf signaling in tumor cells thus inducing anti-proliferative and apoptotic effects or by blocking the vascular endothelial growth factor (VEGF) and Platelet-derived growth factor (PDGF) in the surrounding endothelial cells to exert an anti-angiogenic effect.[179-180]

Meanwhile, Midkine (MK) is a heparin-binding cytokine that is overexpressed in HCC and other malignancies where it is associated with several functions including anti-apoptotic, mitogenic, angiogenic and chemoresistant functions.[47, 181]

In the current project, we propose that combining SOR and siRNA against the MK gene (MK-siRNA) would act synergistically on HCCs and improve the therapeutic outcome of SOR. To our knowledge, this is the first report on the use of such a combination. The outline of our strategy is schemed in **Fig. 5**.

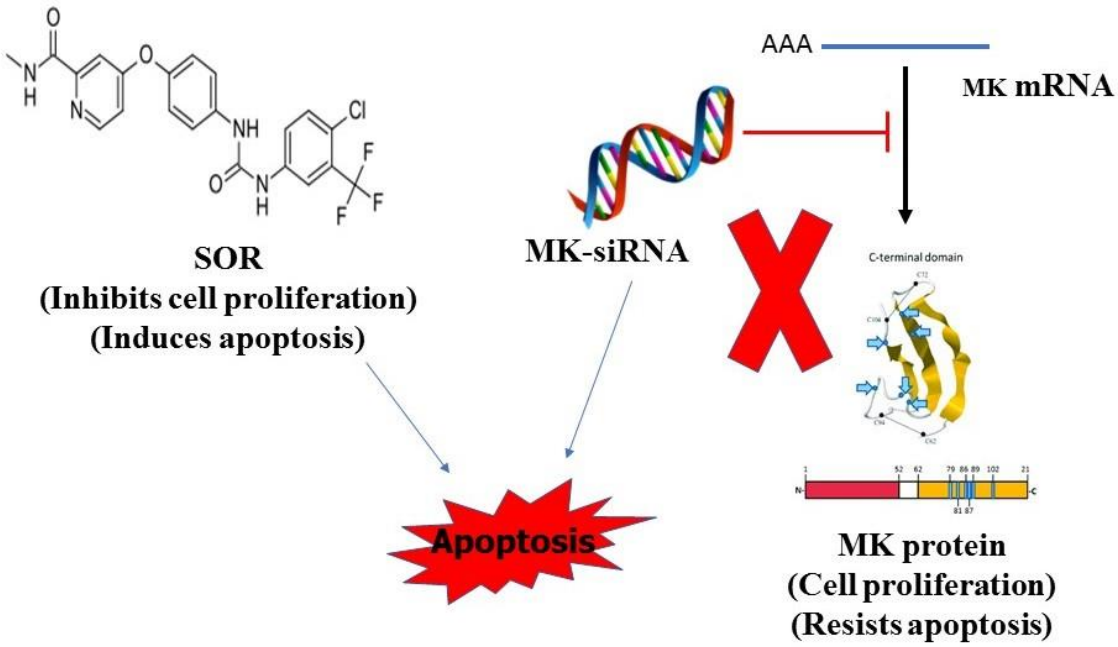

Figure 5. The outline of the novel combinational strategy proposed in this study.

We designed a co-delivery system encapsulating both SOR and MK-siRNA to ensure uniform delivery of both therapeutic agents to HCCs, avoid competition on cellular uptake that is likely to happen if multiple delivery systems encapsulating individual agents are used and to improve the patient compliance. We designed novel smart pH-sensitive lipid nanoparticles (LNPs) based on the pH-sensitive lipid, YSK05, designed in our laboratory[140] and were modified with the highly-selective HCC-targeting peptide, SP94,[116] to impart selectivity.

The current project was divided into three chapters, each represents a step in the research and development to reach our ultimate goal:

Chapter 1: Design and *In Vitro* Evaluation of Multifunctional Lipid Nanoparticles for Highly-Selective Co-delivery of Sorafenib and Midkine-siRNA to Hepatic cancer cells

In this chapter, we attempted to test our hypothesis *in vitro* to obtain a sufficient proof-of-concept (POC) before going deeply to the *in vivo* level. We investigated the impact of different formulation variables on the performance of the proposed delivery system. We compared the performance of the system upon decoration with a commonly-used cell-penetrating peptide (CPP), STR-R8, versus the novel SP94 peptide. We evaluated the system for its efficacy and selectivity using cytotoxicity studies, quantitative real time polymerase chain reaction (qRT-PCR), fluorescence-activated cell sorting (FACS) and confocal laser scanning microscopy (CLSM) in different cancerous and normal cell lines. We tested the hypothesis of the proposed synergism between SOR and MK-siRNA and tried to suggest a potential mechanism. In addition, we evaluated the serum-compatibility and the shelf stability of this system.

Chapter 2: Design and Optimization of Ultra-Small Lipid Nanoparticles for Synergistic Highly-Efficient Eradication of Hepatocellular Carcinoma *In Vivo*

At this stage of work, we extended the application of our strategy to the *in vivo* level using a model of human HCC established in mice. Systemic intravenous administration was adopted to allow real investigation of the delivery performance and simulate the real situation of human cancer therapy. We faced the challenges associated with the *in*

vivo delivery to HCC and established a step-by-step optimization strategy to overcome them. The composition, preparation method, pharmacokinetics and physico-chemical properties were tweaked and their impact on the fate of the delivery system was investigated. Upon reaching the optimum formulation conditions, the therapeutic potential of our combinational strategy was studied on HCC-bearing mice versus SOR or MK-siRNA monotherapies. We recruited a very low dose of SOR (2.5 mg/Kg) aiming at achieving potency and eliminating side effects. Moreover, the biosafety of the delivery system and the treatment was evaluated on both acute and chronic regimens.

Chapter 3: Ultra-Small Lipid Nanoparticles Loaded with Sorafenib and Midkine-siRNA Reverse Resistance to Sorafenib and Eradicate Sorafenib-Resistant Hepatocellular Carcinoma *In Vitro* and *In Vivo*

At this step, we raised the challenge and combated SOR-resistant HCC using our treatment. After establishment of SOR-resistant HCC cell line, the correlation between MK gene expression and the acquired resistance to SOR was elucidated. Then, the impact of using MK-siRNA together with SOR on such resistance was tested. Eventually, the resistant cells were used to establish SOR-resistant HCC in mice and the combinational treatment versus monotherapies were evaluated.

Comprehensively, the data provided in this study indicate that our novel system involving a novel combination of chemotherapy and gene therapy holds promise for potential clinical application in HCC treatment which is nationally demanded in my home country, Egypt. We hope that this project contributes to the development of the health sector in Egypt, which is the main purpose of this studentship jointly supported by the Egyptian and Japanese governments. We wish also that our work contributes to the global knowledge in the fields of drug delivery, gene therapy and cancer treatment.

CHAPTER 1

Design and In Vitro Evaluation of Multifunctional Lipid Nanoparticles for Highly-Selective Co-delivery of Sorafenib and Midkine-siRNA to Hepatic cancer cells

CHAPTER 1

1.1. INTRODUCTION

Delivering genetic materials to their target cells is not an easy task due to the immunogenic and metabolically-labile nature of these materials as well as the presence of several extracellular and intracellular barriers. Several viral and non-viral vectors have been utilized for the delivery of genetic materials with the focus of interest being directed towards non-viral vectors, due to their biosafety and economic feasibility. Non-viral vectors include several forms such as polymeric nanoparticles, lipid nanoparticles and hybrid polymeric-lipid nanoparticles.[136, 182-183] Lipid nanoparticles (LNPs) are among the most widespread delivery vehicles and during last year, the FDA approved the first gene-silencing therapy in the form of LNPs delivered to the liver, Patisiran®, which may trigger the development of additional types of gene therapies and LNPs in the near future. Currently, the use of smart pH-sensitive lipids outweigh those with permanent cationic charge. These smart lipids have pKa values around 6, so they are neutral at physiological pH, but upon internalization by cells, they become positively charged and fuse with the endosomal membrane allowing the release of their payload into the cytosol. Being neutral at physiological pH, these lipids show reduced non-specific interactions with other biological membranes and sensitization of the reticulo-endothelial immune system.[184-185] YSK05, a pH-sensitive lipid that was synthesized in our laboratory, has a pKa value of approximately 6.5, and has shown powerful endosomal escape properties with consequent efficient gene delivery both *in vitro* and *in vivo*. It has been used for the efficient delivery of genes to both the liver and lung.[140, 186]

Successful gene therapy requires the development of systems that protect the genetic material in the circulation and permit intracellular trafficking to be controlled, in order to achieve an improved transfection. We have been in the process of developing various LNPs encapsulating various nucleic acids as efficient nanodevices for gene therapy. The genetic material is first condensed with a polycation such as polyethyleneimine (PEI) or protamine to form a nucleic acid core material, which is then further incorporated into the LNPs. The formation of cores with a polycation helped in neutralizing some of the siRNA charge which reduced the amount of cationic lipids needed to coat it with a subsequent reduction in the toxicity of the nanocarrier.[187] Furthermore, the formation of a nucleic acid condensed core holds several additional advantages including high encapsulation efficiency, protection from nucleases, the controlled intracellular release of nucleic acid as well as the protection of the nucleic acid from degradation during the sonication step used in the preparation of LNPs by the thin lipid film hydration method.[188] The surface of LNPs can be further modified with additional functional devices to improve their cellular uptake and/or endosomal escape capability. Among these devices, the cell penetrating peptide, Octaarginine (R8), showed a high ability to improve both cellular uptake and endosomal escape with the consequent enhancement in transfection efficiency.[189]

In addition to the challenge associated with the delivery of genetic materials, the second accompanying challenge is to deliver them specifically to their target organ or cells, especially, when cytotoxic or genome-editing tools are being used, otherwise, serious off-target effects would arise.[92] Most of the commonly-used targeting ligands target overexpressed receptors in cancer cells such as galactose,[71] folate[101] and

transferrin receptors.[97] It should be noted, however, that these receptors are also expressed to a certain degree in normal cells which subtracts from the selectivity process. Alternatively, attention has been directed to discovering new exclusive targeting ligands using phage display[114] or Systemic Evolution of Ligands by EXponential Enrichment (SELEX) methods.[190] These ligands can bind only to the cancer cells exploiting unique receptors and therefore permit absolute targeting to be achieved. SP94 is a novel 12-amino acid peptide discovered by Albert Lo *et al*. using a phage displayed peptide library. It specifically binds to an unknown cell membrane molecule that is expressed by HCCs but not normal hepatocytes, making it an exclusive targeting ligand for HCC, and showed a high selectivity both *in vitro* and *in vivo*.[116] Li *et al*. utilized the SP94 peptide for the specific *in vivo* imaging and radiotherapy of HCC.[191]

In this chapter, the design, optimization and *in vitro* evaluation of SP94-modified LNPs co-encapsulating SOR and MK-siRNA were studied. The outcome of SOR and MK-siRNA combinational therapy was investigated and the mechanism by which they interact with each other as well as the mode of our delivery system performance were suggested.

1.2. EXPERIMENTAL

1.2.1. Materials

SOR was obtained from AstaTech Inc., USA. MK-siRNA and control siRNA (siGL4) were synthesized by Hokkaido System Science, Japan and their sequences are listed in **Table 5**. Oligonucleotide primers used in qRT-PCR were supplied by Sigma genosys (Japan) and their sequences are listed in **Table 6**. Cysteine-terminated SP94 peptide was synthesized by SMC Co., Japan with the following aminoacid sequence: SFSIIHTPILPL-Cys. YSK05 lipid was synthesized in our laboratory. N-[1- (2,3- dioleoyloxy) propyl] - N, N, N- trimethylammonium chloride (DOTAP), 1,2-dioleoyl-sn-glycero-3-phosphoethanolamine (DOPE), 1,2-dioleoyl-sn-glycero-3-phosphocholine (DOPC) and 1,2-distearoyl-sn-glycero-3-phosphocholine (DSPC) were obtained from Avanti Polar Lipids, USA. 1-Palmitoyl-2-oleoyl-sn-glycero-3-phosphoethanolamine (POPE), egg L-α-phosphatidylcholine (EPC) and 1,2-distearoyl-sn-glycero-3-phosphoethanolamine-N-[maleimide (polyethylene glycol)-2000] (DSPE-PEG_{2k}-MA) were obtained from the NOF corporation, Japan. Cholesterol, Triton X100, the Tri reagent and sinapic acid were obtained from Sigma-Aldrich, USA. Polyethylenimine (PEI)-branched type (average molecular weight = 10 KDa), Acetonitrile, Ethanol, Dextran Sulphate, Chloroform and Isopropanol were obtained from Wako, Japan. Stearylated octaarginine peptide (STR-R8) was synthesized by Kurabo, Japan. Trifluoroacetic acid (TFA) was obtained from Tokyo Chemical Industry Co. (TCI, Japan). HEPES buffer powder was obtained from Dojindo, Japan. Phosphate Buffer Saline (PBS) buffer tablets were obtained from Takara, Japan. Ribogreen was obtained from Invitrogen, USA. 3-(4,5-Dimethylthiazol-2-yl)-2,5-Diphenyltetrazolium Bromide (MTT) cell proliferation assay kit was obtained from Abcam, UK. ReverTra Ace qPCR RT Master Mix kit with gDNA Remover and

Thunderbird SYBR qPCR Mix were obtained from TOYOBO, Japan. Cell culture plates; 2.5 × 150 mm, 6-well plates and 24-well plates were obtained from Corning, USA. 35-mm glass-base dishes were obtained from Iwaki Co., Japan. Nuclease-free water, 1,1'-Dioctadecyl-3,3,3',3'-Tetramethylindodicarbocyanine 4-Chlorobenzenesulfonate Salt (DiD) and 2'-(4-ethoxyphenyl)-5-(4-methylpiperazin-1-yl)-2,5'-bibenzimidazole (Hoechst 33342) were obtained from Thermo Fisher Scientific, USA. Dialysis membranes with cut-off molecular weight of 3.5 KDa (Spectra/Por 6) were obtained from Spectrum Labs, USA.

Table 5. Sequences of siRNAs used in this study.

		sequence (5'→3')
MK-siRNA	Sense	GGA UUG CGG CGU GGG UUU Ctt
	Anti-sense	GAA ACC CAC GCC GCA AUC Ctt
Control siRNA (siGL4)	Sense	GCG CUG CUG GUG CCA ACC CdTdT
	Anti-sense	GGG UUG GCA CCA GCA GCG CdTdT

Table 6. Sequences of primers used in qRT-PCR in the *in vitro* study.

Gene		sequence (5'→3')
Human MK	Forward	AGA TGC AGC ACC GAG GCT
	Reverse	CTT TCT TTT TGG CGA CCG
Human GAPDH	Forward	CCT CTG ACT TCA ACA GCG AC
	Reverse	CGT TGT CAT ACC AGG AAA TGA G
Mouse MK	Forward	GTC AAT CAC GCC TGT CCT CT
	Reverse	CAA GTA TCA GGG TGG GGA GA
Mouse GAPDH	Forward	AGC AAG GAC ACT GAG CAA G
	Reverse	TAG GCC CCT CCT GTT ATT ATG

1.2.2. Cell lines

The human HCC cell line, HepG2, the human cervical adenocarcinoma cell line, HeLa, the mouse hepatocellular carcinoma cell line, Hepa 1-6, and the mouse normal hepatocytes cell line, FL83B, were obtained from the American Type Culture Collection (ATCC, USA). Each cell line was cultured and maintained according to manufacturer's guidelines. HepG2 and Hepa 1-6 cells were cultured in Dulbecco's Modified Eagle Medium (DMEM) containing high proportion of glucose

(4.5 g/L) (Nacalai tesque, Japan) while HeLa cells were cultured in DMEM containing low proportion of glucose (1 g/L) (Sigma Aldrich, USA). FL83B cells were cultured in F-12K medium (ATCC, USA). All media were supplemented with 10% v/v heat-inactivated fetal bovine serum (FBS) (Biosera, USA) and antibiotic solution (Thermo Fisher Scientific, USA) containing 100 unit/mL penicillin and 100 µg/mL streptomycin to prevent microbial contamination. All cells were kept in an incubator (Thermo Electron Corporation, USA) at 37 °C, 5% CO2 and 95% humidity.

1.2.3. Methods

1.2.3.1. Synthesis of SP94-modified DSPE-PEG

Cysteine-terminated SP94 peptide was simply conjugated to DSPE-PEG_{2k}-MA via Micheal reaction schemed in **Fig. 6**. Individual ethanolic or aqueous solution of each reactant was prepared in concentration of 2 mM, then equal volumes of the two solutions were mixed and incubated under shaking at 900 rpm, 30 °C for 24 hours to obtain the conjugate with a final concentration of 1 mM. Matrix-assisted Laser Desorption Ionization-Time of Flight Mass Spectrometry (MALDI-TOF-MS) was used to confirm the completion of reaction and the molecular weight of the conjugate.

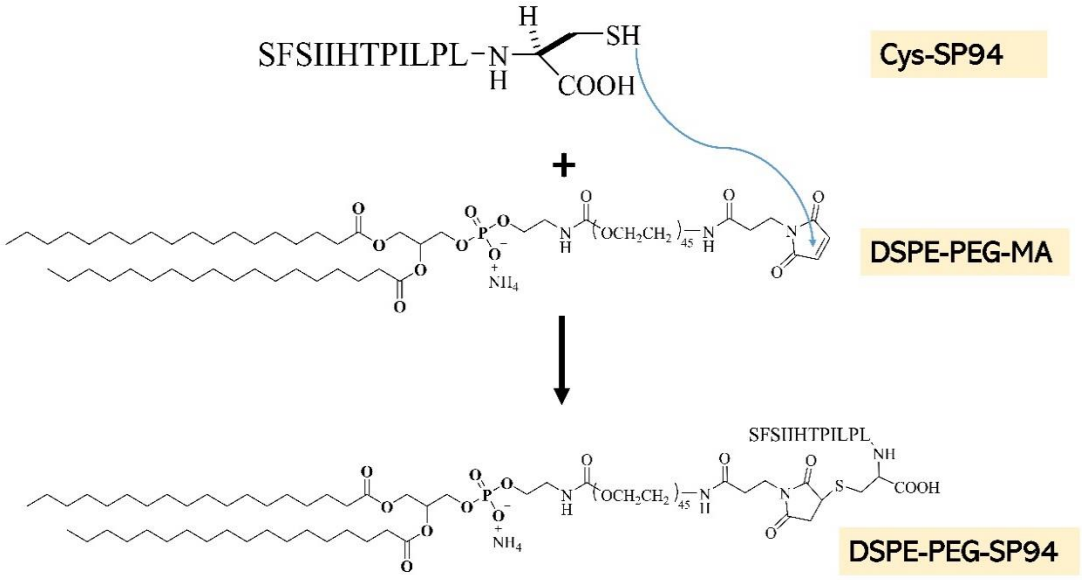

Figure 6. Schematic representation for the synthesis of SP94-modified DSPE-PEG.

1.2.3.2. MALDI-TOF-MS analysis

MALDI-TOF-MS was used after conjugation reaction to confirm molecular weight of reactants and product. Aqueous solution of acetonitrile (30%) containing 0.1% trifluoracetic acid (TFA) and 1% sinapic acid was used as a matrix solution. Molecular weight of each sample was determined using MALDI-TOF Ultraflex II equipment (Bruker Daltonics, USA).

1.2.3.3. Preparation of LNPs

LNPs were prepared by the thin lipid film hydration method. siRNA (3 nmole) and PEI were individually dissolved in HEPES buffer (10 mM, pH 4) and a complex was formed by the gradual addition of PEI solution to the siRNA solution at a nitrogen to phosphate (N/P) ratio equal to 0.5 with vortexing to form a negatively-charged core. After a 30 minute incubation at room temperature, the core solution was used to hydrate the lipid film formed by evaporation of an ethanolic solution of

lipids under a vacuum. SOR was incorporated into the LNPs by the addition of the desired amount of its ethanolic solution to the lipid solutions before evaporation. After a further incubation for 30 minutes at room temperature, the hydrated films were sonicated for 1 minute to form LNPs which were further incubated at room temperature for 30 minutes to allow them to stabilize. The solution of the LNPs was filtered by ultrafiltration–centrifugation (2000 g, for 30 minutes, at room temperature) in a Versatile refrigerated centrifuge (AX-310) (TOMY) using filter tubes with a cut-off molecular weight of 15 KDa (Merck Millipore) to remove unentrapped SOR. The retained LNPs were then re-suspended in HEPES buffer (10 mM, pH 7.4) to neutralize the cationic charge of the pH-sensitive lipid, YSK05. Upon using other pH-independent lipids, all preparations were processed in HEPES buffer (10 mM, pH 7.4). Blank LNPs were prepared in a similar manner without siRNA or SOR and were considered as a negative control. The chemical structures of different lipids used in the optimized formulation are shown in **Fig. 7.**

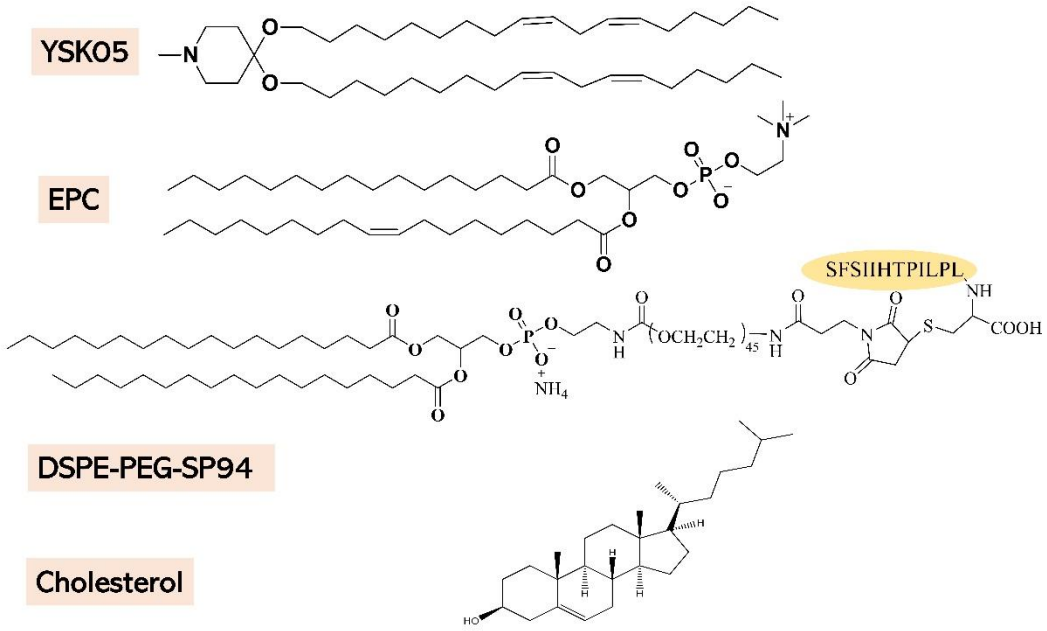

Figure 7. Chemical structures of lipids used in the *in vitro* optimized LNPs (SP94-NPs).

1.2.3.4. Decoration of LNPs with SP94-modified DSPE-PEG

SP94-modified DSPE-PEG was inserted into the LNPs either by a pre-insertion or a post-insertion method. In the pre-insertion method, an ethanolic solution of SP94-modified DSPE-PEG was directly added in the desired amount to an ethanolic solution of the other lipids before the evaporation and formation of the thin lipid film. In the post-insertion method, the desired amount of an aqueous solution of SP94-modified DSPE-PEG was added to the aqueous solution of the LNPs after their formation and the LNPs then were incubated at room temperature or 60 °C for 30 minutes to allow the nanoparticles to stabilize.

1.2.3.5. Characterization of LNPs

The average particle diameter (nm), polydispersity index (PDI) and zeta potential (mV) of the prepared LNPs were determined by a Zetasizer Nano ZS (Malvern Instruments Ltd, UK). SOR encapsulation efficiency (EE) was measured by mixing 30 µL sample of the final LNPs solution

with an appropriate volume of ethanol under vigorous vortexing and SOR content was determined spectrophotometrically (Life Science UV/Vis Spectrophotometer DU730, BECKMAN COULTER, USA) at 266 nm against a blank of empty LNPs treated similarly. A pre-set calibration curve was used to calculate the entrapped SOR amount. SOR EE was calculated by the following equation:

$$\text{SOR EE (\%)} = \frac{\text{Entrapped SOR amount (µg)}}{\text{Total SOR used (µg)}} \times 100 \qquad \textbf{(Equation 1)}$$

siRNA EE was determined by Ribogreen fluorimetric assay method as reported previously.[192]

1.2.3.6. Examination of the morphology of SP94-NPs

A Transmission Electron Microscope (TEM) (Hitachi HD2000, Japan) was used to visualize the morphology of the optimized SP94-NPs as reported previously.[193]

1.2.3.7. Assessment of cytotoxicity

The investigated cells were seeded on 24-well plates at density of 5×10^4 cells/well 24 hours before each experiment. At the time of the experiment, the cells were treated with the prepared LNPs at the desired concentrations in 0.25 mL serum-free medium and incubated at 37 °C for 4 hours. Then, 1 mL of fresh medium containing 10% FBS was added to each well and the cells were incubated for an additional 20 hours. To assess cell viability, MTT assay was performed according to the manufacturer's guidelines. Briefly, the medium was removed and the cells were washed with sterile PBS. 50 µL of MTT reagent and an equal volume of serum-free medium were added to each well and the cells were incubated for 3 hours at 37 °C . Then, 150 µL of MTT solvent was added to each well to dissolve the formazan that had been formed and the plate was shaken on an arbitrary shaker for 15 minutes. The absorbance of the

solution in each well was measured spectrophotometrically using a multiplate reader (Enspire 2300 Multilabel Reader, Perkin Elmer, USA) at 590 nm and compared to the absorbance of non-treated control cells. The negative control serum-free medium that did not contain cells was treated in a similar manner to correct for background absorbance. Cell viability was calculated using the following equation (**Equation 2**):

$$\text{Cell viability}(\%) = \frac{\text{Corrected absorbance of treated cells}}{\text{Corrected absorbance of non-treated cells}} \times 100$$

1.2.3.8. In vitro transfection of cells

Cells were seeded on 6-well plates at a density of 2×10^5 cells/well 24 hours before each experiment. Samples containing the desired concentration of the investigated siRNA-loaded LNPs in 1 mL serum-free medium were added to each well and the cells then were incubated for 4 hours at 37 °C. Fresh medium (4 mL) containing 10% FBS was added to each well and the cells were then incubated for a further 20 hours. The cells were then washed with PBS and lysed using 500 µL of Tri reagent and saved at -80 ºC until the measurements were made.

1.2.3.9. Measurement of gene expression

The Tri reagent containing cell lysate was mixed with chloroform and centrifuged for separation of the total RNA from the DNA and protein. The upper RNA layer was separated and the RNA pellet was precipitated with isopropanol and washed twice with 75% cold ethanol. The final RNA pellet was then dissolved in a suitable volume of nuclease-free water and quantified by UV spectrophotometry (NanoDrop Lite, Thermo Fisher Scientific, USA). 500 ng of total RNA were reverse-transcribed into complementary DNA (cDNA) using ReverTra Ace qPCR RT Master Mix kit with gDNA Remover (TOYOBO, Japan) according to

the manufacturer's protocol. qRT-PCR analysis was performed on the obtained cDNA using Thunderbird SYBR qPCR Mix (TOYOBO, Japan) and the specific primers listed in Supporting Information file. qRT-PCR was conducted on a 96 well plate using a Light Cycler 480 (Roche Diagnostics, Basel, Switzerland) under the conditions reported previously [194]. The relative MK mRNA amount was calculated by ddCt method and normalized to Glyceraldehyde 3-phosphate dehydrogenase (GAPDH) mRNA as a house-keeping gene, as reported previously.[194]

1.2.3.10. Cellular uptake study by Fluorescence-Activated Cell Sorting (FACS) analysis

The cellular uptake of the prepared LNPs was evaluated in different cell lines. The investigated cells were seeded on 6-well plates at a density of 2×10^5 cells/well 24 hours before each experiment. LNPs were labeled with the lipophilic fluorescent probe, DiD, (0.1 mol%). Samples containing the tested LNPs were mixed with serum-free cell culture medium to give a final concentration equivalent to 10 µM SOR in a total volume 1 mL, and the cells were incubated for 4 hours at 37 °C. The medium was removed and cells were washed with PBS and detached by treatment with 0.05% trypsin. The cell suspension was then centrifuged at 500 g, 4°C for 10 minutes and the cell pellet was suspended in 1 mL FACS buffer containing 0.5% bovine serum albumin and 0.1% sodium azide). After two cycles of centrifugation and washing the cell pellet with FACS buffer, the cell pellet was thoroughly-suspended in 750 µL FACS buffer, and then passed through a nylon mesh to remove any cell aggregates. The mean fluorescence intensity (MFI) of the cells was determined by FACSCalibur™ flow cytometry (BD Biosciences, USA), normalized to the MFI of the non-treated cells and

was used to compare the cellular uptake of different LNPs by the different cell lines.

1.2.3.11. Competitive inhibition of the uptake of SP94-NPs

HepG2 and Hepa 1-6 cells, which showed the maximum uptake for SP94-NPs, were selected for this experiment, while FL83B cells, which showed negligible uptake of these LNPs, were excluded as they were likely lacking specific receptors for SP94 peptide. The cells were incubated with increasing concentrations of free SP94 peptide in serum-free medium at 37 °C for 1 hour before the experiment to saturate its specific receptors. Then, the medium was replaced with fresh serum-free medium and the cells were co-incubated with fixed concentration of SP94-NPs (equivalent to 10 μM SOR dose) and increasing concentrations of free SP94 for additional 4 hours. The cells were harvested and the cellular uptake was measured by FACS as described above. Mean fluorescence intensity (MFI) of each sample was normalized to MFI of cells that received SP94-NPs without incubation with free SP94 peptide, which was considered as 100% cellular uptake.

1.2.3.12. Confocal Laser Scanning Microscopy (CLSM)

Cells were seeded at a density of 3×10^4 cells/well on a 35-mm glass-base dish 24 hours before the experiment. LNPs were labeled with DiD (0.1 mol%). The cells were treated with LNPs in concentration equivalent to 10 μM SOR in 1 mL serum-free medium and incubated for 4 hours at 37 °C. The medium was then replaced with serum-containing medium and nuclei were stained with Hoechst 33342 (5 μg/mL) 30 minutes before being examined. The medium was replaced again with fresh serum-containing medium and the cells were examined and imaged using CLSM (Olympus, Japan).

1.2.3.13. In vitro drug release

In vitro drug release profile from LNPs was determined at two different pH values; 7.4, which represented the physiologic pH, and 5.5, representing endosomal pH. To ensure sink condition, amount of LNPs equivalent to SOR dose 17.43 µg was diluted to total volume 500 µL with HEPES buffer (pH 7.4), introduced into pre-hydrated dialysis membrane (cut-off molecular weight = 3.5 KDa) and dialyzed against 2 L of HEPES buffer (pH 7.4 or 5.5) over a magnetic stirrer (300 rpm, 37 °C) for 48 hours. At different time intervals, samples of 10 µL of LNPs were diluted with ethanol and assayed spectrophotometrically for the remaining SOR content. The amount of SOR released was determined by subtracting the remaining SOR content in LNPs from the initial SOR content at zero time and expressed as percentage of SOR dose released against time.

1.2.3.14. Kinetic analysis of drug release from LNPs

The mechanism of drug release from LNPs was determined by linear regression analysis according to zero-order, first-order and Higuchi-diffusion models which are the most common models for controlled-release delivery systems. The correlation coefficient (r) value was calculated for each model. The highest value of the calculated correlation coefficients assigned the kinetic model of the drug release. The drug release data were fitted to the following equations:[195]

Zero-order model: $M_t / M_\infty = K_0 t$. (**Equation 3**)

First-order model: $M_t / M_\infty = e^{-K1t}$ (**Equation 4**)

Higuchi-diffusion model : $M_t / M_\infty = k_H t^{½}$. (**Equation 5**)

Where (M_t / M_∞) is the fractional release of the drug at time t, k_0 = Zero-order rate constant, k_1 = First-order rate constant, k_H = Higuchi rate constant and t = time of release.

Then, the release data were analyzed using the equation proposed by Ritger and Peppas:[195]

$$M_t / M_\infty = Kt^n \qquad \textbf{(Equation 6)}$$

Where M_t / M_∞ is the fractional release of the drug at time t, K is the release rate constant and n is the diffusional exponent that characterizes the type of release mechanism during the dissolution process. In case of LNPs (spherical sample) , n= 0.43 for Fickian diffusion; while in case of non-Fickian release, the value of (n) falls between 0.43 and 0.85; for zero order release (case II transport), n= 0.85 and for supercase II transport, n > 0.85.

1.2.3.15. Long-term stability testing of LNPs

The optimum LNPs were stored in refrigerator (4 °C) for two months. Average particle size was measured weekly to investigate nanoparticles liability for aggregation upon long-term storage.

1.2.3.16. Statistical analysis

Statistical analyses were performed using the GraphPad Prism 8 software. Comparisons between the means of different groups were made using the one-way analysis of variance (ANOVA) followed by the Bonferroni test. When applicable, two-way ANOVA was used for analysis of experiments involving two factors or for verifying the interactive effect between SOR and MK-siRNA. Pair-wise comparisons between means were made using a two-tail Student t-test. P-value <0.05 was considered to be significant.

1.3. RESULTS

1.3.1. Characterization of LNPs

Table 7 shows the results for the physico-chemical characterization of the prepared LNPs. The average particle diameter of MK-siRNA-PEI core ranged from 48-64 nm with the average zeta potential ranging between -4.95 and -12 mV. LNPs containing STR-R8 (STR-R8-NPs) showed an average particle diameter of 168.8-191.2 nm with a highly-positive zeta potential (42.5-55.5 mV), while the SP94-modified LNPs (SP94-NPs) showed a lower particle diameter (140.6-159.4 nm) with a negative zeta potential between -6.75 and -14.25 mV. PEGylation resulted in a lower particle size and improved particle size distribution, as indicated from the polydispersity index (PDI) values for the SP94-NPs that contain DSPE-PEG-SP94 in comparison with non-PEGylated LNPs (STR-R8-NPs). The SOR encapsulation efficiency (EE) ranged from 80-100% in the case of a low drug loading (5 mol%) while this value decreased to around 50% upon increasing the drug loading to 10 mol% (**Table 8**). MK-siRNA recovery ranged from 70-85% with an encapsulation efficiency 70-90%. According to the previous physico-chemical properties, the prepared LNPs were acceptable for use in further studies.

Table 7. Results of the physico-chemical characterization of the prepared LNPs for the *in vitro* study (average ± standard deviation, n=6).

	Average diameter (nm)	PDI	Zeta potential (mV)	SOR EE (%)	siRNA EE (%)
siRNA/PEI core	56±8	0.270±0.045	-8.5±3.5	-	-
STR-R8-NPs	180±11.2	0.332±0.061	49±6.5	90±8.25	75±6.4
SP94-NPs	150±9.4	0.205±0.035	-10.5±3.7	91.5±9.8	80.5±8.5

Table 8. Effect of drug loading relative to total amount of lipids on SOR encapsulation efficiency in the prepared LNPs for the *in vitro* study (average ± standard deviation, n=6, total lipid amount=1500 nmole).

SOR amount (nmole)	SOR loading (mol%)	SOR EE (%)
75	5	91.5±9.8
112.5	7.5	70.4±5.5
150	10	50±7.2

1.3.2. Assessment of cytotoxicity of SOR-loaded LNPs

Based on our modified protocol for assessing cytotoxicity, the free SOR showed a concentration-dependent cytotoxicity to human HCCs, HepG2, with a half maximal inhibitory concentration (IC_{50}) equal to 14±2.8 μM (**Fig. 8A**). In the next experiments, we compared the cytotoxic effect of different LNPs encapsulating SOR at a low SOR concentration (10 μM) aiming to achieve maximum efficiency at a lower drug dose. **Table 9** shows the composition of the investigated SOR-

loaded LNPs and their corresponding IC_{50} values measured in HepG2 cells. LNPs based on different main lipids; namely the pH-sensitive lipid, YSK05, the pH-independent cationic lipid, DOTAP, and a combination of YSK05 and DOTAP were tested, but none showed a significant efficiency over the free drug (**Fig. 8B**). Introduction of the cell-penetrating peptide (CPP) STR-R8 (10 mol%) was attempted in order to improve the cellular uptake and endosomal escape of the LNPs. Modification with STR-R8 resulted in a significant improvement in efficiency, with the highest efficiency shown by LNPs based on YSK05/STR-R8 which reduced the cell viability to about 47.40±2.65% compared to 65.66±1.51% in the case of the same concentration of free SOR (**Fig. 8C**).

1.3.3. Effect of MK-siRNA-loaded LNPs on MK gene expression and HepG2 cell viability

The LNPs investigated in the above section were loaded with MK-siRNA alone (no SOR) and their capabilities for knocking down the MK gene in HepG2 cells were compared. At a fixed MK-siRNA concentration (100 nM), the LNPs based on YSK05/STR-R8 showed the strongest knockdown activity among all of the LNPs that were investigated (about 87% knockdown) (**Fig. 9**). Upon transfection of HepG2 cells with the latest LNPs in amounts equivalent to different concentrations of MK-siRNA, the qRT-PCR data showed a concentration-dependent MK gene silencing with a half maximal effective concentration (EC_{50}) of 44±6.5 nM, while this silencing was not obtained using control siRNA (siCntrl) in place of MK-siRNA (**Fig. 8D**). Based on the results of cytotoxicity and knockdown studies, the YSK05/STR-R8 LNPs were used in subsequent experiments. Upon testing the effect of these LNPs on HepG2 cell viability at high siRNA

concentrations that achieved maximum gene silencing, we failed to achieve a high level of cytotoxicity to the cells (**Fig. 8E**), indicating that silencing the MK gene alone is not an efficient strategy for inducing cytotoxicity. This prompted us to hypothesize that using a combination of SOR and MK-siRNA might be necessary to achieve a higher efficiency.

1.3.4. Investigation of the potential value of a combination of SOR and MK-siRNA

Based on the previous results, we combined SOR and MK-siRNA into the same LNP. To investigate the potential value of this combination, LNPs containing SOR alone, MK-siRNA alone, control siRNA (siCntrl), SOR/MK-siRNA and SOR/siCntrl were tested on HepG2 cells. Interestingly, LNPs containing the SOR/MK-siRNA combination showed the highest efficiency among all of the LNPs that were investigated, as indicated from the results of cytotoxicity assessment (**Fig. 8F**). LNPs containing the SOR/MK-siRNA combination reduced HepG2 cell viability to 34.98±3.82% compared to LNPs containing SOR alone or MK-siRNA alone (50.47±4.13 and 54.68±5, respectively) while combining SOR with control siRNA showed a cell viability of 50.19±6.1%. These results suggested that SOR and MK-siRNA may function synergistically, thus confirming our hypothesis, and encouraged us to explore this combination further.

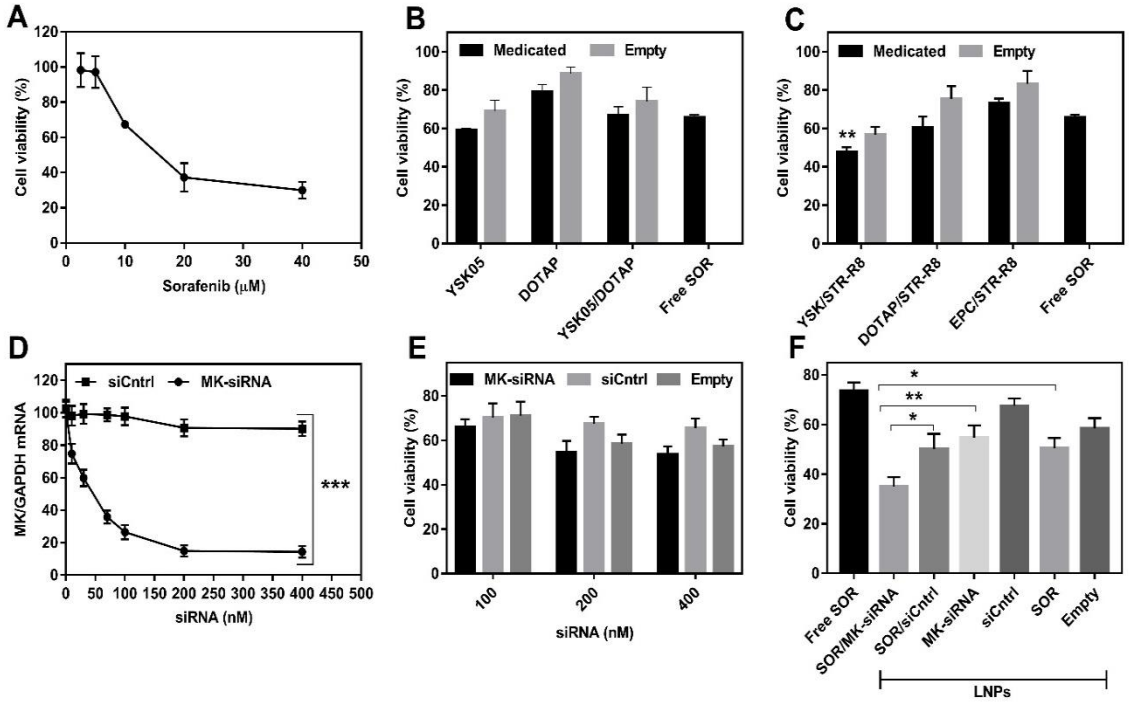

Figure 8. Effect of free SOR and different LNPs loaded with SOR and/or MK-siRNA on HepG2 cells. A) Effect of different concentrations of free SOR. B) Effect of SOR-loaded LNPs based on different main lipids (SOR concentration= 10 μM). C) Effect of LNPs containing 10 mol% STR-R8 (SOR concentration= 10 μM) (**P<0.001 versus other LNPs and free SOR). D) Effect of different concentrations of MK-siRNA encapsulated in YSK05/STR-R8 LNPs on MK gene expression (***P<0.0001). E) Effect of different concentrations of MK-siRNA encapsulated in YSK05/STR-R8 LNPs on cell viability. F) Investigation of the potential value of SOR and MK-siRNA combination using YSK05/STR-R8 LNPs (SOR concentration= 10 μM, MK-siRNA concentration= 400 nM) (*P<0.05, **P<0.001). In all panels, the average of three independent experiments is expressed ± standard deviation.

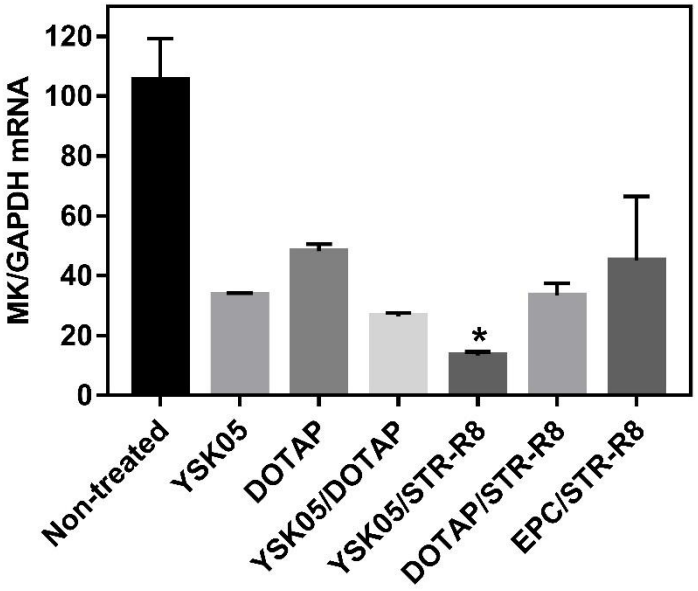

Figure 9. Effect of LNPs based on different main lipids encapsulating MK-siRNA on MK gene expression in HepG2 cells at fixed siRNA dose (*P<0.05 versus the other LNPs). MK-siRNA concentration=100 nM. The average of three independent experiments was considered and expressed ± standard deviation.

Table 9. Composition of the investigated SOR-loaded LNPs[a] based on different main lipids with/without CPP (STR-R8) and their corresponding IC_{50} values measured after 24 hour-incubation with HepG2 cells.

Formulation	Lipid composition and their molar ratios	IC_{50} (μM)[b]
Free SOR	-	14±2.80
YSK	YSK05/Cholesterol (7:3)	12±2
DOTAP	DOTAP/DOPE/Cholesterol (4:3:3)	18±4.75
YSK/DOTAP	DOTAP/YSK05/Cholesterol (4:3:3)	14.64±2.50
YSK/STR-R8	YSK05/Cholesterol/STR-R8 (6:3:1)	9±1.70
DOTAP/STR-R8	DOTAP/DOPE/Cholesterol/STR-R8 (4:3:3:1)	13±3.40
EPC/STR-R8	EPC/Cholesterol/STR-R8 (6:3:1)	17±4.10

[a]SOR loading was 5 mol% of the total lipid amount (75 nmole SOR/1500 nmole lipids).

[b]The average of three independent experiments was considered and expressed ± standard deviation.

1.3.5. Optimization of SOR/MK-siRNA-loaded LNPs

Since empty YSK05/STR-R8 LNPs were found to exert a relatively high toxicity to HepG2 cells (cell viability of around 60%, **Fig. 8 C,E,F**), we attempted to optimize these LNPs with the objective of eliminating the toxicity of the nanocarriers and maximizing their efficiency. In our attempts to identify the source of the cytotoxicity exerted by the empty YSK05/STR-R8 LNPs, we investigated the impact of the YSK05 ratio on both the efficiency and toxicity of the nanocarriers. Surprisingly, reducing the YSK05 ratio to 50 mol% or lower with partial substitution with a neutral helper lipid, DOPE, nearly eliminated this toxicity, with cell viability values >90% for empty LNPs (**Fig. 10A**). In

terms of efficiency, the most efficient LNPs contained 40 mol% YSK05, and therefore, this was considered to be the optimum ratio and was used in subsequent experiments. After solving the problem of the toxicity of the carrier, we further optimized other formulation parameters to maximize the efficiency of the system. Optimizing the cholesterol ratio (**Fig. 10B**) revealed that there was no significant difference in the efficiency of LNPs containing 20-40 mol% cholesterol, while LNPs containing 10 mol% cholesterol showed a lower efficiency. Therefore, the lowest effective ratio (20 mol%) was selected for further optimization. We then optimized the total amount of lipids in the LNPs by screening different amounts of lipid, ranging from 750-2250 nmole in the formulation while maintaining the amounts of SOR and siRNA fixed (**Fig. 10C**). We found that the optimum amount of lipid was 1500 nmole (siRNA/lipid molar ratio 1:500). Lower or higher lipid amounts resulted in a lower efficiency. We also varied the siRNA/drug molar ratio in the LNPs and tested them at a fixed SOR concentration in order to evaluate whether the efficiency of the SOR and MK-siRNA combination was ratio-dependent or not. Surprisingly, we found a significant difference in the efficiency by varying the siRNA/drug molar ratio (cell viability ranged from 28.67% to 60%) (**Fig. 10D**). This result indicates that there is an optimum ratio for the drug and siRNA for obtaining maximum efficiency. In this case, the optimum siRNA/drug molar ratio was 1:25 which reduced cell viability to 28.67±4.57%. We also investigated the effect of using different helper lipids; namely DOPE, POPE, DOPC, EPC and DSPC in the formulations. Although most formulations showed an efficient cytotoxicity, the maximum efficiency was obtained using EPC (cell viability was 21.68±5.60) (**Fig. 10E**). The final composition of the optimized STR-R8-LNPs was YSK05/EPC/cholesterol/STR-R8 (4:3:2:1 molar ratio) and these nanoparticles are referred to as STR-R8-NPs in the

next sections. In addition, we verified the value of the STR-R8 peptide in the optimized formulation by screening different ratios of the peptide (0-10 mol%). Regardless of the payload, reducing the STR-R8 ratio significantly lowered the cytotoxic efficiency (**Fig. 10F**). Therefore, the STR-R8 ratio was fixed at 10 mol% in the next experiments. To show the impact of the above optimization on the performance of the system, we compared the initial YSK05/STR-R8 LNPs (YSK05/cholesterol/STR-R8 6:3:1 molar ratio) with the optimized STR-R8 NPs (YSK05/EPC/cholesterol/STR-R8 4:3:2:1 molar ratio). It was obvious that the optimization resulted in a significant enhancement in the cytotoxic efficiency of the formulation (HepG2 cell viability was reduced from 39.24±4.50% to 22.31±5.55%) as well as a significant reduction in the toxicity of the empty nanocarrier (cell viability was increased to 86±3.85% in case of the optimized LNPs compared to 60.72±5.91% before optimization) (**Fig. 11A**). In terms of MK knockdown activity, the optimized formulation reduced the EC_{50} value from 44 nM to 30 nM revealing a higher delivery efficiency for the MK-siRNA (**Fig. 11B**).

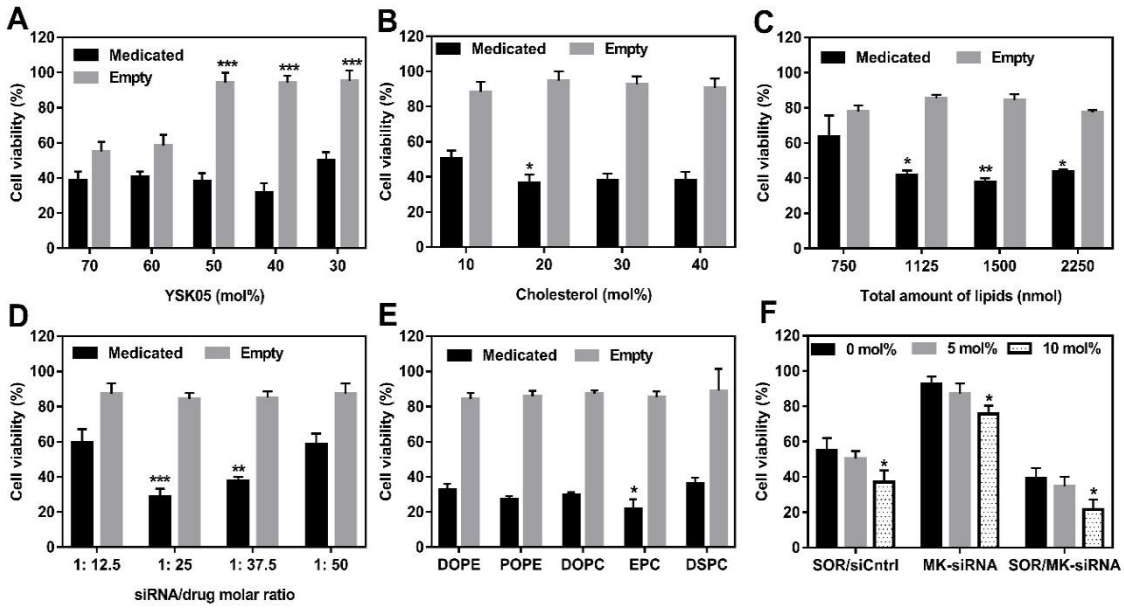

Figure 10. Optimization of different components of the STR-R8-LNPs. The evaluation was done using HepG2 cells. A) Optimization of the YSK05 ratio (***P<0.0001 versus empty LNPs containing 60 or 70 mol% YSK05). B) Optimization of the cholesterol ratio (*P<0.05 versus 10 mol%). C) Optimization of the total amount of lipid used (*P<0.05 versus 750 nmole, **P<0.001 versus 750 nmole). D) Optimization of the siRNA/drug molar ratio (**P<0.001 versus 1:12.5 and 1:50, ***P<0.0001 versus 1:12.5 and 1:50). E) Optimization of helper lipid type (*P<0.05 versus DOPE and DSPC). F) Effect of STR-R8 ratio on the performance of the optimized LNPs encapsulating different payloads, as evidenced by their cytotoxic effect (*P<0.05 versus 0 mol% and 5 mol%). In all optimization steps, SOR concentration= 10 µM, MK-siRNA concentration= 400 nM except in (D) where the SOR concentration was fixed at 10 µM, the MK-siRNA was varied according to the ratio under consideration. The average of three independent experiments is expressed ± standard deviation.

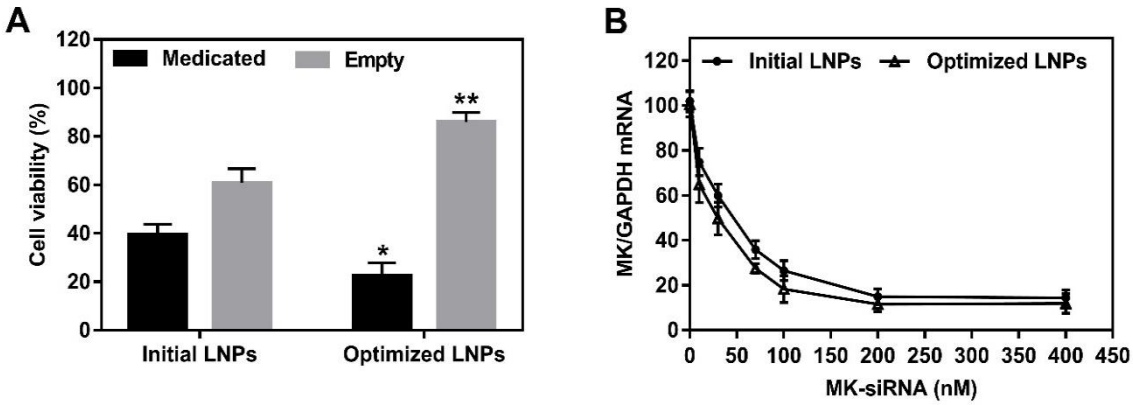

Figure 11. Comparison between the performance of the initial and optimized STR-R8 NPs in HepG2 cells. A) Evaluation of cytotoxic effect (*P<0.05 versus medicated initial LNPs, **P<0.001 versus empty initial LNPs). SOR concentration= 10 µM, MK-siRNA concentration=400 nM. B) Evaluation of MK gene knockdown activity at different MK-siRNA doses. The average of three independent experiments was considered and expressed ± standard deviation.

1.3.6. HCC targetability of the optimized STR-R8 NPs

After obtaining an optimum and efficient co-delivery system (STR-R8-NPs), we examined the targetability of these nanoparticles by investigating their cytotoxicity in HCCs, HepG2, compared to normal hepatocytes, FL83B. Free SOR showed a non-specific cytotoxicity for both cell lines with a higher cytotoxicity to normal hepatocytes (cell viability was 64.90±8.10% and 54.18±5.89% for HepG2 and FL83B, respectively). Unfortunately, the STR-R8-NPs also demonstrated a high non-selective cytotoxicity for both cell lines with superior selectivity to normal hepatocytes (cell viability was 24.93±3.25% and 8.03±3.26% for HepG2 and FL83B, respectively) (**Fig. 12A**). A similar pattern was observed in cellular uptake study by FACS where the uptake of STR-R8-NPs in FL83B cells was 5.26-fold higher than that in HepG2 cells (**Fig. 12B**). These results indicated that it was necessary to introduce another specific targeting ligand to improve the selectivity of the system to HCCs while maintaining the high efficiency of the system.

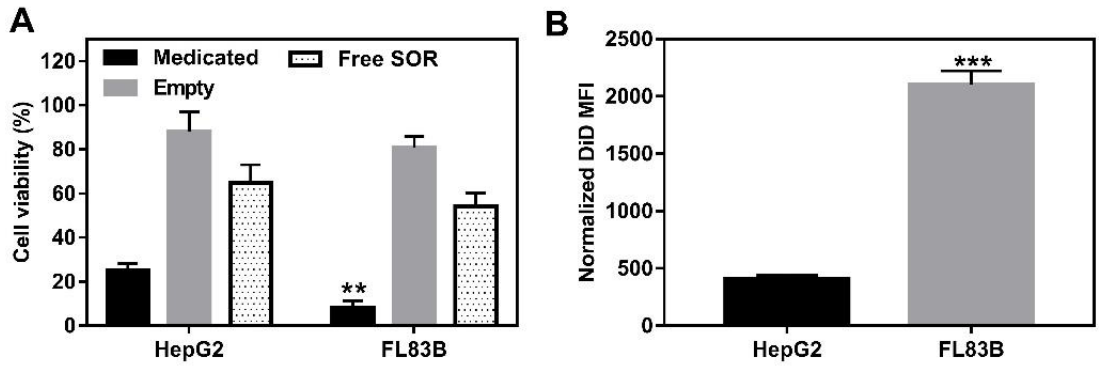

Figure 12. Effect of STR-R8-NPs on HepG2 and FL83B cells. A) Effect on cell viability (**P<0.001 versus HepG2). B) Effect on cellular uptake (***P<0.0001 versus HepG2). SOR concentration= 10 μM, MK-siRNA concentration= 400 nM. The average of three independent experiments was considered and expressed ± standard deviation.

1.3.7. Introduction of SP94 peptide to improve the system's targetability to HCC

Despite their high efficiency, the STR-R8-NPs failed to be a highly-specific co-delivery system for HCC. This prompted us to use the novel HCC targeting ligand, the SP94 peptide, in preparing SP94-LNPs loaded with both SOR and MK-siRNA. First, we conjugated the cysteine-terminated SP94 peptide to DSPE-PEG_{2k}-MA (**Fig. 6**) and determined the molecular weights of the reactants and product using MALDI-TOF-MS (**Fig. 13**). The molecular weights of DSPE-PEG_{2k}-MA and the SP94 peptide were 2940.696 and 1446.118, respectively, very close to the exact molecular weights reported by their manufacturers. The molecular weight of the conjugation product was 4427.495 which is approximately the same as the sum of both reactants confirming that the desired conjugation product was formed. There were no peaks related to reactants in the spectra of the conjugate confirming that the reaction was complete that there were no impurities in the preparation.

Second, we inserted different ratios of SP94-modified DSPE-PEG (0-10 mol%) into LNPs that did not contain STR-R8 to evaluate their effect on cellular uptake in HepG2 and FL83B cells. Interestingly, at 5 mol% SP94-modified DSPE-PEG, the uptake of LNPs by HepG2 cells was 27-fold higher than that by FL83B cells which showed almost no uptake of these nanoparticles (**Figs. 14A**, **15**). This effect was not observed at lower or higher concentrations of SP94-modified DSPE-PEG. Furthermore, we compared LNPs modified with the SP94 peptide at the optimum concentration (5 mol%) by either pre-insertion or post-insertion methods. We found that LNPs modified with DSPE-PEG-SP94 by the pre-insertion method showed a significantly higher cellular uptake and efficiency in HepG2 cells than those modified by the post-insertion method as indicated by FACS and cytotoxicity studies (data not shown). The optimized SP94-modified LNPs had a lipid composition of YSK05/EPC/cholesterol/DSPE-PEG-SP94 (molar ratio is 4:3:3:0.5), modified by the pre-insertion method, and are referred to as SP94-NPs in the next sections.

Fig. 16 shows a schematic representation for the composition of SP94-NPs as well as a TEM image showing their morphology. To verify the importance of the SP94 peptide, the optimized SP94-NPs were loaded with SOR/siCntrl, MK-siRNA or SOR/MK-siRNA and their cytotoxic efficiency in HepG2 and FL83B cells were evaluated in the presence or absence of SP94 peptide (+/-). The results revealed that the SP94 peptide has a significant impact on the selectivity to HCCs regardless of the payload being investigated (**Fig. 14B**).

The SP94-NPs were as efficient as the previously optimized STR-R8-NPs in HepG2 cells (**Fig. 17A**). However, only the SP94-NPs showed a limited cytotoxicity to FL83B cells, which confirms the higher

selectivity for HCCs. Cellular uptake studies by FACS confirmed that, in opposite to the STR-R8-NPs, the SP94-NPs were selective for HCCs compared to normal hepatocytes (**Fig. 17B-C**). In attempting to increase efficiency without losing selectivity, we also investigated the cytotoxicity of LNPs modified with both STR-R8 and SP94 peptides (**Fig. 18**). The use of low STR-R8 concentrations (1-3 mol%) did not result in a significant improvement in efficiency. Meanwhile, increasing the STR-R8 concentration to 5 or 10 mol% decreased both the efficiency and selectivity of the system, with efficiency in HepG2 cells being decreased and cytotoxicity to FL83B cells being increased. These results indicated that SP94-NPs were more efficient and selective for HCCs than LNPs modified with STR-R8 or STR-R8 and SP94.

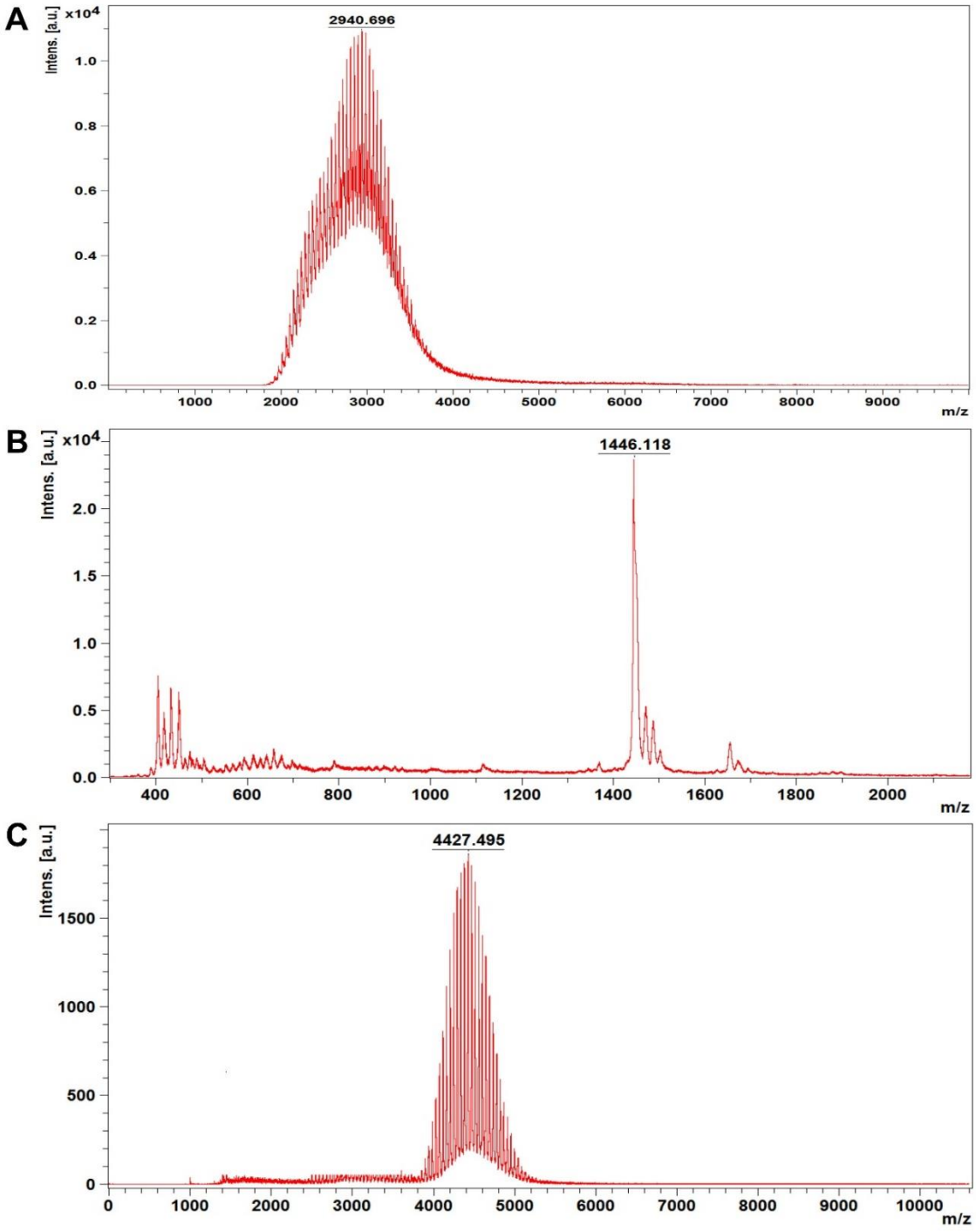

Figure 13. MALDI-TOF-MS spectra for DSPE-PEG_{2K}-MA (A), SP94 peptide (B) and SP94-modified DSPE-PEG (C).

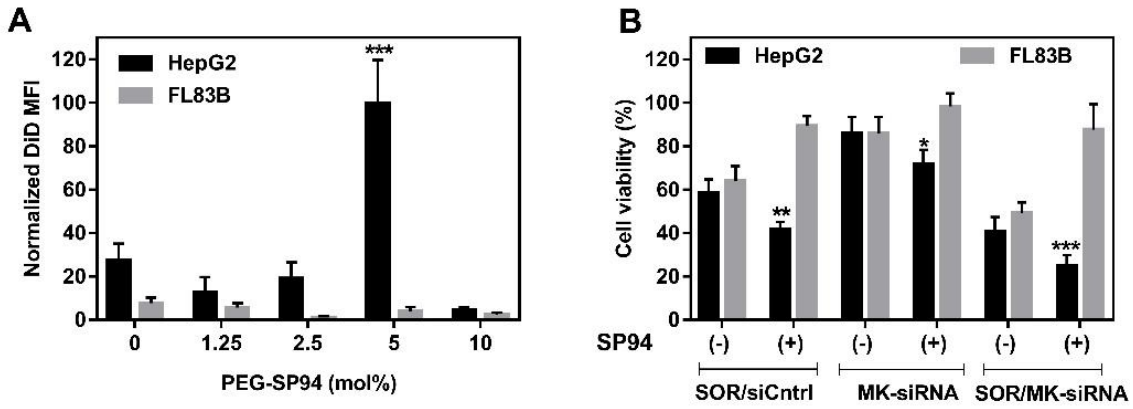

Figure 14. Effect of modifying the LNPs with the SP94 peptide on their selectivity for HCC. A) Effect of LNPs modified with different concentrations of DSPE-PEG-SP94 on cellular uptake in two cell lines (***P<0.0001 versus FL83B). B) Effect of the presence or absence of SP94 peptide at the optimum concentration (5 mol%) on the performance of LNPs encapsulating different payloads, as evidenced by their cytotoxic effect on HepG2 and FL83B cells (*P<0.05, **P<0.001, ***P<0.0001 versus FL83B). SOR concentration= 10 μM, MK-siRNA concentration= 400 nM. The average of three independent experiments was considered and are expressed as ± standard deviation.

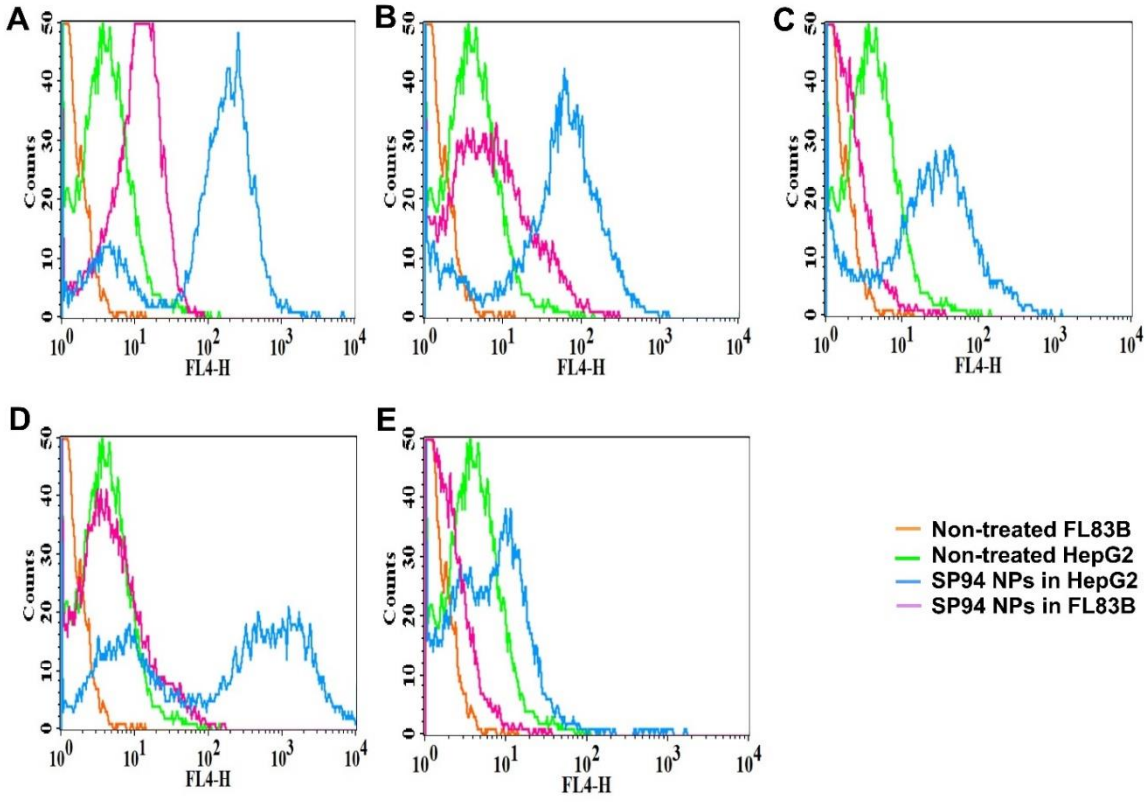

Figure 15. FACS histogram plots for the uptake of LNPs modified with different concentrations of DSPE-PEG-SP94 in HepG2 and FL83B cells. A) 0 mol%. B) 1.25 mol%. C) 2.5 mol%. D) 5 mol%. E) 10 mol%. SOR concentration= 10 µM, MK-siRNA concentration=400 nM.

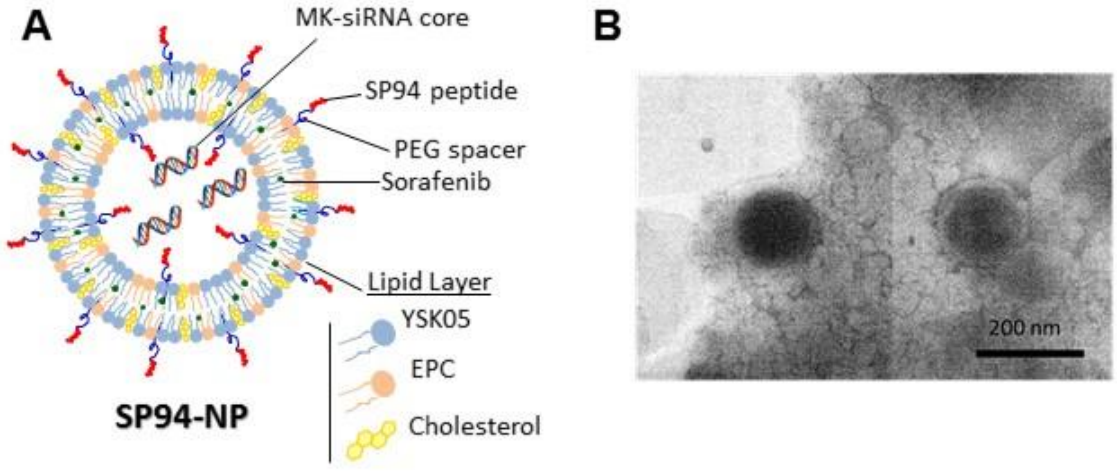

Figure 16. Structure of the optimized SP94 NPs. A) A schematic representation for the composition of SP94 NPs. B) TEM image for the optimized SP94 NP.

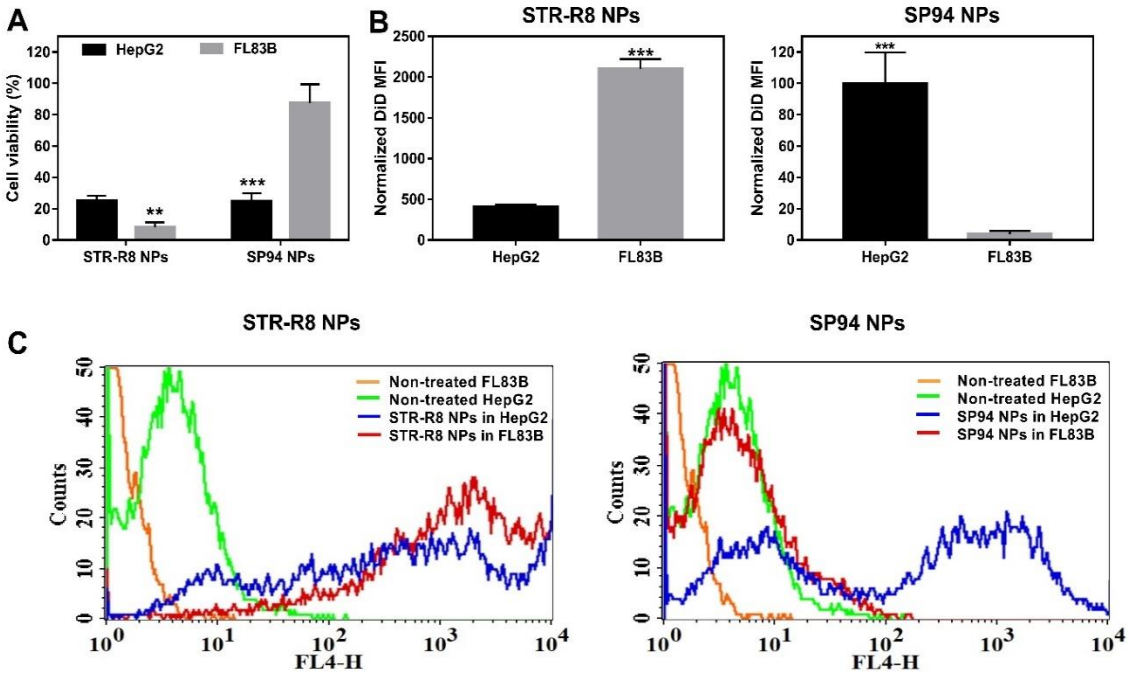

Figure 17. Comparison between STR-R8-NPs and SP94-NPs in HepG2 and FL83B cells. A) Effect on cell viability (**P<0.001 versus HepG2, ***P<0.0001 versus FL83B). B) Evaluation of cellular uptake (***P<0.0001 versus the other cell line). C) FACS histogram plots for the uptake of STR-R8-NPs and SP94-NPs in HepG2 and FL83B cells. SOR concentration= 10 μM, MK-siRNA concentration= 400 nM. The average of three independent experiments was considered and expressed ± standard deviation.

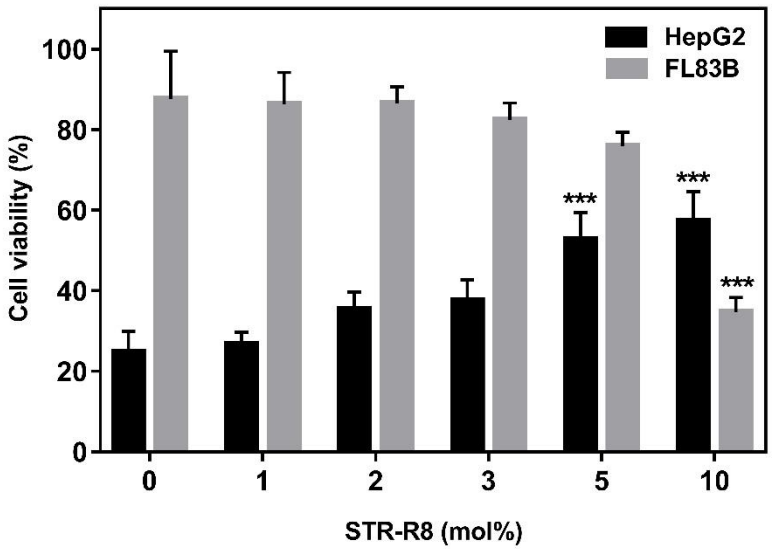

Figure 18. Effect of LNPs modified with 5 mol% PEG-SP94 and different concentrations of STR-R8 on the cell viability of HepG2 and FL83B cells (***P<0.0001 versus 0-3 mol% in HepG2 cells, ***P<0.0001 versus 1-5 mol% in FL83B cells). SOR concentration= 10 μM, MK-siRNA concentration=400 nM. The average of three independent experiments was considered and expressed ± standard deviation.

1.3.8. Confirming the value of using a combination of SOR and MK-siRNA under different conditions

We further re-investigated the value of using a combination of SOR and MK-siRNA using the optimized SP94-NPs. We compared SP94-NPs encapsulating a combination of SOR and MK-siRNA with those encapsulating SOR and control siRNA (siCntrl), the MK-siRNA alone or siCntrl alone and investigated the cytotoxic effect of these nanoparticles on HepG2 cells (**Fig. 19A**). The value of the combination was confirmed, since the SOR and MK-siRNA combination showed the highest cytotoxicity compared to the other formulations (IC_{50} was 5±1.50 μM compared to 9±2.20 μM and 17±2.60 μM for SOR+siCntrl and MK-siRNA, respectively). We varied the SOR concentration (5 or 10 μM) and the duration of the experiment (24 or 48 hours) to test the combination

under different conditions. Interestingly, the value of the combination was clearer upon using a low SOR concentration (5 μM) where HepG2 cell viability was reduced to 50.72±7.34% after a 24-hour incubation with SP94-NPs encapsulating SOR and MK-siRNA, but such a low concentration was significantly less effective when MK-siRNA was replaced with siCntrl (cell viability was 75.48±3.55% after the same incubation period) (**Fig. 19B**). Moreover, such an impact was much clearer when the incubation period was extended to 48 hours (**Fig. 19C**) where HepG2 cell viability was 40.72±5.90% for SOR and MK-siRNA compared to 73.52±4.55% for SOR and siCntrl. SP94-NPs encapsulating siCntrl showed negligible cytotoxicity to HepG2 cells (cell viability around or higher than 90%) (**Fig. 19A**) which eliminated the probability of significant cytotoxicity arising from the carrier itself.

1.3.9. *In vitro* drug release

The *in vitro* release profile of SOR from the optimized SP94-NPs was determined in media representing physiological or endosomal pH (7.4 and 5.5, respectively) followed by kinetic analysis, as described in the methods section.[195] SP94-NPs exhibited a controlled-release pattern over 48 hours which was pH-dependent with a significantly-higher drug release at pH 5.5 compared to that at pH 7.4 (cumulative percentage of SOR dose released after 48 hours was 80.48±2.45% and 34.42±3.51, respectively) (**Fig. 19D**).

Table 10 shows the results of the kinetic analysis of the SOR release data which were best-fitted to the Higuchi-diffusion model. Fitting the drug release data to the equation proposed by Ritger and Peppas[196] revealed that the release of SOR from SP94-NPs exhibited a non-fickian behavior (**Table 11**) indicating that the drug release occurred

by a combination of diffusion and molecular relaxation of the lipid bilayer.

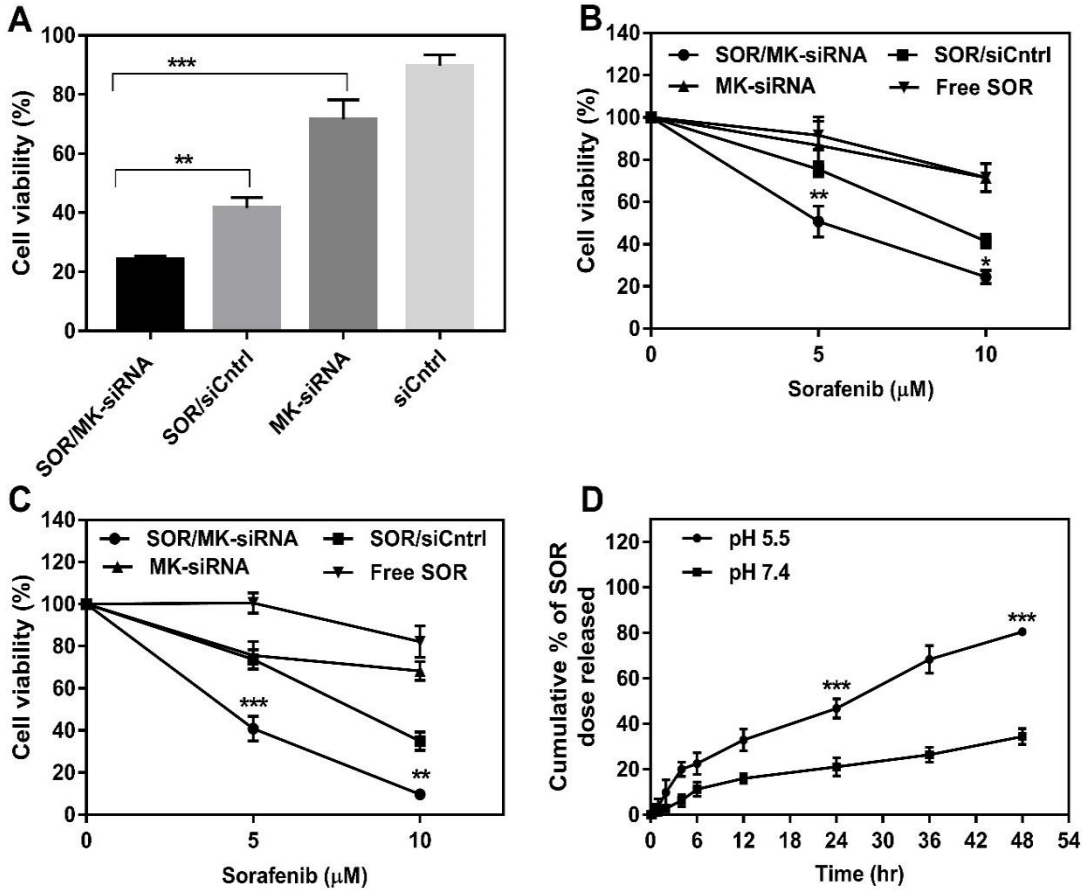

Figure 19. MK-siRNA increases the sensitivity of HepG2 cells to SOR and evaluation of the release profile of SOR. A) Confirming the value of the SOR and MK-siRNA combination under ordinary experimental conditions (SOR concentration= 10 μM, MK-siRNA concentration= 400 nM, incubation time= 24 hr) (**P<0.001, ***P<0.0001). B) Effect of MK-siRNA on SOR dose response curve after 24 hours (**P<0.001 versus SOR/siCntrl, *P<0.05 versus SOR/siCntrl). C) Effect of MK-siRNA on SOR dose response curve after 48 hours (***P<0.0001 versus SOR/siCntrl, **P<0.001 versus SOR/siCntrl). D) *In vitro* SOR release profile from SP94-NPs at different pH values (***P<0.0001 versus pH 7.4). When the SOR concentration= 5 μM, MK-siRNA concentration= 200 nM; when the SOR concentration= 10 μM, MK-siRNA concentration= 400 nM. The average of three independent experiments was considered and expressed ± standard deviation.

Table 10. Kinetic analysis of the release of SOR from SP94-NPs at different pH values (the average cumulative percentage of SOR dose released at different time points for three independent experiments was used in the calculations).

	Correlation coefficient (r)				
pH	Zero-order model	First-order model	Higuchi-diffusion model	$t_{50\%}$[a] (hr)	K_{rel}[b]
5.5	0.9809	0.1749	0.9934	24	10.2062
7.4	0.9739	0.3559	0.9925	>48	N/A

[a]$t_{50\%}$: the time required for the release of 50% of SOR dose.

[b]$K_{rel.}$: drug release rate constant calculated based on the best-fit kinetic model.

Table 11. Analysis of SOR release data from SP94-NPs according to the Ritger and Peppas equation (the average cumulative percentage of SOR dose released at different time points for three independent experiments was used in the calculations).

pH	n[a]	K[a]	r[b]	Mechanism
5.5	0.777605	4.572692	0.9836	non-fickian
7.4	0.742614	2.103373	0.9896	non-fickian

[a]n and K are the parameters of Ritger and Peppas equation defined in methods section (**Equation 6**).

[b]r is the correlation coefficient calculated by linear regression analysis of the Logarithm of cumulative percentage of drug released (Log M_t / M_∞) versus the Logarithm of the corresponding different time points (Log t).

1.3.10. Evaluation of SP94-NPs in different cell lines

We expanded the study of SP94-NPs to four different cell lines; human HCC (HepG2), mouse HCC (Hepa 1-6), human cervical adenocarcinoma (HeLa), which was considered as a model of a cancerous cell line other than HCC, and normal mouse hepatocytes (FL83B). The selectivity and efficiency of the system were evaluated by FACS, CLSM, cytotoxicity, and MK gene silencing studies. The uptake study by FACS revealed that the highest cellular uptake of SP94-NPs occurred in both HepG2 and Hepa 1-6 cells, while the uptake in HeLa cells was 2.5-fold lower than HepG2 cells and almost no uptake was found in FL83B cells (**Fig. 20A**). CLSM images confirmed this selective pattern of uptake (**Fig. 20B**). Upon the incubation of different cell lines with the SP94-NPs for 24 hours, the cell viability values were 25.81±6.52%, 35.88±3.66%, 71.09±11.53% and 86.97±3.75% for HepG2, Hepa 1-6, HeLa and FL83B, respectively (**Fig. 20C**). Furthermore, the SP94-NPs resulted in an efficient MK gene silencing in both HepG2 and Hepa 1-6 cells with EC_{50} values of 7.50±2.50 and 10±3.50 nM, respectively (**Fig. 20D**). Surprisingly, these EC_{50} values were much lower than that for the initial LNPs containing STR-R8 (44±6.5 nM in HepG2 cells, **Fig. 8D**). On the other hand, in HeLa cells, a significantly lower MK gene silencing was observed with an EC_{50} value of 70±8.25 nM. No significant MK gene silencing was observed in FL83B cells. These collective results serve to confirm the high selectivity of SP94-NPs for HCCs.

The cellular uptake of SP94-NPs was competitively-inhibited by pre-treatment and co-incubation of cells with increasing concentrations of free SP94 peptide (**Fig. 21**).

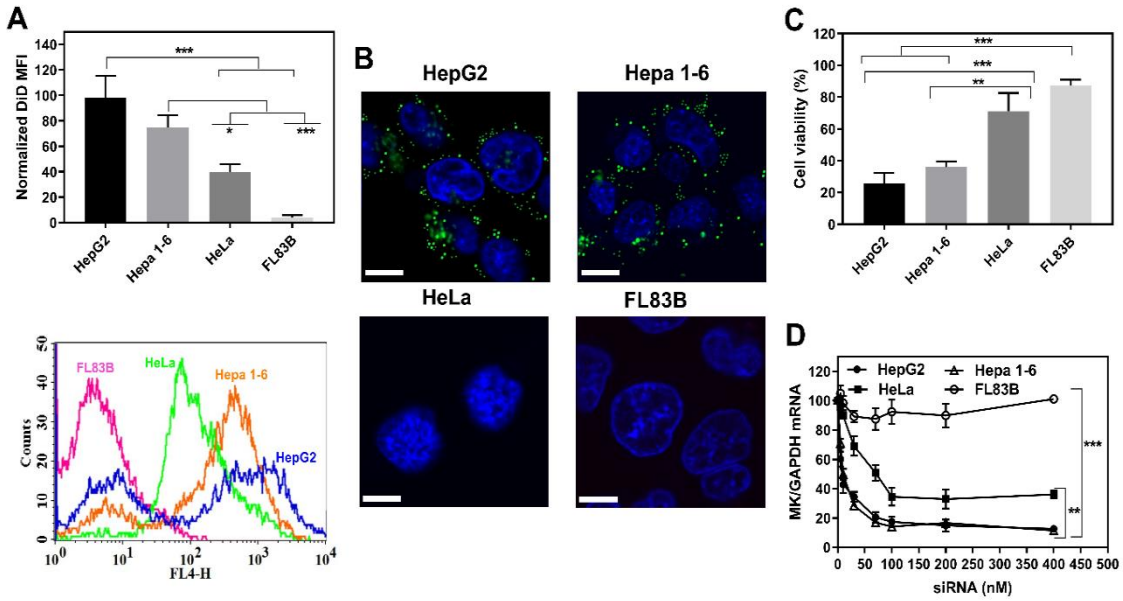

Figure 20. Evaluation of the optimized SP94-NPs in different cell lines. A) Uptake study by FACS (*P<0.05, ***P<0.0001) and FACS histogram plots for the uptake of SP94-NPs in different cell lines. B) Cellular uptake study by CLSM (blue; nuclei, green; SP94-NPs, scale bars represent 20 μm). C) Cytotoxicity in the various cell lines (**P<0.001, ***P<0.0001). D) MK gene silencing in different cell lines (**P<0.001, ***P<0.0001). SOR concentration= 10 μM, MK-siRNA concentration= 400 nM. The average of three independent experiments was considered and values are expressed ± standard deviation.

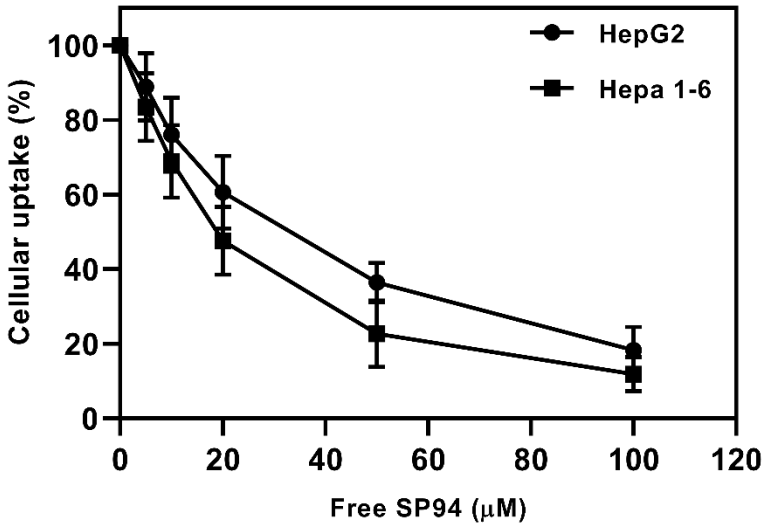

Figure 21. Competitive inhibition of SP94-NPs uptake in HepG2 and Hepa 1-6 cells by co-incubation with increasing concentrations of free SP94 peptide. SOR concentration= 10 μM, MK-siRNA concentration=400 nM. MFI of each sample was normalized to MFI of cells that received SP94-NPs without incubation with free SP94 peptide, which was considered as 100% cellular uptake. The average of three independent experiments was considered and expressed ± standard deviation.

1.3.11. Serum compatibility and long-term stability of SP94-NPs

To judge the *in vivo* potential of the optimized SP94-NPs, we compared their cytotoxicity to HepG2 cells in the presence or absence of serum. Surprisingly, the presence of serum had no significant effect on the efficiency of the system (**Fig. 22A**) which confirms that the SP94-NPs are serum-compatible and serum-stable. Moreover, we investigated the long-term shelf stability of these nanoparticles after two months of storage. **Fig. 22B-C** show the frequency size distribution curves for freshly prepared SP94-NPs (zero-time) and for those stored for 2 months at 4 °C. The average particle sizes were 149.9±7.5 and 161.5±8.3 nm at zero-time and 2 months, respectively, indicating a non-significant change in particle size and the absence of any particle aggregates.

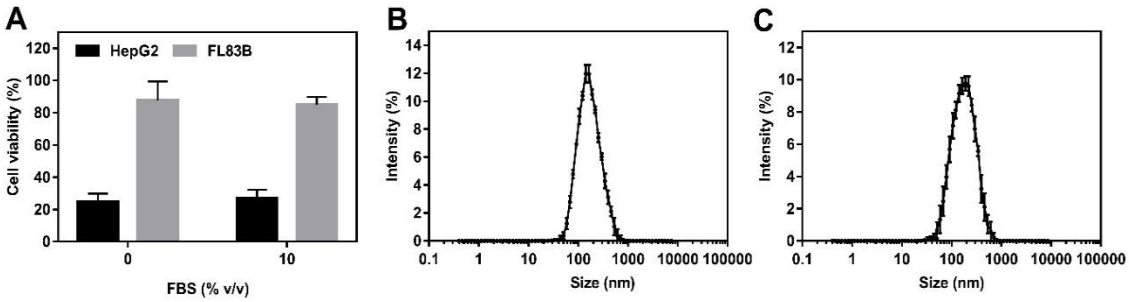

Figure 22. Serum compatibility and long-term stability of SP94-NPs. A) Effect of FBS on efficiency of SP94-NPs in HepG2 cells (SOR concentration= 10 μM, MK-siRNA concentration=400 nM). The average of three independent experiments was considered and expressed ± standard deviation. B) Frequency particle size distribution curve for SP94-NPs at zero-time. C) Frequency particle size distribution curve for SP94-NPs after 2-month storage at 4 °C (average ±standard deviation, n=6).

1.4. DISCUSSION

In the current study, we proposed a novel strategy for the treatment of HCC based on a combination of chemotherapy and gene therapy. We selected the cytotoxic drug, Sorafenib (SOR), which has been approved by the FDA as the first line therapy for the treatment of resistant non-resectable HCC.[197] Based on previous studies, Midkine gene (MK) is overexpressed by several folds in HCC compared to normal hepatocytes and has been considered to be a novel diagnostic marker for HCC where it exerts several malignant functions. [48, 198] This triggered us to target the MK gene in our approach for treating HCC. We propose that SOR, if it were to be combined with MK gene-silencing therapy (MK-siRNA), this would represent a synergistic combination. To our knowledge, this is the first report of an investigation of such a possible synergistic combination. **Fig. 23** provides a schematic illustration for our hypothesis regarding the proposed mechanism of action of the investigated combination encapsulated in the targeted SP94-NPs and the proposed role for each component in the nanocarrier.

We optimized a protocol for assessing the cytotoxicity of different formulations using MTT assay. In our protocol, we treated the cells with the desired concentration of SOR (free or encapsulated in LNPs) in 0.25 mL of serum-free medium and after a 4-hour incubation; we made a 5-fold dilution with fresh serum-containing medium (1 mL) to limit the effect of uninternalized drug/nanoparticles. Therefore, the difference in efficiency between the different formulations and the free drug would be related to the efficiency of cellular internalization during the first 4 hours. This protocol enabled us to compare the efficiencies of the different formulations. Moreover, this is closer to the actual *in vivo* environment in which the drug concentration would not remain fixed near tumor cells for

a long time period due to the dynamic environment and clearance mechanisms. Decoration of the investigated LNPs with STR-R8 resulted in an improved cytotoxic efficiency to HepG2 cells which was in agreement with previous results reported by our group.[12, 199-200] The highest efficiency was obtained using LNPs based on YSK05, a smart pH-sensitive lipid, which can be attributed to its powerful endosomal escape properties.[140]

After obtaining a promising nanocarrier candidate, we investigated its ability to deliver MK-siRNA. During core formation with PEI, we selected a nitrogen to phosphate (N/P) ratio lower than 1 to form a negatively-charged core which was reported to have a superior intracellular availability and activity.[201] The prepared LNPs showed acceptable physico-chemical properties and resulted in a concentration-dependent silencing of the MK gene, but this silencing alone was not sufficient to efficiently kill HepG2 cells. Therefore, this encouraged us to investigate the effect of a combination of SOR and MK-siRNA. Interestingly, the combination showed a synergistic cytotoxic effect on HepG2 cells suggesting that MK-siRNA has a role in enhancing SOR activity.

We further optimized the system to improve its efficiency and biosafety. Reducing YSK05 ratio to 50 mol% and lower eliminated the toxicity of the empty nanocarrier which can be attributed to the high endosomolytic effect of YSK05 that might be toxic when an inappropriate ratio was used. Upon investigating the cholesterol ratio used, we found that a low cholesterol ratio (10 mol%) resulted in a lower efficiency which can be attributed to the instability of the formed LNPs leading to premature drug release and/or siRNA leakage from nanoparticles with a subsequent reduction in efficiency. Cholesterol has

been reported to improve the integrity and stability of LNPs as well as their membrane fusion ability.[202] Regarding the total amount of lipid, we found that the optimum amount was 1500 nmole (siRNA/lipid molar ratio 1:500). Lower lipid amounts resulted in lower SOR encapsulation efficiency (~50%) and lower cytotoxic efficiency, probably due to the insufficiency for coating the payload and/or exerting sufficient endosomal escape activity. On the other hand, increasing the total amount of lipid to above 1500 nmole resulted in a slight lowering in efficiency, probably due to the retardation of drug release by the high amount of lipids. Surprisingly, upon varying the siRNA/drug molar ratio in the nanocarrier, a significant variation in efficiency was observed, in spite of the fixed SOR dose (10 μM). This cannot be explained by the effect of increasing the siRNA dose because, at a siRNA/drug ratio 1:12.5, the siRNA dose was the highest (800 nM), but the poorest efficiency was obtained. Instead, this finding can be explained by a possible ratio-dependent synergism between SOR and MK-siRNA which would require an optimum ratio between the two components for achieving maximal activity (1:25 siRNA to drug molar ratio). A recent study reported a similar finding for synergism between two drugs,[203] but to our knowledge, there is no study reporting such a finding regarding siRNA and drug combination. Our study is the first to provide experimental evidence to show that the efficiency of a drug and an siRNA combination is ratio-dependent. Thus, the selection of the optimum combination ratio should be taken into consideration in any future studies in which combinational therapy is being investigated.

We also investigated the effect of different helper lipids in the system and found that the highest efficiency was obtained with EPC. This could not be explained in terms of endosomal escape activity because it is

well known that DOPE has higher endosomal escape properties than EPC owing to its capability of undergoing conformational change to an inverted hexagonal shape in the endosomal pH with enhanced fusogenic properties.[204] Alternatively, this could be attributed to the difference in stability of these LNPs. It has been reported that phosphatidyl choline phospholipids (e.g. EPC) form more stable bilayer structures than phosphatidyl ethanolamine phospholipids (e.g. DOPE)[205] and thus, forming more stable LNPs with a lower tendency for premature drug release. On the other hand, DSPC contains saturated fatty acids which result in the formation of highly-stable LNPs that may hinder the interaction with endosomal membrane leading to impaired endosomal escape activity[206] which might explain the lower efficiency of the DSPC-containing LNPs compared to LNPs containing EPC with unsaturated fatty acids.[207]

The optimized STR-R8-NPs showed a higher affinity for normal hepatocytes rather than HCCs as indicated by the cytotoxicity and FACS results. This indicated that the STR-R8-NPs might cause significant side effects, since high levels are taken up by normal hepatocytes. Previous studies done in our laboratory as well as other laboratories showed that the use of R8-modified LNP resulted in a highly-efficient gene delivery in normal hepatocytes.[208-209] The higher affinity of the STR-R8-modified LNPs to normal hepatocytes can be rationalized in terms of the mechanism of cellular uptake of the STR-R8 peptide. A previous study reported by our laboratory [189] showed that a high density of the R8 peptide stimulates cells for macropinocytosis via interactions with cell surface heparan sulfate proteoglycans. Recent reports have shown that the expression of the major family of cell surface heparan sulfate proteoglycans, Syndecans, is down regulated in HCC (e.g. Syndecan-

1/CD138)[210] which may explain the difference in the uptake of STR-R8 NPs in HCC cells compared to normal hepatocytes.

In order to achieve our goal of targeting HCC, we introduced a novel HCC targeting peptide, SP94, in place of STR-R8 by conjugating it to DSPE-PEG_{2k}-MA and screening LNPs containing different molar ratios of this conjugate. Surprisingly, a high degree of selectivity was achieved at molar ratio 5 mol% of DSPE-PEG_{2k}-SP94 with almost no uptake and limited cytotoxicity to normal hepatocytes. This confirmed the high selectivity of SP94-targeted LNPs for HCC and indicated that there is an optimum ratio for the peptide for exerting its maximum effect on the cellular uptake. The ratio of DSPE-PEG_{2k}-SP94 may need to be further optimized in future studies in which the system will be extended to *in vivo* tumor delivery. The efficiency of the new co-delivery system was comparable to that for STR-R8-NPs in HCC with the additional advantage of a high selectivity.

After confirming the system's selectivity and efficiency, we re-investigated the cytotoxic impact of the combination of SOR and MK-siRNA using the final lipid composition (SP94-NPs). Interestingly, the value for the combination became clearer upon comparing the cytotoxicity of these LNPs at a lower SOR dose (5 μM rather than 10 μM) or after incubation for 48 hours. These observations confirm that MK-siRNA increases the sensitivity of HepG2 cells to SOR at low doses and this effect is enhanced by prolonged silencing of the MK gene. This effect would be promising in reducing the chemotherapeutic dose required for HCC treatment. On the other hand, the superior cytotoxicity of LNPs encapsulating SOR+siCntrl over free SOR seen in **Fig. 19B-C** could be mainly attributed to the value of our drug delivery system (DDS) which might have increased the cellular uptake and/or endosomal escape

of SOR. Since LNPs encapsulating only siCntrl showed cell viability value of ~90%, the cytotoxicity from the carrier itself could also be considered.

Comparing our findings with recent studies in which liposomal SOR was used in combination with siRNA or other agents, Sun *et al.*[211] reported on the co-delivery of SOR and siRNA against the Glypican-3 gene (siGPC3) to HepG2 cells using PEI-modified liposomes. Using a 10 μM SOR dose, 5×10^3 cells/well, 48 hours incubation, their system reduced HepG2 cell viability to about 20%. Our system showed a similar effect at the same dose, but using a 10-fold higher number of cells (5×10^4 cells/well) and half the incubation period (24 hours). Xiao *et al.*[212] reported on the co-delivery liposomes encapsulating SOR and Gadolinium for the treatment and imaging of HCC. Their system reduced HepG2 cell viability to about 60% after 48 hours using a 10 μg/mL SOR concentration (21.5 μM) and 8×10^3 cells/well. Our system showed a much higher cytotoxicity (cell viability about 25%) using a 6.25-fold higher number of cells, half the drug concentration and half the incubation period. This clearly proves the higher efficiency of our system in addition to its amazingly high selectivity. Compared to commercially available transfection reagents which have no selectivity, the system developed in this study is highly specific for hepatic cancer cells. Furthermore, the system is more suitable for *in vivo* use since the two therapeutic tools are combined in one system which is covered with a PEG coat that is expected to reduce nonspecific interactions in the circulation.

We studied the release of SOR from the optimized SP94 NPs at two different pH values considering the pH-sensitive nature of our main lipid, YSK05. The drug release profile was pH-dependent with a

significantly-higher dissolution rate at an acidic pH 5.5 compared to the physiological pH of 7.4. This gives an additional advantage to our system because a limited drug release will occur in the physiological pH in the extracellular environment, but upon internalization inside HCC cells, the pH becomes acidic in the endosome, which imparts a cationic charge to YSK05, leading to the repulsion and dissociation of the lipid bilayer with subsequent drug release. This inhibits the off-target cytotoxicity caused by SOR and increases the selectivity of the system. This also explains the biosafety of the system for normal hepatocytes which showed a cell viability near 90% after a 24-hour incubation despite the well-known non-selective cytotoxicity of SOR. FACS and CLSM studies confirmed that the SP94-NPs were not taken up by normal hepatocytes, and, as a result limited drug release occurred (no more than 20%) in the extracellular medium (pH 7.4). Kinetic analysis revealed that the release of SOR from SP94-NPs followed the Higuchi-diffusion model with non-fickian behavior which confirms the controlled-release nature of our LNPs with additional advantages of controlled-release drug delivery systems including dosage control, decreasing administration frequency, decreasing side effects and increasing patient acceptability.[213] These results come in agreement with previous studies included the use of LNPs for the delivery of other drugs.[214-215]

We expanded our study to include different types of cancerous and normal cell lines. Interestingly, the cellular uptake in HeLa cells was 2.5-fold lower than that for HepG2 cells and nearly 2-fold lower than that for Hepa 1-6 cells. This indicates that the SP94 peptide is highly selective for HCCs not only compared to normal cells, but to other cancerous cells as well. A similar observation was reported by Li *et al.* who used the SP94 peptide as a specific probe for HCC imaging and found that the uptake in

Huh-7 human HCC cells was 2.72-fold higher than in HeLa cells.[191] Although the molecular target receptor(s) for the SP94 peptide are still unknown, our collective data suggest that these receptors are highly-expressed in HCCs, expressed at lower levels in other cancers and absent in normal cells. The competitive inhibition of the cellular uptake of SP94-NPs by pre-treatment and co-incubation of cells with excess free SP94 peptide confirms that these LNPs are uptaken through specific receptors for SP94 peptide. We are now planning to investigate the underlying mechanism behind such selectivity and the target receptors in future studies.

Interestingly, we found that MK gene silencing by the SP94-NPs was much higher than in the case of initial LNPs containing STR-R8 (about 6-fold lower EC_{50} in HepG2 cells). This indicated that our optimization improved the MK gene silencing capability of MK-siRNA. Furthermore, it appears that LNPs with a neutral surface charge are better for delivering siRNA than cationic LNPs. Cationic LNPs may strongly bind to short siRNA molecules, thus limiting their intracellular availability. This phenomenon may not apply to pDNA, with a larger molecular size, which commonly shows a high transfection ability using cationic LNPs.[216-217] Lastly, we evaluated the stability of the optimized SP94-NPs. The presence of 10% FBS had no significant impact on the efficiency in HepG2 cells, which confirmed the serum-compatibility of these nanoparticles. Furthermore, no significant change in particle size of the SP94-NPs was detected after a 2-month storage at 4 °C, which revealed the absence of aggregate formation, which confirms the shelf stability of SP94-NPs.

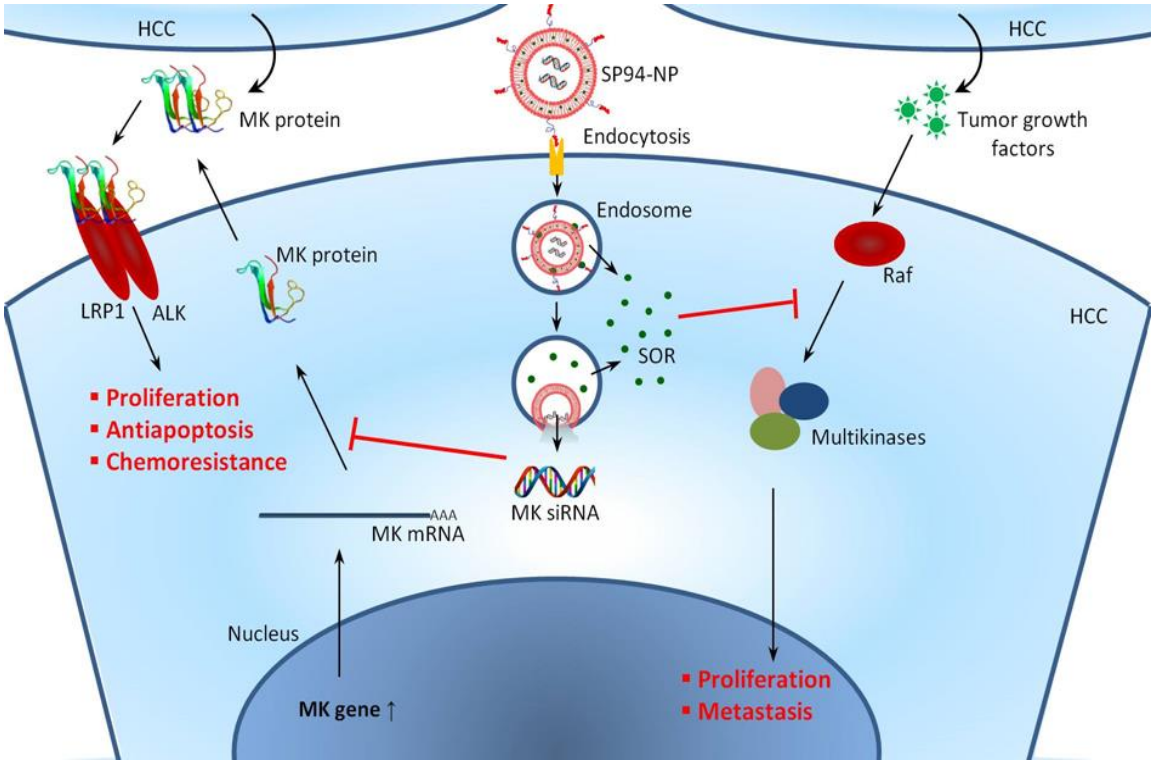

Figure 23. A schematic illustration for the proposed mechanism of performance of SP94-NPs and the role of its different components. SP94-NPs are internalized into HCCs via specific SP94 receptors. The fusogenic lipid, YSK05, mediates a strong endosomal escape to release the payload into the cytosol. SOR inhibits Raf signaling and the action of other multikinases leading to apoptosis, while MK-siRNA prevents the translation of MK-mRNA into MK protein eliminating its proliferative, anti-apoptotic and chemoresistant functions which consequently, increases the sensitivity of HCCs to SOR. Abbreviations: HCC, Hepatic cancer cell; MK, Midkine; LRP1, LDL-receptor-related protein 1; ALK, anaplastic lymphoma kinase; mRNA, messenger RNA; siRNA, small interfering RNA; Raf, rapidly accelerated fibrosarcoma tyrosine kinase effector; SOR, sorafenib; NP, nanoparticle.

1.5. CONCLUSIONS

We designed a novel targeted pH-sensitive LNPs which successfully and selectively delivered both SOR and MK-siRNA to HCCs. Cytotoxicity studies confirmed the value of using a combination of SOR and MK-siRNA. The optimization of different formulation variables resulted in the production of a highly-efficient and highly-specific delivery system (SP94-NPs). The SP94-NPs showed a high selectivity for HCCs compared to other cancerous and normal cells, which was not observed in the case of STR-R8-NPs. The optimized SP94-NPs had the following advantages: efficient and selective uptake into HCCs, efficient and selective cytotoxicity to HCCs, efficient MK gene silencing, high biosafety of the carrier and a smart pH-responsive drug release profile. These collective advantages clearly delineate our goal of creating a highly-selective and efficient co-delivery system for the combined chemotherapy and gene therapy of HCC.

CHAPTER 2

Design and Optimization of Ultra-Small Lipid Nanoparticles for Synergistic Highly-Efficient Eradication of Hepatocellular Carcinoma In Vivo

CHAPTER 2

2.1. INTRODUCTION

In the previous chapter, we demonstrated that MK-siRNA increases the sensitivity of HCC cells to SOR *in vitro* which offers a potential synergistic combination. Yet, the *in vivo* application of HCC gene therapies is challenged by multiple obstacles. The leaky vasculature and poor lymphatic drainage in most tumors make them accessible for nano-sized drug delivery systems by Enhanced Permeability and Retention (EPR) effect.[125] However, HCC is a stroma-rich tumor depositing a dense extracellular matrix of collagen, hyaluronan and fibroblasts which functions as a physical barrier hindering nanomedicines from accessing the tumor cells. Such barrier mostly accounts for the failure of Doxil®, the first FDA-approved cancer nanomedicine, in the treatment of HCC and similar stroma-rich tumors.[218] The challenges associated with the *in vivo* delivery to HCC have been schemed previously in **Fig. 4**. Modulating the tumor microenvironment via anti-stromal agents has been proposed, yet, the complexity of such systems is a demerit.[90]

Microfluidic devices has led a revolution in nanotechnology with the ability of tuning the particle size for diverse applications. The concept of ultra-small nanoparticles with average diameter less than 100 nm has been introduced as an alternative to enhance the penetration through the stroma barrier in tumors. Nevertheless, these nanoparticles are challenged by poor serum stability limiting their *in vivo* efficiency, especially for the delivery of nucleic acids.[219]

In the current chapter, we applied invasive lipid nanoparticle production microfluidic device (iLiNP) developed by our partners[220] to generate ultra-small lipid nanoparticles (usLNPs) co-encapsulating SOR and MK-siRNA for the synergistic *in vivo* eradication of HCC in mice. The device is schemed in **Fig. 24**. We designed a step-by-step optimization strategy to cope with the successive challenges hindering the *in vivo* gene delivery to HCC including pharmacokinetics, tumor penetration, selectivity and endosomal escape. We tweaked the composition and physico-chemical properties of the usLNPs and explored their impact on the nanoparticles' fate and the delivery performance to elucidate the optimum conditions. The optimized usLNPs were subjected to extensive *in vivo* evaluation prior to therapeutic application. Then, the therapeutic potential against aggressive HCC model in mice was investigated recruiting very low dose of SOR and siRNA to achieve potency and avoid side effects. Deep evaluation of the therapeutic performance of our usLNPs as well as their biosafety were performed to increase the potential for clinical application.

The simple, rapid and economic one-step preparation method of our nanoparticles would be beneficial for scalable industrial application.

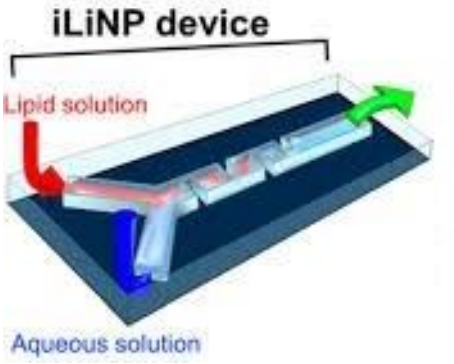

Figure 24. Schematic illustration for iLiNP microfluidic device (adapted from Kimura N. *et al.*[220]).

2.2. Experimental

2.2.1. Materials

In addition to those mentioned in Chapter 1, the following materials were used:

Heparin sodium and Sodium dodecyl sulfate (SDS) were obtained from Sigma-Aldrich, USA. 2-morpholinoethanesulfonic acid monohydrate (MES) was obtained from Wako, Japan. Matrigel® solution was obtained from Corning, USA. Alexa Fluor 488-labeled siRNA was obtained from Qiagen, USA. Amicon centrifugal filtration units (100 KDa) were obtained from Merck Millipore, USA.

2.2.2. Animals

Male BALB/c nude mice (4-6 weeks old) were purchased from Sankyo laboratories, Japan and they were kept in sterile, pathogen-free (SPF) environment. The experimental protocols were reviewed and approved by the Hokkaido University Animal Care Committee according to the ethical guidelines for handling laboratory animals. Animals had free access to food and water during experiments.

2.2.3. Methods

In addition to the methods described in Chapter 1, the following methods were adopted:

2.2.3.1. Creation of HCC tumor model in mice

For the creation of aggressive HCC mouse model in mice, HepG2 cells were cultured as described above. Cells in the logarithmic growth phase were harvested, counted, resuspended in a mixture of sterile PBS and Matrigel® (1:1 v/v) and kept over ice. Matrigel® helps in the

localization of the inoculated cells and increases their aggressiveness and growth rate.[221] Cells were inoculated subcutaneously in the right flanks of mice at a density of 2×10^6 cells/mouse. The growth of the tumors was monitored and evaluated with a digital caliper (Mitutoyo, Japan) using the following equation:

Tumor volume (mm^3) = Length × $(Width)^2$ × 0.52 (**Equation 7**) [222]

Animals with tumor volume 100-200 mm^3 were used in the gene knockdown experiments.

2.2.3.2. Preparation of LNPs by microfluidic mixing

Our previously-developed invasive lipid nanoparticle production microfluidic device (iLiNP) was employed.[220] Lipids and SOR were dissolved in Ethanol to form the organic phase (7.5 mM) while siRNA was dissolved in acidic buffer (pH 4) to form the aqueous phase (1.25 μM). The two phases were rapidly mixed through the iLiNP device with a total flow rate of 500 μL/minute. The aqueous phase to organic phase flow rate ratio, the buffer system used and the lipid composition were varied to tune the size of the formed LNPs. LNPs were dialyzed against MES buffer (20 mM, pH 6) for 2 hours followed by overnight dialysis against HEPES buffer (10 mM, pH 7.4) or PBS (pH 7.4) for the gradual increase of the pH and removal of Ethanol. LNPs solution was finally concentrated through Amicon filter units and resuspended in 10 mM HEPES buffer or PBS (pH 7.4).

2.2.3.3. Biodistribution of the prepared LNPs

LNPs were labeled by DiD (0.1 mol%) and administered intravenously to HCC-bearing mice via the marginal tail vein at siRNA dose of 0.5 mg/Kg. 24 hours following the administration, mice were euthanized and the tumors as well as major organs were collected.

Biodistribution was visualized using FluorVivo™ IVIS *in vivo* imaging system (INDEC Biosystems). In addition, to ensure accurate estimation of the tumor accumulation, DiD in the collected organs/tumors was extracted by 1% sodium dodecyl sulfate (SDS) solution and assayed using a microplate reader (Tecan Infinite M200) at excitation/emission wavelengths of 641/685 nm, respectively. A pre-constructed calibration curve was used to calculate the percentage of the injected dose distributed to each gram of the investigated tissues (%ID/g tissue).[222]

2.2.3.4. Evaluation of the in vivo gene knockdown activity

HCC-bearing mice were injected with LNPs encapsulating MK-siRNA intravenously via the marginal tail vein. 24 hours post-injection, mice were euthanized and the tumors as well as the major organs were harvested, immersed in liquid nitrogen and kept at -80 °C. 20 mg samples of the investigated tissues were homogenized with 500 µL Tri reagent in PreCellys 24 homogenizer (Bertin Technologies, France). The supernatant was collected, mixed with chloroform and processed similarly to what was described in the relevant section in Chapter 1.

For comparing the gene expression of diverse HCC markers in the different treatment groups, the mRNA expression in each group was normalized to that of HEPES buffer-treated group.

In addition to the oligonucleotide primers listed in Chapter 1, the primers listed in **Table 12** were used.

Table 12. Sequences of additional primers used in the *in vivo* study.

Gene		sequence (5'→3')
Human AFP	Forward	GCA GAG GAG ATG TGC TGG ATT G
	Reverse	CGT GGT CAG TTT GCA GCA TTC TG
Human OSP	Forward	CGA GGT GAT AGT GTG GTT TAT GG
	Reverse	GCA CCA TTC AAC TCC TCG CTT TC
Human VEGF-1	Forward	CTA CCT CCA CCA TGC CAA GT
	Reverse	GCA GTA GCT GCG CTG ATA GA

2.2.3.5. Evaluation of the circulation time of LNPs

DiD-labeled LNPs were administered to mice intravenously at siRNA dose of 0.5 mg/Kg. At different time intervals post administration, venous blood samples were collected and DiD was extracted by 1% sodium dodecyl sulfate (SDS) solution. DiD mean fluorescence intensity was assessed using a microplate reader (Tecan Infinite M200) as described above. The percentage of injected dose per each milliliter of blood (%ID/mL) was estimated from a pre-constructed calibration curve. The semi-logarithmic plot of %ID/mL versus time was analyzed using PK solver add-in linked to Microsoft Office Excel software and the various pharmacokinetic parameters were assessed.[223]

2.2.3.6. Evaluation of usLNPs stability

2.2.3.6.1. siRNA leakage and pharmacokinetic performance

To evaluate the pharmacokinetic performance of the optimum usLNPs and their encapsulated siRNA payloads, a double-labelling process was adopted. Lipids were labeled with DiD (0.1 mol%) while Alexa Fluor 488-labeled siRNA replaced the MK-siRNA cargo.

Following intravenous administration to mice (siRNA dose = 0.5 mg/Kg), venous blood samples were collected at different time points and the fluorescent probes were retrieved using 1% SDS solution. A microplate reader (Tecan Infinite M200) was used to determine the fluorescence intensity at excitation/emission wavelength of 495/519 nm and 641/685 nm for Alexa Fluor 488 and DiD, respectively. Pre-constructed calibration curves were used to individually-estimate the percentage of injected dose per each milliliter of blood (%ID/mL) for LNPs and siRNA. The semi-logarithmic plots of %ID/mL versus time were analyzed using PK solver add-in linked to Microsoft Office Excel software and the various pharmacokinetic parameters were assessed.

LNPs stability index (SI) was used as an indicator for siRNA leakage from the LNPs in the serum and was calculated by the following equation:

SI= AUC siRNA/AUC LNPs (**Equation 8**)

where AUC is the area under the semi-logarithmic curve of %ID/mL versus time. SI values close to unity are considered to be ideal.

2.2.3.6.2. Long-term ex-vivo stability

The optimized usLNPs were kept at 4 °C for 2 months. The physico-chemical characteristics were determined using a Zetasizer Nano ZS (Malvern Instruments Ltd, UK) and compared with the initial values at zero-time.

2.2.3.7. Therapeutic potential of usLNPs

The optimum usLNPs encapsulating various payloads were administered to HCC-bearing mice intravenously each three days for overall seven shots, starting from the 7th day post tumor challenge. Mice

were terminated three days after receiving the last treatment dose. Treatment schedule is schemed in **Fig. 25**. The optimum doses of SOR and MK-siRNA (2.5 mg/Kg and 0.5 mg/Kg, respectively) were selected according to individual dose-response curves.

In a separate study, the survival of the mice receiving different treatments was monitored after the end of treatment until 60 days post tumor challenge and Kaplan–Meier survival curves were constructed using Graphpad prism 8 software.

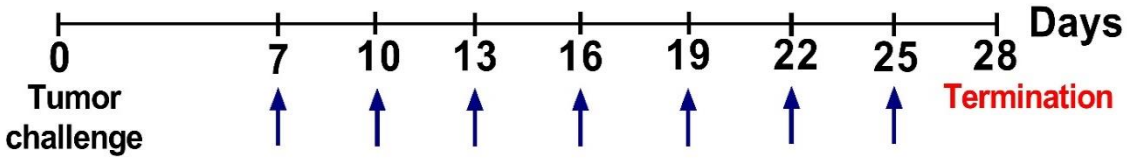

Figure 25. The protocol of anticancer treatment applied throughout this study. Arrows represent the dose timing.

2.2.3.8. Verification of the synergism between SOR and MK-siRNA

The *in vivo* therapeutic anticancer effect obtained at different SOR and MK-siRNA doses was analyzed using Chou and Talalay mathematical model and the combination index (CI) values were calculated using CompuSyn software. CI<1 suggests a synergistic relationship, CI=1 suggests additive relationship while CI>1 suggests antagonism.[224]

2.2.3.9. Immunohistostaining of HCC markers in tumors

Tumor tissues harvested from the different treatment groups at the end of treatment were immediately fixed in 4% paraformaldehyde at 4 ºC overnight, washed, dehydrated in ascending concentrations of ethanol, cleared in xylene and impregnated in melted paraffin. 3 µm paraffin sections were prepared and used for immunohistostaining of the investigated HCC markers.

Following deparaffinization and antigen retrieval, the sections were incubated with the specific primary antibodies and biotin-conjugated goat anti-rabbit secondary antibodies, followed by incubation with streptavidin-peroxidase conjugate for 30 minutes at room temperature according to streptavidin-biotin method reported previously.[225] The antibodies used, working dilutions and methods for antigen retrieval are listed in **Table 13**. The color for a positive reaction was developed by incubating the sections in a 3,3-diaminobenzidine tetrahydrochloride-H2O2 solution and the nuclei were lightly stained with Mayer's hematoxylin. The BZ-X710 inverted microscope (Keyence, Osaka, Japan) was used for capturing images for histometric measurements. The average results from five mice in each group were expressed as positive cells (%) or positive area (%) relative to the examined field.

Table 13. List of antibodies used in immunohistostaining of various HCC markers, working dilutions and methods used for antigen retrieval.

Antibody	Source	Working dilution	Antigen retrieval method	Heating conditions
Rabbit anti-CC3	Cell signaling	1:300	10 mM citrate buffer (pH 6)	105ºC, 15 min
Rabbit anti-Ki-67	Abcam	1:150	10 mM citrate buffer (pH 6)	105ºC, 20 min
Rabbit anti-CD31	Abcam	1:200	10 mM citrate buffer (pH 6)	105ºC, 15 min
Mouse anti-AFP	BioLegend	1:300	10 mM citrate buffer (pH 6)	105ºC, 15 min

2.2.3.10. Biosafety of usLNPs

Acute and chronic toxicity studies were conducted to confirm the biosafety of the optimum usLNPs. In acute toxicity study, HCC-bearing mice were injected intravenously with usLNPs at siRNA dose of 3 mg/Kg (30-fold higher than the half-maximal effective silencing dose, ED_{50}). 24 hours post administration, serum samples were collected, centrifuged for 10 minutes (10,000 rpm, 4 °C) and the plasma was separated. Various markers associated with hepato-renal functions were assayed according to the standard methods listed in **Table 14**. JCA-BM6050 automatic analyzer (JEOL, Tokyo, Japan) was used and the assay was performed at 37ºC. The results were normalized to HEPES buffer-treated mice with similar tumor volume.

In chronic toxicity study, serum was collected from mice at the end of repeated treatment by usLNPs encapsulating various cargos according to the same schedule schemed in **Fig. 25**. SOR and siRNA doses were adjusted to 2.5 mg/Kg and 0.5 mg/Kg, respectively. Hepato-renal function markers were assayed in plasma and normalized to HEPES buffer-treated mice.

Furthermore, histo-pathological examination for the major organs of mice (liver, lung, kidney, heart) was carried out after chronic treatment to detect any potential organ injury as described below.

Table 14: Standard methods used in the assay of plasma hepatorenal markers in mice.

Plasma biomarker	Standard method used
Aspartate aminotransferase (AST)	Japan Society of Clinical Chemistry (JSCC) Recommended method
Alanine aminotransferase (ALT)	JSCC Recommended method
Lactate dehydrogenase (LDH)	JSCC Recommended method
Alkaline phosphatase (ALP)	JSCC Recommended method
Cholinesterase (ChE)	Butyrylthiocholine-DTNB method
Creatine kinase (CK)	JSCC Recommended method
Lipase (LIP)	1,2-diglyceride substrate TOOS method
Glucose (GLU)	Enzymatic method (HK-G6PDH)
Total cholesterol (T-CHO)	Enzymatic method (CE-COD-POD)
Triglycerides (TG)	Enzymatic method (LPL-GK-GPO), Free glycerol elimination method
Non-esterified fatty acids (NEFA)	Enzymatic method (acylation of coenzyme A , CoA)
Total protein (TP)	BUIret method
Albumin (ALB)	BCG method
Blood urea nitrogen (BUN)	Enzymatic method (Urease-GLDH)
Creatinine (CRE)	Enzymatic method (Creatinine amidohydrolase-Creatinine amidinohyrolase-SOX-POD)
Calcium (Ca)	o-CPC method
Inorganic phosphorus (IP)	Enzymatic method (PNP-XOD-POD)
Sodium (Na)	Ion selective electrode method
Potassium (K)	Ion selective electrode method
Chloride (Cl)	Ion selective electrode method
Total bilirubin (T-Bil)	Stabilized diazo method

2.2.3.11. Histo-pathological examination of the major organs after chronic treatment

Three µm paraffin sections of the fixed tissues were subjected to hematoxylin and eosin (H&E) staining at room temperature. Digital images were acquired with the BZ-X710 microscope (Keyence, Osaka, Japan). Photos were compared with HEPES buffer-treated mice to check for any signs of abnormalities or organ damage.

2.3. RESULTS

2.3.1. *In vivo* evaluation of the previously-prepared LNPs based on *in vitro* optimization

We tested the *in vivo* potential of our LNPs that have been optimized *in vitro* as described in Chapter 1. Despite their high *in vitro* efficiency and selectivity, the aforementioned LNPs failed to accumulate in the tumor tissue following intravenous administration to HCC-bearing mice while they only distributed between liver and spleen (**Fig. 26A**). About 40% MK gene knockdown activity was shown in the healthy liver while no significant silencing was observed in the tumor. Presence or absence of SP94 peptide did not significantly affect the delivery performance to HCC at this stage (**Fig. 26 B**). Upon evaluating the pharmacokinetic behavior of these LNPs, they exhibited very short circulation time with mean residence time less than 20 minutes (**Fig. 26C**).

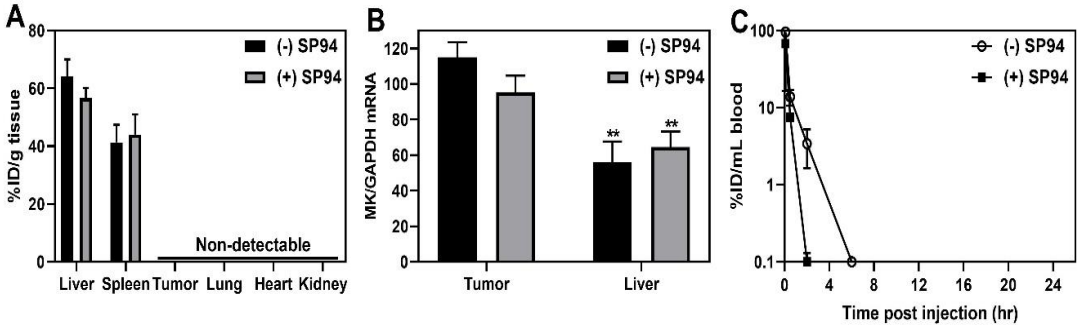

Figure 26. *In vivo* evaluation of the previously-optimized LNPs (YSK05/EPC/Cholesterol/PEG-SP94 4:3:3:0.5) in HCC-bearing mice. A) Biodistribution in major organs 24 hours after intravenous administration of DiD-labeled LNPs. B) MK gene silencing activity in HCC tumor versus healthy liver 24 hours after intravenous administration. **P<0.01 versus the tumor. C) Circulation time profile of DiD-labeled LNPs in mice after intravenous administration. In all treatments, MK-siRNA dose was adjusted to 0.5 mg/Kg. N=3, the average was expressed ±standard deviation.

2.3.2. Optimization of the co-delivery LNPs for *in vivo* delivery to HCC

We attempted the optimization of our LNPs to accomplish the challenging delivery to HCC *in vivo*. First, we manipulated PEG-SP94 ratio in the LNPs to control their pharmacokinetics. Surprisingly, upon increasing the ratio from 5 to 10 mol%, circulation time was dramatically improved with MRT exceeded 9 hours. However, increasing such ratio to 15 mol% decreased the circulation time. Therefore, 10 mol% ratio was considered to be the optimum (**Fig. 27A**). The optimum SP94 density did not significantly impair the circulation time of the PEGylated LNPs (**Fig. 27B**). At the optimum PEG-SP94 ratio, LNPs could induce about 30% MK gene silencing in the HCC tumor at MK-siRNA dose of 0.5 mg/Kg. Nevertheless, stronger gene silencing was detected in the healthy liver (~50%). No gene silencing could be obtained when SP94 peptide was eliminated from the system (**Fig. 27C**).

Second, we applied microfluidic device, iLiNP, to tune the particle size aiming at improving LNPs penetration through the stroma barrier in HCC. Operating conditions were varied and their impact on the LNPs physico-chemical properties was studied. Increasing the aqueous phase: organic phase flow rate ratio from 2:1 to 4:1 linearly reduced the average particle diameter from 220.14±8 nm to 104±9.5 nm. However, further increase of such ratio above 4:1 did not reduce the average particle size while having a negative effect on the homogeneity of particle size distribution (PDI higher than 0.3) (**Table 15**). The preparation of LNPs in acidic HEPES buffer (pH 4) followed by gradual increase in pH via dialysis and final replacement with neutral HEPES buffer (pH 7.4) maintained a moderate particle size (~100 nm) and PDI (~0.2) which could not be obtained using acetate or citrate buffers under the same

conditions (**Table 16**). Aiming at further reduction of particle size, we attempted the increase in the cationic component (YSK05) ratio to facilitate compact packaging of siRNA. Increasing YSK05 ratio from 40 to 70 mol% resulted in a linear reduction in the particle size down to 50 nm (**Table 17**). We then evaluated the MK gene knockdown activity of these nanoparticles in the tumor versus the healthy liver. Interestingly, reducing the particle size from 160 nm to 70 nm dramatically improved the selective knockdown activity in the tumor compared to the healthy liver. Nevertheless, smaller LNPs obtained by increasing YSK05 ratio above 50 mol% showed higher affinity to the healthy liver and diminished silencing activity in the tumor (**Fig. 27D**). We considered 70 nm LNPs (50 mol% YSK05) to be the optimum. To avoid harming the liver, additional DSPE-PEG_{2K}-MA was inserted to mask the hepatic recognition of our LNPs. At optimum ratio (3 mol%), our LNPs maintained strong MK gene silencing in the tumor while demonstrating minimal effect on the healthy liver (**Fig. 27E**). Moreover, the particle size of LNPs was further reduced to 60 nm by the effect of the additional PEG (**Table 18**). The activity in the tumor was impaired upon increasing such ratio to 5 mol% despite having smaller particle size.

Third, we screened diverse helper lipids aiming at improving the endosomal escape capability of our LNPs. MK-siRNA dose was reduced to 0.3 mg/Kg to allow the recognition of the difference between the investigated helper lipids. Interestingly, LNPs containing DOPE showed the most superior gene silencing compared to EPC or DOPC (**Fig. 27F**). All the investigated helper lipids maintained the HCC selectivity.

A summary of the *in vivo* optimization process is schemed in **Fig. 28**. The optimum LNPs had the following composition (YSK05/DOPE/Cholesterol/PEG-SP94/PEG 5:2:3:1:0.3) and are referred

to as ultra-small lipid nanoparticles (usLNPs) in the next sections. A schematic representation for the composition of the optimized usLNPs is shown in **Fig. 29A**. Examination by TEM indicated the spherical morphology of usLNPs with an average diameter of 50-60 nm, in which siRNA is condensed as a core material surrounded by lipid membrane (**Fig. 29B**). Dynamic light scattering revealed particle size distribution with narrow polydispersity (**Fig. 29C**). The physico-chemical characteristics of usLNPs compared to the original LNPs are shown in **Table 19**.

The optimized usLNPs prepared by microfluidic mixing had higher SOR loading capacity compared to those prepared by thin lipid film hydration method. Although the SOR encapsulation efficiency (EE) decreased by increasing the drug loading (mol%) in both cases, microfluidic-based usLNPs demonstrated ~70% EE at high drug loading (10 mol%) compared to ~40% in case of hydration-based LNPs. At 7.5 mol% drug loading, SOR EE exceeded 90%, so this ratio was considered in the next experiments (**Table 20**).

In vitro dissolution study revealed a pH-responsive controlled-release profile for SOR from the optimized usLNPs favoring the acidic pH (5.5) compared to physiological pH (7.4). usLNPs sustained the SOR release for 60 hours without demonstrating initial burst release commonly seen with other nanomedicines (**Fig. 30**).

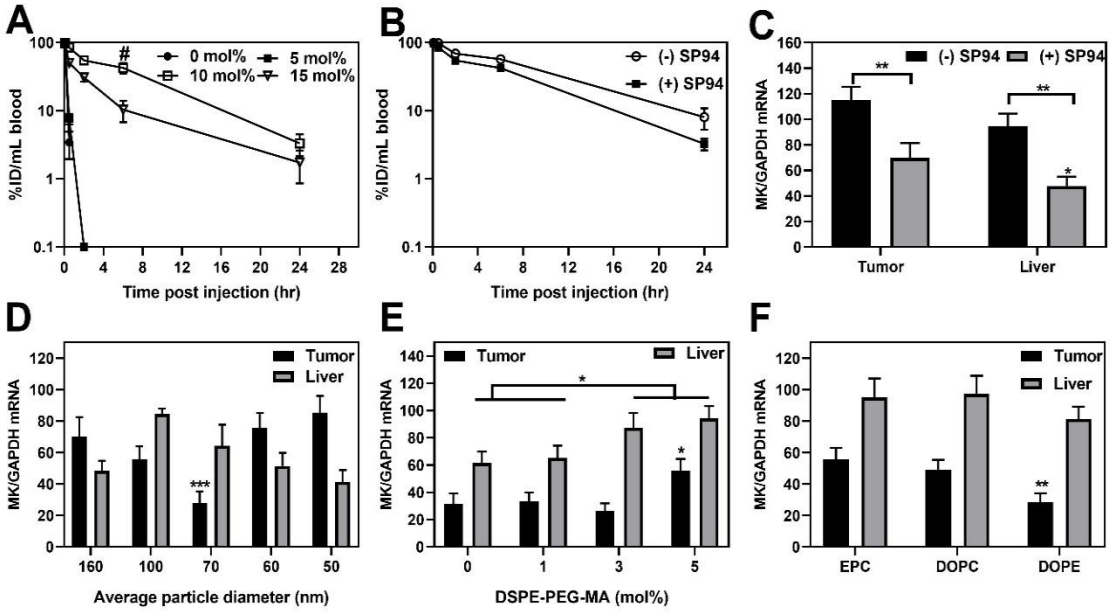

Figure 27. Optimization of LNPs for siRNA delivery to HCC tumor in mice. A) Effect of PEG-SP94 ratio on circulation time profile of DiD-labeled LNPs after intravenous administration in mice. #P<0.0001 versus other ratios. B) Effect of SP94 peptide on circulation time profile of DiD-labeled LNPs modified with 10 mol% PEG±SP94 after intravenous administration. C) Evaluation of MK gene knockdown in HCC tumor versus healthy liver 24 hours after intravenous administration of LNPs modified with 10 mol% PEG±SP94. *P<0.05 versus tumor in case of (+) SP94, **P<0.01 for (+) versus (-) SP94. D) Effect of average particle diameter of LNPs prepared by microfluidic mixing on MK gene knockdown in HCC tumor versus healthy liver 24 hours after intravenous administration in mice.***P<0.001 versus the tumors in case of the other investigated particle diameters. E) Impact of inserting additional DSPE-PEG_{2K}-MA into the optimized LNPs on the selective MK gene silencing in HCC tumor versus healthy liver 24 hours after intravenous administration in mice. *P<0.05 for the tumor in case of 5 mol% ratio versus the tumors in case of the other ratios, and for the livers in case of 3 and 5 mol% ratios versus the livers in case of the other ratios. F) Effect of helper lipid type on MK gene silencing in HCC tumor versus healthy liver 24 hours after intravenous administration in mice. **P<0.01 versus the tumors in case of the other helper lipids. In all treatments, MK-siRNA dose was adjusted to 0.5 mg/Kg except in F, where the dose was reduced to 0.3 mg/Kg. N=3, the average was expressed±standard deviation.

Table 15. Effect of aqueous phase: organic phase flow rate ratio on the physico-chemical properties of LNPs prepared by iLiNP microfluidic mixer (N=6, average±standard deviation).

Flow rate ratio	Average diameter (nm)	PDI	Zeta potential (mV)	SOR EE (%)	siRNA EE (%)
2:1	220.14±8	0.325±0.045	-15.2±3.55	90±8.25	75±6.4
3:1	146.3±11.2	0.271±0.061	-16.5±6.5	91.5±9.8	77.5±8.5
4:1	104±9.5	0.217±0.024	-13.8±7.73	100±5.5	80.76±9.9
5:1	111.7±6.12	0.315±0.042	-10.5±5.15	95±9	82±5.5
9:1	100±6.16	0.371±0.084	-12.4±4.83	80±11.25	71.2±8.9

Table 16. Effect of the used buffer system on the physico-chemical properties of LNPs prepared by iLiNP microfluidic mixer (N=6, average±standard deviation).

Buffer system	Average diameter (nm)	PDI	Zeta potential (mV)	SOR EE (%)	siRNA EE (%)
HEPES	110.4±8	0.225±0.029	-11.8±5.57	100±8.25	85±7.4
Citrate	180.3±14.2	0.386±0.074	-16.4±7.9	90.8±10	80.5±6.5
Acetate	164±9.12	0.355±0.064	-18.1±5.22	90±8.15	82.21±6.8

Table 17. Effect of the used YSK05 ratio on the physico-chemical properties of LNPs prepared by iLiNP microfluidic mixer (N=6, average±standard deviation).

YSK05 ratio (mol%)	Average diameter (nm)	PDI	Zeta potential (mV)	SOR EE (%)	siRNA EE (%)
40	112.43±8	0.207±0.035	-14.5±6.55	100±7.5	85±7.14
50	69.47±6.9	0.154±0.011	-11.4±5	96.5±4.8	92.5±6.5
60	60.22±5.7	0.135±0.028	-16.7±6.83	100±8.5	95.16±7.94
70	50.64±5.12	0.144±0.022	-14.3±6.9	100±9.5	92±6.5

Table 18. Effect of the ratio of additional DSPE-PEG_{2K}-MA[A] on the physico-chemical properties of LNPs prepared by iLiNP microfluidic mixer (N=6, average±standard deviation).

DSPE-PEG_{2K}-MA (mol%)	Average diameter (nm)	PDI	Zeta potential (mV)	SOR EE (%)	siRNA EE (%)
0	71.74±5.12	0.139±0.015	-14.8±4.5	97.3±5.5	91.8±7.1
1	65.3±7.5	0.116±0.014	-16.9±5.45	94.8±9.8	92.5±5.5
3	61.4±6.4	0.092±0.008	-19.5±3.88	100±8.1	90.21±6.6
5	50.17	0.095±0.013	-24.67±6.1	90.8±7.7	84.12±5.71

[A] Additional amount of DSPE-PEG_{2K}-MA (0-5 mol%) was added to fill the interspaces in the hydrophilic shield of LNPs aiming to mask them from being recognized by ApoE.

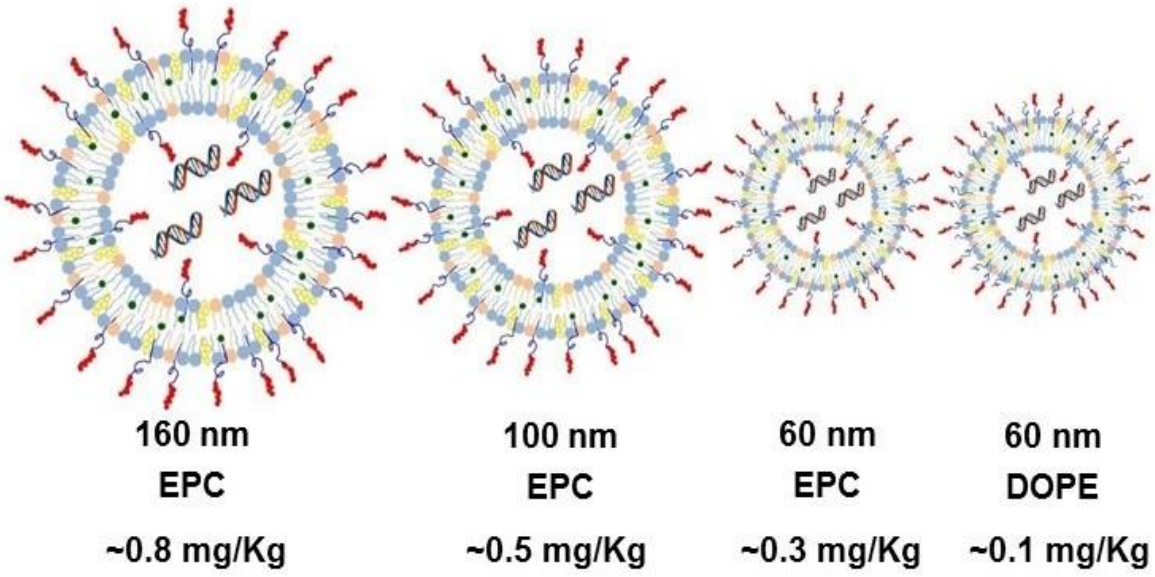

Figure 28. A Schematic representation summarizing LNPs optimization process to achieve maximum MK gene silencing in the tumor tissue after intravenous administration to HCC-bearing mice. The average particle diameter and helper lipid used correlate with the siRNA half-maximal effective dose (ED_{50}) in the tumor.

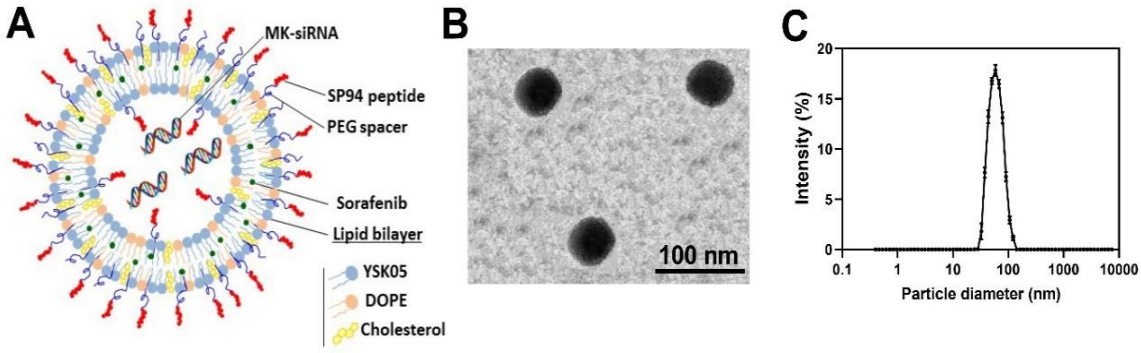

Figure 29. Structure and morphology of the optimized usLNPs. A) A Schematic representation for the composition of optimized usLNPs. B) TEM image showing the particle size and morphology of optimized usLNPs. C) Particle size distribution of the optimized usLNPs as measured by dynamic light scattering (average±standard deviation, N=6).

Table 19. Physico-chemical properties of the optimized usLNPs versus the original LNPs (average ± standard deviation, N=6).

Formulation	Average diameter (nm)	PDI	Zeta potential (mV)	SOR EE (%)	siRNA EE (%)
Original LNPs	160±9.4	0.235±0.035	-10.5±3.75	91.5±9.8	77.5±8.5
Optimized usLNPs	60.47±6.9	0.101±0.011	-17.4±5	96.5±4.8	94.5±6.5

Table 20. Effect of the drug loading (mol%)[A] on SOR encapsulation efficiency in LNPs prepared by thin lipid film hydration method versus microfluidic mixing (N=6, average±standard deviation).

Drug loading (mol%)	SOR EE (%)	
	Hydration method	Microfluidic mixing
5	90.12±8.22	100±6.12
7.5	73.13±9.62	92.16±6.36
10	43.4±6.81	68.25±7.14

[A] Drug loading was calculated as molar ratio (%) of the total lipid amount (1500 nmole).

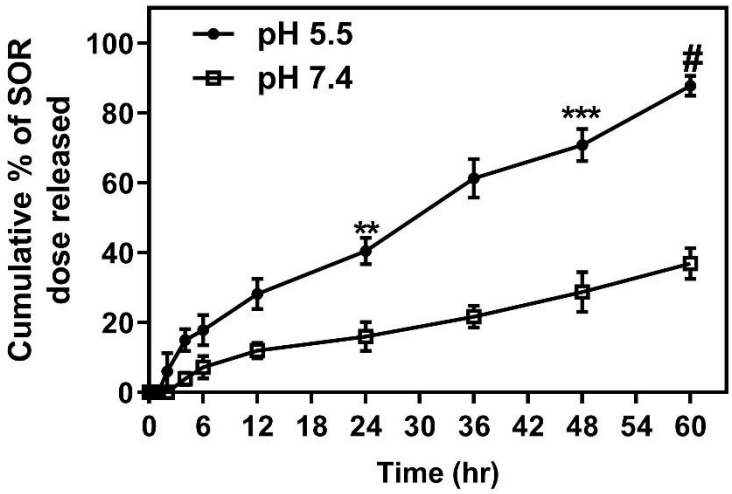

Figure 30. *In vitro* release of SOR from the optimized usLNPs at different pH conditions. **P<0.01, ***P<0.001, #P<0.0001 versus pH 7.4. The average of three independent experiments was considered and expressed±standard deviation.

2.3.3. *In vivo* evaluation of the optimized usLNPs

The optimized usLNPs were subjected to extensive *in vivo* evaluation to confirm their performance. Pharmacokinetic analysis revealed long circulation time with minimal siRNA leakage from the usLNPs (**Fig. 31A**). The estimated stability index (SI) obtained by comparing the area under siRNA and LNPs circulation curves (AUC_{siRNA}/AUC_{LNPs}) was 0.83 suggesting high serum stability in spite of the small particle size. Other calculated pharmacokinetic parameters are presented in **Table 21**. In addition, usLNPs demonstrated good shelf stability *ex-vivo*. No signs of particle aggregation could be detected after 2-month storage at 4 °C (**Table 22**).

The biodistribution of usLNPs was monitored 24 hours following intravenous administration. Our usLNPs showed efficient accumulation in HCC tumor (15% ID/g tissue) (**Fig. 31B-C**).

We screened different MK-siRNA doses (0.05-1 mg/Kg). Encapsulation of MK-siRNA into usLNPs exhibited high gene

knockdown activity in the tumor with a half-maximal effective dose (ED_{50})~0.1 mg/Kg. The maximum gene silencing activity (~80%) was obtained at a dose of 0.5 mg/Kg, which was selected for further therapeutic studies (**Fig. 31D**). No significant gene silencing could be obtained upon replacing MK-siRNA with a control siRNA (siCntrl).

In order to select the optimum SOR dose for potential therapeutic application, usLNPs were loaded with SOR and siCntrl and their therapeutic anticancer effect on HCC-bearing mice was monitored at various SOR doses (1.25-5 mg/Kg). Surprising, despite the relatively-low doses screened, significant inhibition in the tumor growth was observed which followed a dose-dependent manner (**Fig. 31E**). No significant body weight loss was observed in mice during the treatment (**Fig. 31F**).

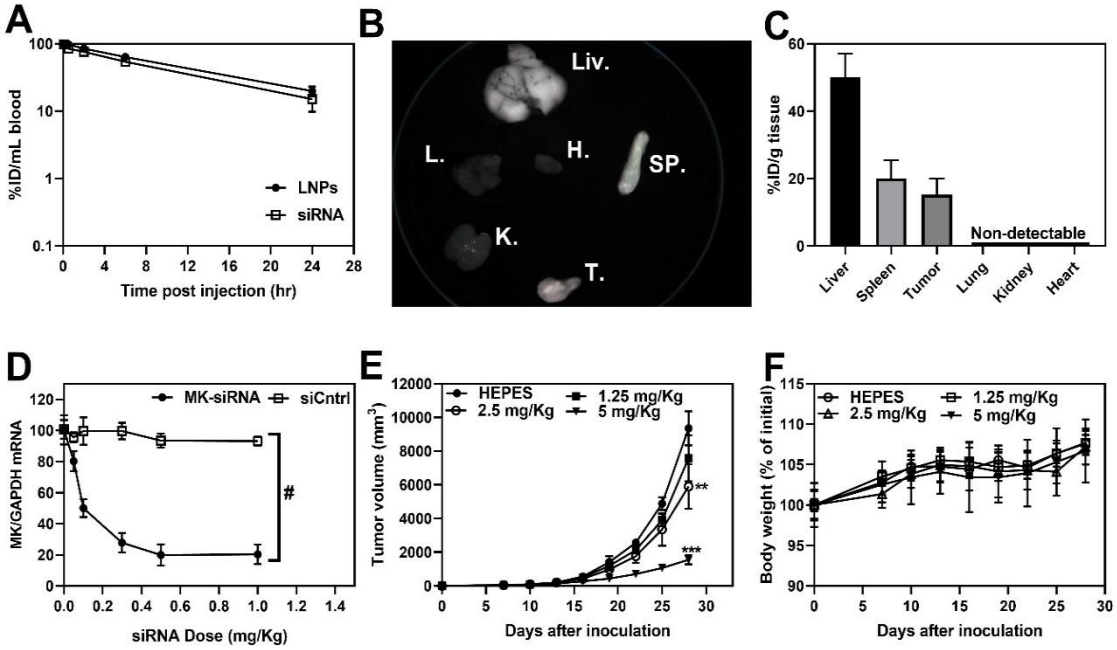

Figure 31. *In vivo* evaluation of the optimized usLNPs in HCC-bearing mice. A) Blood circulation time profile of usLNPs after intravenous administration in mice. DiD and Alexa Fluor 488 were used as fluorescent probes for lipids and siRNA, respectively. B) Biodistribution of DiD-labeled usLNPs in HCC-bearing mice 24 hours after intravenous administration as visualized by in vivo imaging system (IVIS). Liv., liver; SP., spleen; T., tumor; H., heart; L., lung, K., kidney. C) Quantitative biodistribution of DiD-labeled usLNPs in HCC-bearing mice 24 hours after intravenous administration. In panels A-C, siRNA dose was adjusted to 0.5 mg/Kg, N=3, results were expressed as average±standard deviation. D) Dose-silencing curve of MK-siRNA or siCntrl encapsulated in usLNPs measured in tumor tissues 24 hours after intravenous administration in HCC-bearing mice. #P<0.0001. N=3, the average is expressed±standard deviation. E) Effect of different doses of SOR loaded in usLNPs on the tumor growth in HCC-bearing mice. MK-siRNA was replaced with siCntrl to show SOR effect only. The protocol of the treatment is shown in **Fig. 25**. **P<0.01, ***P<0.001 versus HEPES-treated group. F) Changes of mice body weight during treatment with different doses of SOR-loaded usLNPs. In panels E-F, N=5 and the average is expressed±standard deviation.

Table 21. Pharmacokinetic parameters of the optimized usLNPs following intravenous administration to mice (siRNA dose=0.5 mg/Kg, N=3, average ± standard deviation).

Pharmacokinetic parameter	LNPs	siRNA
$t_{1/2}$ (h)	9.73±0.53	8.08±0.31
V (mL)	1.00±0.11	1.08±0.24
CL (mL/h)	0.07±0.015	0.09±0.019
AUC 0-t (%ID. h/mL)	1147.21±298	944.68±175.11
AUC 0-inf (%ID. h/mL)	1400.45±331.5	1083.03±227.1
AUMC (%ID. h^2/mL)	19653.03±981.9	12631.66±636.7
MRT (h)	14.03±2.8	11.66±1.95

Table 22. Changes in the physico-chemical properties of the optimized usLNPs after storage at 4 °C for 2 months (N=6, average±standard deviation).

	Average diameter (nm)	PDI	Zeta potential (mV)
Zero-point	62.33±5.25	0.091±0.013	-19.4±6.2
After 2 months	68.12±7.5	0.105±0.018	-16.3±4.38

2.3.4. Therapeutic application of the optimized usLNPs

Based on the previous results, we evaluated the therapeutic activity of our optimized usLNPs against aggressive HCC tumor in mice. The purpose of our integrative therapy approach was to maximize the therapeutic benefit at low SOR dose. Therefore, a low SOR dose (2.5 mg/Kg) was selected in combination with MK-siRNA (0.5 mg/Kg). At the end of treatment, usLNPs loaded with MK-siRNA monotherapy resulted in a low inhibitory effect on the tumor growth (~18%) while a moderate effect was shown by SOR+siCntrl (~40%). Surprisingly,

usLNPs encapsulating SOR+MK-siRNA resulted in dramatic eradication of the tumor (~85%) which much exceeded the additive values of individual monotherapies suggesting the presence of synergism between SOR and MK-siRNA (**Fig. 32A-B**). The interactive effect between SOR and MK-siRNA was statistically-significant, P(SOR*MK-siRNA)<0.001. Verification of the interaction by applying Chou and Talaly's model [224] favored the synergy hypothesis with combination index (CI) values less than the unity (**Table 23**). In a separate study, SOR+MK-siRNA combination extended the survival of mice after treatment cessation up to 60 days post tumor challenge which could not be achieved by other monotherapies (**Fig. 32C**).

The integrative treatment resulted in 3-fold downregulation in the gene expression of the characteristic HCC marker, Alpha fetoprotein (AFP), in the tumor tissues and 4-fold downregulation in the gene expression of Osteopontin (OSP) and vascular endothelial growth factor (VEGF-1) (**Fig. 32D**).

Furthermore, evaluation of biochemical markers by immunohistostaining of tumor tissues at the end of treatment revealed significant elevation of the apoptosis marker, cleaved caspase 3 (CC-3), and significant decrease in other markers associated with HCC growth including cell proliferation protein (Ki-67), Alpha fetoprotein (AFP) and cluster of differentiation 31 (CD31). These effects were prominent in mice that received SOR+MK-siRNA treatment (**Fig. 33**).

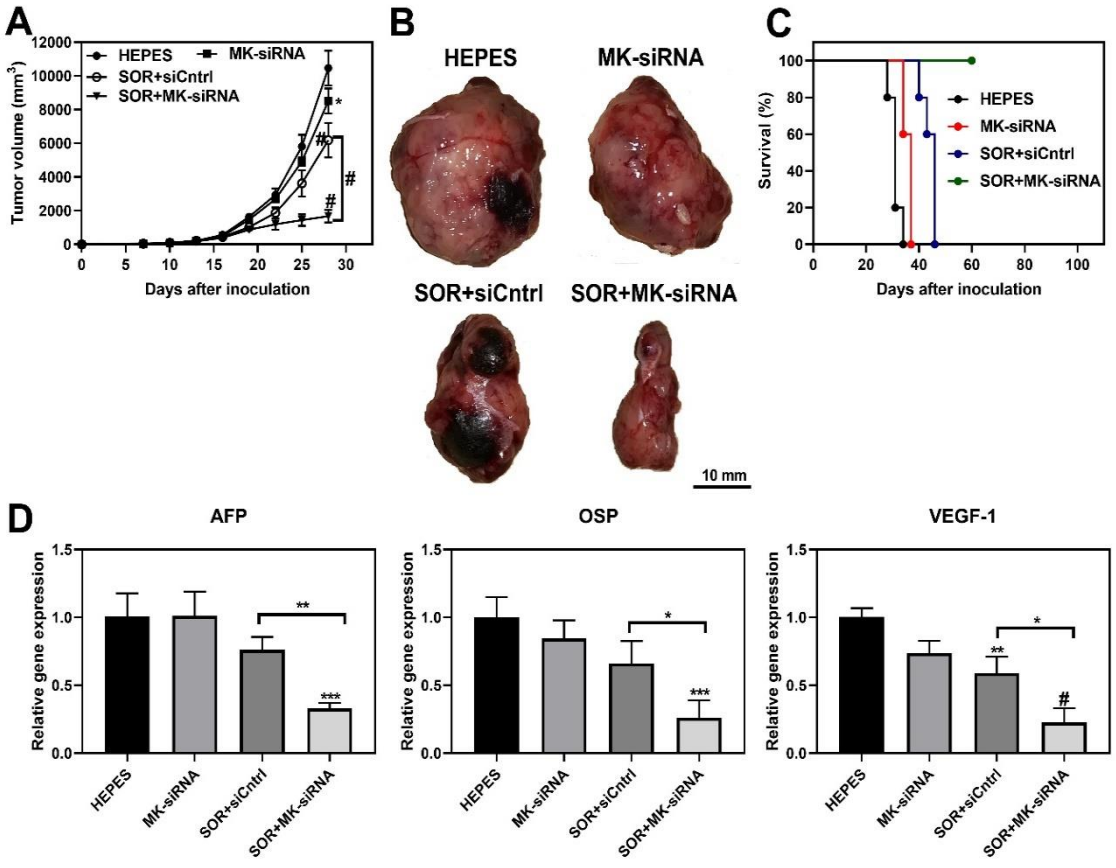

Figure 32. Therapeutic effect of usLNPs with different payloads on HCC-bearing mice. A) Effect on tumor growth. *P<0.05 versus HEPES, #P<0.0001 for SOR+siCntrl and SOR+MK-siRNA versus HEPES and for SOR+MK-siRNA versus SOR+siCntrl. Two-way ANOVA was applied to verify the interaction between SOR and MK-siRNA, P(SOR*MK-siRNA)<0.001. B) Representative photos showing tumor tissues from different treatment groups after the end of treatment. C) Survival rates of mice in different treatment groups followed-up until 60 days post tumor inoculation. D) Gene expression of various tumor markers evaluated in the tumor tissues of different treatment groups after the end of treatment. AFP, Alpha fetoprotein; OSP, Osteopontin; VEGF-1, Vascular endothelial growth factor-1. *P<0.05, **P<0.01 for SOR+MK-siRNA versus SOR+siCntrl, **P<0.01,***P<0.001, #P<0.0001 versus HEPES. In all panels, SOR dose and siRNA dose were adjusted to 2.5 mg/Kg and 0.5 mg/Kg, respectively. N=5, the average is expressed±standard deviation. Treatment schedule is shown in **Fig. 25**.

Table 23. Combination index (CI) values for SOR+MK-siRNA combination according to Chou and Talaly's model (N=5, the average response was considered).

SOR dose (mg/Kg)	MK-siRNA dose (mg/Kg)	Fa[A]	CI[B]
2.5	0.5	0.85	0.55
1.25	0.25	0.5	0.66
0.625	0.125	0.2	0.67

[A] Fa represents the average response, i.e. reduction in the tumor volume relative to the control and expressed as fraction from the unity.

[B] CI values were calculated using Compusyn® software, CI<1 suggests synergism.

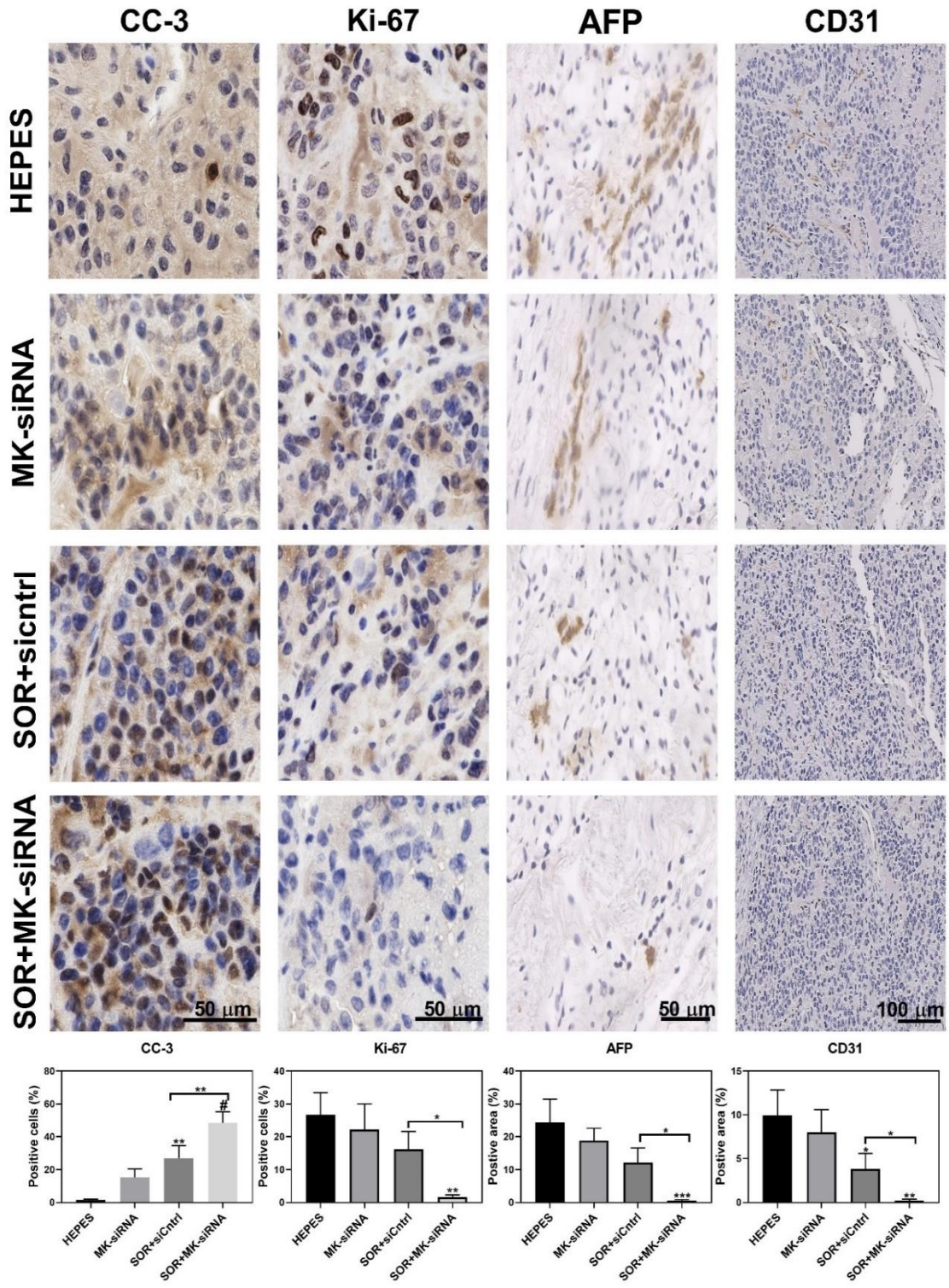

Figure 33. Evaluation of HCC markers in tumor tissues by immunohistochemistry after treatment of HCC-bearing mice with usLNPs encapsulating different payloads. Treatment protocol is shown in **Fig. 25**. Representative photos are presented while quantitative data were calculated from five mice in each treatment group and expressed as average±standard deviation. CC-3, Cleaved caspase 3; Ki-67,

Proliferation protein marker; AFP, Alpha fetoprotein; CD31, Cluster of differentiation 31. In CC-3: **P<0.01 for SOR+MK-siRNA versus SOR+siCntrl and for SOR+siCntrl versus MK-siRNA and HEPES, #P<0.0001 versus MK-siRNA and HEPES. In Ki-67 and AFP: *P<0.05 for SOR+MK-siRNA versus SOR+siCntrl, **P<0.01, ***P<0.001 versus MK-siRNA and HEPES. In CD31: *P<0.05 for SOR+MK-siRNA versus SOR+siCntrl and for SOR+siCntrl versus MK-siRNA and HEPES, **P<0.01 versus MK-siRNA and HEPES.

2.3.5. Biosafety of usLNPs

We evaluated the biosafety of our usLNPs on acute and chronic levels. In acute treatment, there was no significant elevation in hepato-renal function markers measured in the mice plasma 24 hours after the administration of usLNPs at siRNA dose 30-fold higher than ED_{50} which can represent a clinically-relevant dose (**Fig. 34A**). Moreover, chronic treatment with the aforementioned usLNPs was biosafe as suggested from the normal levels of plasma hepatorenal markers in the usLNPs-treated mice compared to HEPES buffer-treated mice. Alternatively, there was a significant reduction in the levels of Aspartate transaminase (AST), Alanine aminotransferase (ALT), Alkaline phosphatase (ALP), Lactate dehydrogenase (LDH) and Creatine kinase (CK) in mice received SOR+MK-siRNA treatment which correlate with the prognosis of HCC (**Fig. 34B**). Chronic treatment of mice with usLNPs encapsulating diverse payloads did not result in body weight loss (**Fig. 34C**). Furthermore, histo-pathological examination of the major organs following chronic treatment did not reveal any signs of injury or damage (**Fig. 35**).

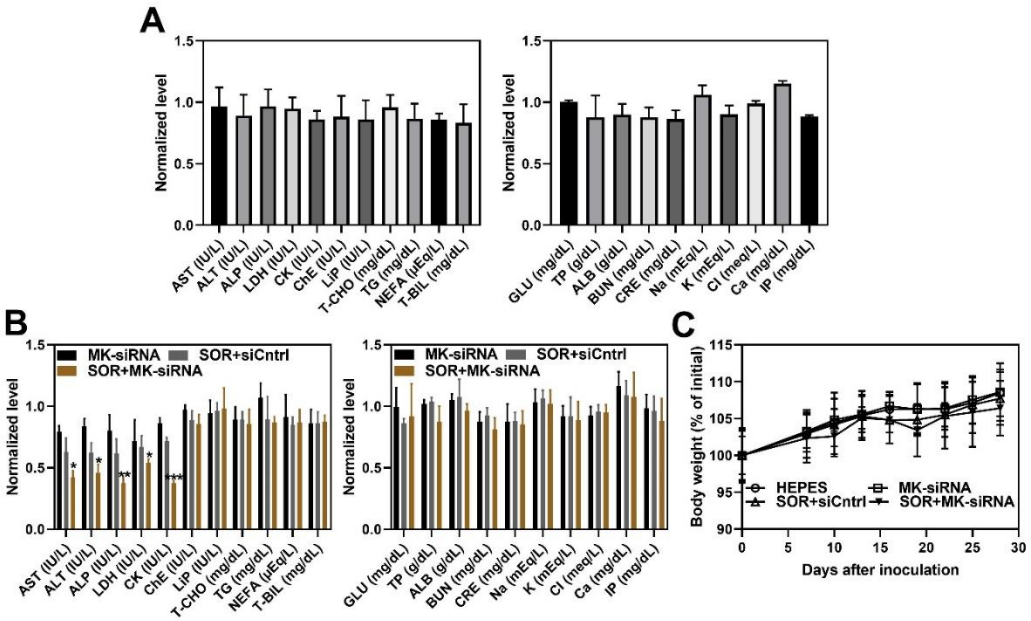

Figure 34. Evaluation of plasma hepato-renal function markers in HCC-bearing mice after acute and chronic treatment with usLNPs. A) Levels of plasma hepato-renal function markers after acute treatment of mice with a single intravenous dose of usLNPs (siRNA dose= 3 mg/Kg). Serum was collected 24 hours after administration and the plasma was separated for analysis. N=3, results were normalized to HEPES-treated mice with similar tumor volume and expressed as average±standard variation. B) Levels of plasma hepato-renal function markers after chronic treatment of mice with usLNPs encapsulating different payloads. Mice were treated on days 7,10,13,16,19,22 and 25 post tumor inoculation. SOR dose and siRNA dose were adjusted to 2.5 mg/Kg and 0.5 mg/Kg, respectively. Serum was collected on day 28 and the plasma was separated for analysis. N=5, results were normalized to HEPES-treated mice and expressed as average±standard variation. *P<0.05, **P<0.01, ***P<0.001 versus SOR+siCntrl and MK-siRNA. C) Changes in the body weight of mice after chronic treatment with usLNPs encapsulating different payloads. Treatment protocol was the same as in B, N=5, body weight data were expressed as average percentage of initial body weight (day 0) ± standard deviation. Abbreviations: AST, Aspartate transaminase; ALT, alanine aminotransferase; ALP, Alkaline phosphatase; LDH, Lactate dehydrogenase; CK, Creatine kinase; ChE, Cholinesterase; LiP, Lipase; T-CHO, Total cholesterol; TG, Triglycerides; NEFA, Non-Esterified Fatty Acid; T-BIL, Total bilirubin; GLU, Glucose; TP, Total protein; ALB, Albumin; BUN, Blood Urea nitrogen; CRE, Creatinine; Na, Sodium; K, Potassium; Cl, Chloride; Ca, Calcium; IP, Inorganic phosphate.

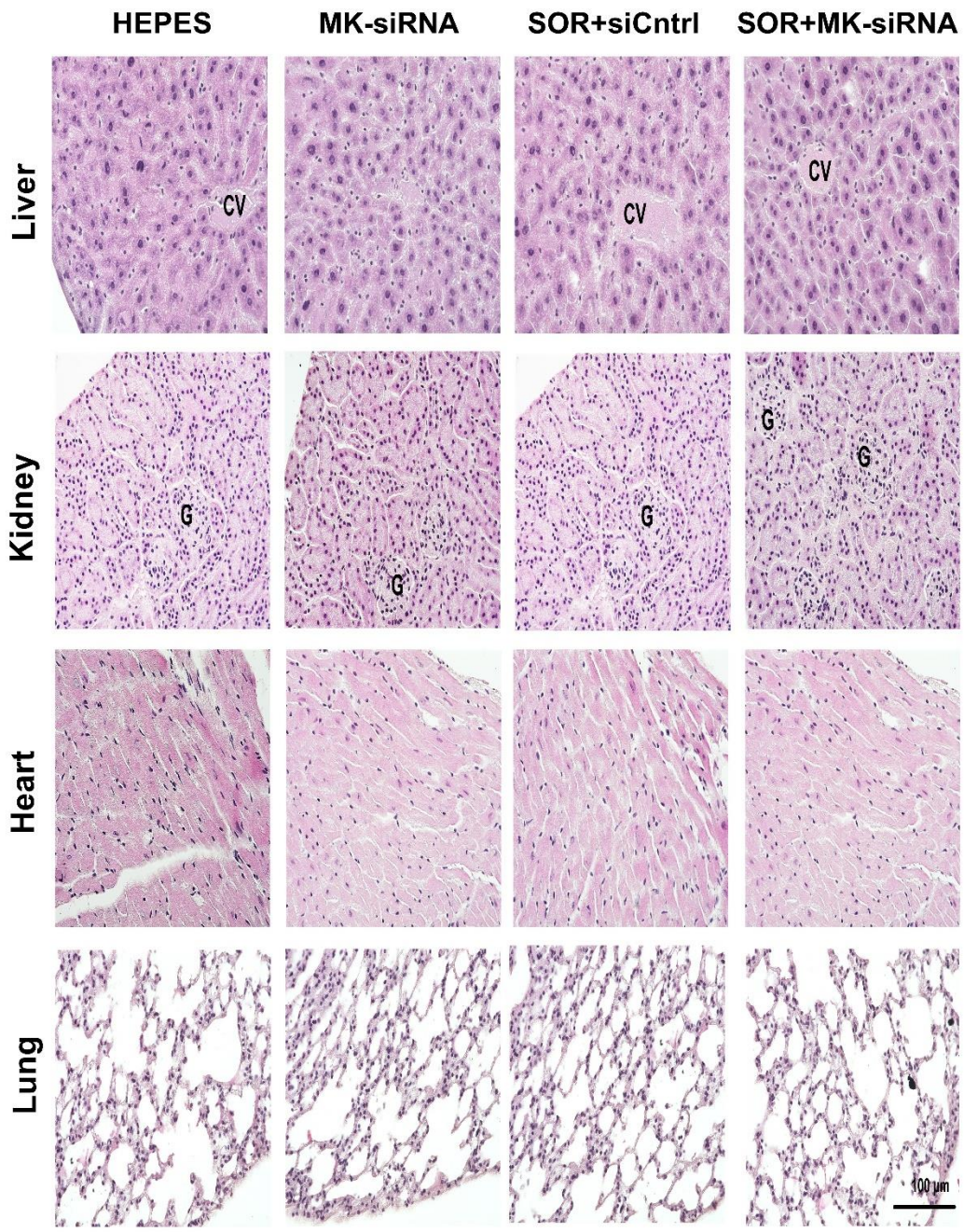

Figure 35. usLNPs with different payloads are biosafe upon chronic administration. Hematoxylin and eosin (H&E) staining in major organs shows no signs of organ damage. Mice were treated with usLNPs according to the protocol schemed in **Fig. 25**. Abbreviations: CV, central vein; G, glomerulus. Scale bar represents 100 µm.

2.4. DISCUSSION

Hepatocellular carcinoma is a global lethality without efficient therapeutic approaches. In the previous chapter, we introduced a novel combination of SOR, a potent multiple kinase inhibitor, and siRNA targeting the MK gene (MK-siRNA) for synergistic eradication of HCC *in vitro*. In the current chapter, we attempted the extension of such strategy to the *in vivo* application. We were challenged by multiple obstacles facing the *in vivo* delivery of gene therapies to HCC. First, the delivery vehicle should exhibit good pharmacokinetics and secure sufficient circulation time following the systemic administration to avoid rapid clearance by the first-pass organs; liver and spleen or the reticuloendothelial system such as macrophages.[91] Second, the carriers should possess a certain nano-scaled particle size to extravasate and accumulate in the tumor region. Third, unlike other tumors that can easily accessed by EPR effect, the presence of stroma barrier in HCC stagnates nanomedicines before reaching the tumor cells.[89] Eventually, the nanocarriers should sufficiently internalize into HCC cells and escape from lysosomal degradation to release their cargos safely into cytosol.[125] These challenges collectively may account for the failure of our initial *in vitro*-optimized LNPs in achieving MK gene silencing in the HCC tumor *in vivo* post intravenous administration. By understanding these hampers, we designed a step-wise optimization process to cope with them. In this study, we selected animal model based on human HCC cells to maximize similarity to the tumor microenvironment of human HCC. The characteristic stroma barrier was observed histologically.

The initial LNPs modified with 5 mol% PEG-SP94 demonstrated poor pharmacokinetics and rapidly disappeared from the circulation. The situation was resolved by increasing such ratio to 10 mol%. However, at

15 mol% ratio, the reticuloendothelial system was likely sensitized by the excessive SP94 density resulting in impaired circulation profile.[226] Although the circulation-optimized LNPs demonstrated considerable MK gene silencing in the tumor, their selectivity was poor, probably due to the inadequate penetration of 160 nm nanoparticles through the stroma barrier in the tumor microenvironment.[227]

iLiNP is a novel microfluidic device that can tune the size of LNPs down to 10 nm.[220] However, the very small size of LNPs accounts for poor stability in serum via the excessive adsorption of serum components on the massive surface area presented by these nanoparticles.[219] Previous studies in our laboratory revealed poor *in vivo* performance of siRNA-loaded LNPs with average particle diameter below 40 nm (unpublished data). Therefore, we attempted controlling the average particle diameter of our LNPs in the range of 50-100 nm to balance the stability and the tumor penetration efficiency. Controlling the aqueous phase: organic phase flow rate ratio during microfluidic mixing affected the particle size of the prepared LNPs. Increasing the flow rate ratio results in rapid dilution of the organic phase with consequent deposition of small-sized nanoparticles. Nevertheless, excessive increase in the flow rate ratio results in too fast dilution of the organic phase with subsequent deposition of the extra free lipids which tend to aggregate increasing the PDI of the system.[228] Diverse buffer systems were investigated to optimize the particle size. Citrate and acetate buffers yielded relatively-large particles (160-180 nm) with high polydispersity (>0.3), probably the presence of sodium ions in the latter buffers tend to partially complex with siRNA forming nuclei that contribute to the increased particle size. This phenomenon is less likely to occur using buffers that do not contain metal ions such as HEPES.[229] We manipulated YSK05 ratio and

investigated its impact on the size of LNPs. Increasing such ratio linearly reduced the particle size, probably due to the increased compact packaging of the negatively-charged siRNA by the increase in the cationic component in lipids.[230] Upon testing these LNPs *in vivo*, reducing the particle size from 160 to 70 nm increased the MK gene silencing in the tumor and decreased the silencing in the healthy liver reflecting improved efficiency and selectivity. This may be attributed to the enhanced penetration through the stroma barrier in the tumor by the small-sized LNPs.[231] Interestingly, increasing YSK05 ratio to 60 or 70 mol% to produce 60 or 50 nm LNPs, respectively resulted in inversed selectivity favoring the healthy liver. This may be explained by the sensitization of the serum Apolipoprotein E (ApoE) transporter by the high density of YSK05 leading to the redirection of LNPs from the tumor to the liver. Our laboratory previously reported that YSK05 has high affinity to ApoE which mediates the delivery of LNPs to the healthy hepatocytes via low density lipoprotein (LDL) receptors.[232] ApoE might have penetrated through the interspaces in the PEG-SP94 hydrophilic shield exploiting the increase in the nanoparticle surface curvature driven by particle size reduction.[233] We selected 70 nm LNPs containing 50 mol% YSK05 as the optimum for HCC targeting. Furthermore, to mask their recognition by ApoE, we inserted additional DSPE-PEG_{2K}-MA aiming at filling the interspaces in the curved surfaces of LNPs. At an optimum ratio of 3 mol%, gene silencing in the healthy liver was almost masked suggesting successful escape from the ApoE recognition. Meanwhile, strong gene silencing was maintained in the tumor tissues. The additional PEG further reduced the average particle diameter to 60 nm by improving the particles stability and reducing their tendency to aggregate.[234] Further PEGylation to 5 mol% impaired the knockdown activity in the tumor probably due to the interference with the cellular

uptake and endosomal escape functions by the excessive PEG density, known as PEG dilemma.[235]

The selection of helper phospholipid affected the gene silencing efficiency with the superiority of DOPE over EPC or DOPC. This might be explained by the promotion of the formation of inverted hexagonal lipid structures in case of phosphoethanol amines such as DOPE with consequent improvement of fusogenicity and endosomal escape capability compared to phosphatidyl choline lipids.[186]

The optimized usLNPs prepared by iLiNP device possessed high SOR loading capacity compared to those prepared by thin lipid film hydration method. Hamano *et al*. reported that microfluidic mixing allows fast and efficient interaction between the hydrophobic drug and the lipids with subsequent higher and more homogenous distribution of the drug within the lipid bilayer compared to the hydration method.[236] Moreover, the optimized usLNPs demonstrated a prolonged controlled-release of SOR without initial burst release or dose dumping owing to their high stability and homogenous encapsulation of SOR.[236-237] The prolonged SOR release helps to reduce the dose frequency with potential improvement of patient compliance, convenience and reduction of side effects. The pH-sensitive nature of YSK05 imparted a pH-responsive release pattern which is beneficial to minimize the off-target release of SOR.[50]

In vivo evaluation of our optimized usLNPs revealed good pharmacokinetic profile in terms of the prolonged circulation time necessary to secure sufficient tumor delivery and other pharmacokinetic aspects. Surprisingly, our usLNPs demonstrated minimal siRNA leakage in the blood circulation in spite of their relatively-small size nature. Our

data suggest that the selected particle size range (~60 nm) can balance between stability and tumor penetration issues. Our usLNPs could efficiently accumulate in the HCC tumor following intravenous administration as high as 15% ID/g tissue which much exceeded other reported tumor delivery systems exhibiting a tumor accumulation around or lower than 5% ID/g tissue.[238-240] Wo owe this interestingly-high tumor accumulation to the collective contribution of diverse integrative factors: the excellent pharmacokinetic performance with high area under the circulation time curve (AUC) driving high tumor accumulation,[241] the small particle size facilitating efficient extravasation and subsequent transport through the stroma barrier shielding the tumor, and the active targeting by SP94 peptide facilitating high cellular uptake while avoiding PEG dilemma associated with passively-targeted PEGylated liposomes which impairs their cellular uptake. Our novel delivery system secured a potent gene silencing in the tumor with ED_{50} ~ 0.1 mg/Kg, 15-30 fold lower than other reported nanocarriers.[194, 242-243] As to our knowledge, our delivery system may be among the most potent non-viral vectors for systemic delivery of siRNA to tumor so far.

To accomplish the goal of this study though lowering the effective therapeutic dose of SOR, we screened the anticancer effect of low SOR doses (1.25-5 mg/Kg) encapsulated in our usLNPs and the dose demonstrating moderate antitumor activity was selected (2.5 mg/Kg). Surprisingly, combining the aforementioned dose with low dose of MK-siRNA (0.5 mg/Kg) eradicated HCC in mice by approximately 85%. This dramatic effect could be obtained at very low dose of SOR compared to 10 mg/Kg dose or higher recruited in previous studies [160, 244] and at lower number of doses.[211] These results suggest that MK-siRNA synergize with SOR and increase the sensitivity of HCC to SOR by more than 2-fold.

Extended survival of mice received the combinational treatment, the upregulation of apoptosis marker CC-3 and downregulation of other HCC growth markers confirmed the therapeutic potential of our strategy.

Toxicity studies revealed the biosafety of our treatment as concluded from serological and histo-pathological examinations thanks to its high selectivity with minimal effects on the non-tumorous tissues. In addition, lowered serum levels of AST, ALT, ALP, LDH and CK reflected efficient inhibition of HCC progression with consequent positive prognosis.

2.5. CONCLUSIONS

We designed size-controlled usLNPs for selective co-delivery of SOR and MK-siRNA to HCC tumor *in vivo*. Tweaking the lipid composition and physico-chemical properties of LNPs dramatically affected their pharmacokinetics, biodistribution, selectivity, tumor penetration and cellular delivery with consequent impact on their *in vivo* fate and therapeutic potential. Our optimized 60 nm usLNPs achieved high tumor penetration efficiency while demonstrating good *ex-vivo* and *in vivo* stability. Following intravenous administration, they silenced MK gene with ED_{50} ~0.1 mg/Kg reflecting high potency. The novel combination carried by our delivery system synergistically eradicated an aggressive HCC tumor in mice at surprisingly low doses of SOR and MK-siRNA with high biosafety on both acute and chronic levels. The simple and rapid one-step preparation method would be beneficial for economic industrial scale-up.

CHAPTER 3

Ultra-Small Lipid Nanoparticles Loaded with Sorafenib and Midkine-siRNA Reverse Resistance to Sorafenib and Eradicate Sorafenib-Resistant Hepatocellular Carcinoma In Vitro and In Vivo

CHAPTER 3

3.1. INTRODUCTION

SOR is the FDA drug of choice for resistant HCC.[179] However, there are no alternative therapeutic options so far if the tumor develops resistance to it. The emergence of chemoresistance remains one of the major obstacles for cancer chemotherapy. The chemoresistance accounts for poor recovery rates of HCC which range from 10-15%, without improvement in the last three decades.[7]

The recruitment of gene therapy to overcome chemoresistance and increase the efficiency of chemotherapy has been investigated in literature. One widely-investigated example involves combining doxorubicin (DOX) and small interfering RNA (siRNA) against the multidrug resistance gene (mdr1) to inhibit the production of the P-glycoprotein protein (P-gp), which is responsible for the development of resistance to DOX. The outcome was an increased cell sensitivity to DOX with a subsequent improvement in therapeutic efficiency.[245-246]

Previous reports discussed the contribution of various pathways to chemoresistance in tumors including MDR1, Survivin, Notch and MK.[181, 247-249] Yet, the mechanism for resistance to SOR is still unclear.

In the previous two chapters, we demonstrated that MK-siRNA synergizes with SOR and increases the sensitivity of HCC to SOR by approximately 2-fold both *in vitro* and *in vivo*. In the previous chapter, we could create a highly-efficient and selective co-delivery system for the *in vivo* eradication of HCC, called usLNPs. In the current chapter, we raised the challenge and attempted to contribute to the understanding and combating SOR-resistant HCC aiming at opening a new therapeutic

window for unresolved health problem. We established a SOR-resistant HCC cell line *in vitro* and studied the contribution of MK pathway to such acquired resistance. We then attempted the reversal of the aforementioned resistance recruiting MK-siRNA in our delivery system. Eventually, the resistant cells were used to create SOR-resistant HCC tumor model in mice and we attempted its eradication using our novel combination.

3.2. EXPERIMENTAL

3.2.1. Materials

The same materials previously mentioned in Chapter 1 and Chapter 2 were used in this chapter.

3.2.2. Methods

In addition to the methods mentioned in Chapter 1 and Chapter 2, the following methods were applied:

3.2.2.1. Establishment of SOR-resistant HCC cell line

HepG2 cells were cultured as previously mentioned in Chapter 1. A low concentration of SOR (3 μM) was added to the cell culture medium and the cells were continuously allowed to grow in the presence of SOR for four weeks to acquire resistance to SOR. The cells were maintained in complete growth medium containing 3 μM SOR.

3.2.2.2. Assessment of the cell sensitivity to SOR

MTT assay was used to evaluate the cell viability after 24-hour incubation with usLNPs encapsulating SOR+MK-siRNA or SOR+siCntrl. The cytotoxicity assessment protocol applied in Chapter 1 was used in this study.

3.2.2.3. Evaluation of MK gene expression

MK gene expression in the investigated cells/tissues was evaluated by qRT-PCR as previously described in Chapter 1 and Chapter 2.

3.2.2.4. Creation of SOR-resistant HCC mice model

The SOR-resistant HepG2 cell line established in section 3.2.2.1 was used. Cells were cultivated and maintained as previously described. Then, the cells were suspended in PBS: Matrigel solution (1:1 v/v) and inoculated into the right flanks of male BALB/c nude mice in a density of 2×10^6 cells/mouse. The tumor growth was monitored as previously described in Chapter 2.

3.2.2.5. Treatment of SOR-resistant HCC in mice

The treatment protocol schemed in **Fig. 25** was used. usLNPs encapsulating SOR+MK-siRNA or SOR+siCntrl were administered to the mice at the specified time points. SOR dose was 2.5 mg/Kg, siRNA dose was 0.5 mg/Kg.

3.3. RESULTS

3.3.1. MK-siRNA reverses the acquired resistance to SOR *in vitro*

We established a SOR-resistant HepG2 cell line by prolonged cultivation in the presence of SOR. The cells became almost insensitive to SOR+siCntrl combination compared to regular HepG2 cells (cell viability values were 95.61±8.11 and 45.01±5.53%, respectively). Surprisingly, upon combining MK-siRNA with SOR, such resistance was significantly reversed (cell viability was 50.48±8.32%) (**Fig. 36**). To understand the molecular basis of such resistance, we compared MK gene expression in both resistant and regular HepG2 cells. Interestingly, MK gene was upregulated by 3-fold in the resistant cells (**Fig. 37**).

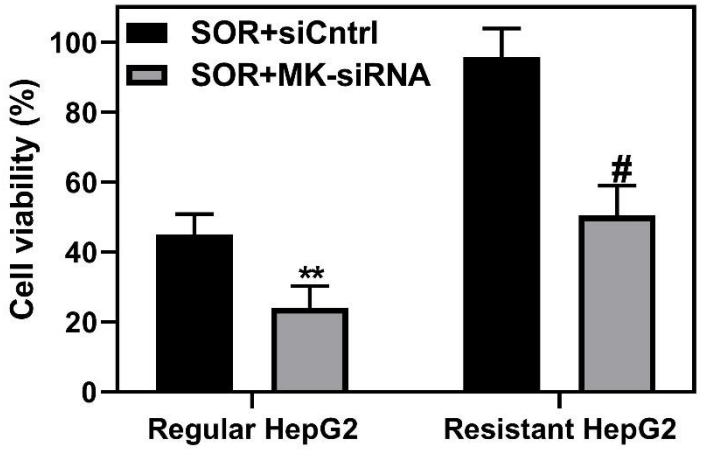

Figure 36. MK-siRNA reverses the resistance to SOR in established SOR-resistant HepG2 cells. **P<0.01, #P<0.0001 versus SOR+siCntrl. SOR dose = 10 μM, siRNA dose= 400 nM, N=3, results are expressed as average±standard deviation.

Figure 37. Overexpression of MK gene correlates with the acquired resistance to SOR in HepG2 cells. ***P<0.001 versus regular HepG2 cells.

3.3.2. SOR and MK-siRNA co-therapy resensitizes SOR-resistant HCC to SOR allowing its efficient eradication in mice

The resistant cells were inoculated into mice to establish SOR-resistant tumors *in vivo*. Surprisingly, the combinational treatment with SOR+MK-siRNA obviously resumed the tumor's sensitivity to SOR with ~70% inhibition of tumor growth. On the other hand, the tumor was negligibly sensitive to the combination upon replacing MK-siRNA with siCntrl (**Fig. 38A-B**).

The treatment demonstrated high biosafety without significant weight losses (**Fig. 38C**).

The treatment with SOR+MK-siRNA could maintain a sustained MK gene silencing of about 70% in the tumor tissues up to 3 days following the treatment cessation (**Fig. 38D**).

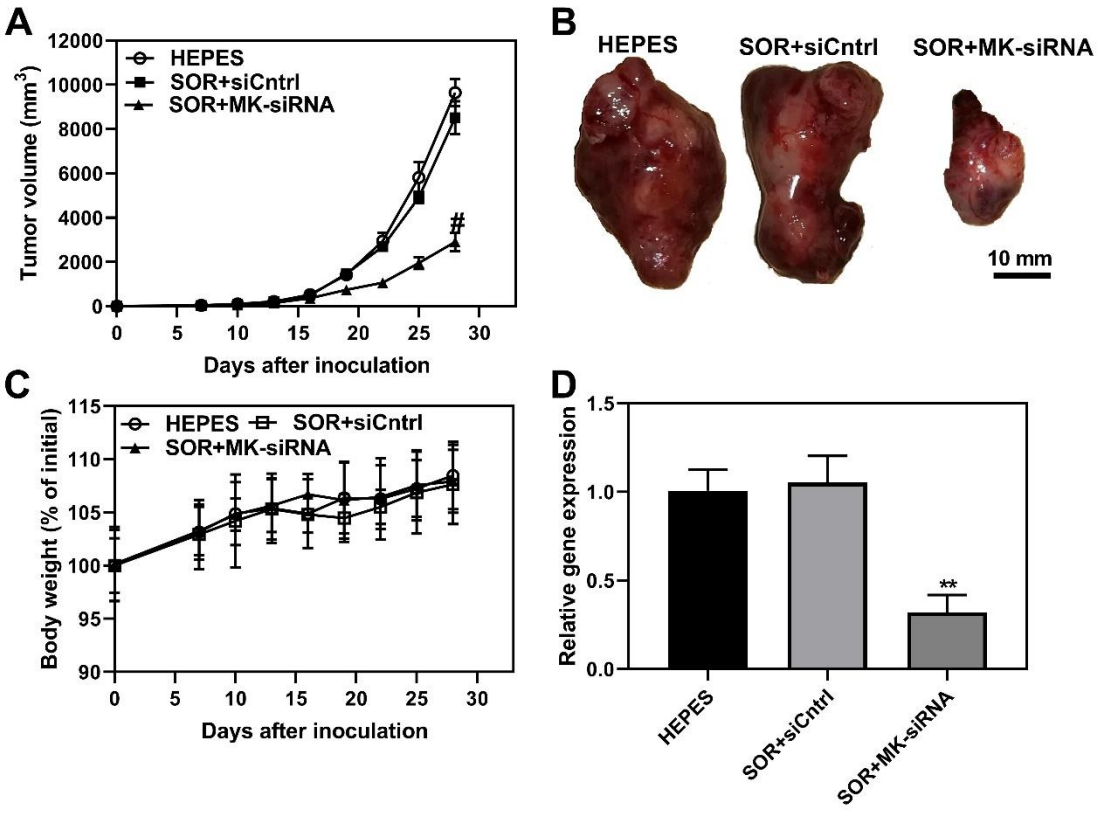

Figure 38. usLNPs loaded with SOR and MK-siRNA eradicate SOR-resistant HCC in mice. A) Treatment of SOR-resistant HCC in mice using SOR and MK-siRNA combination. #P<0.0001 versus the other treatment groups. SOR dose= 2.5 mg/Kg, siRNA dose = 0.5 mg/Kg, N=5, results are expressed as average±standard deviation. Treatment schedule is shown in **Fig. 25**. B) Representative photos for tumors harvested from mice that received different treatments at the end of treatment. C) Changes in the body weight of mice during different treatments. D) MK gene expression in tumor tissues harvested from mice at the end of treatment. **P<0.01 versus the other treatment groups.

3.4. DISCUSSION

Taking into consideration being the last choice for resistant HCC, We raised the challenge and attempted the eradication of SOR-resistant HCC. We established a SOR-resistant HCC cell line by prolonged exposure to low concentration of SOR. The used SOR concentration was selected based on a previously-constructed dose-response curve shown in **Fig. 8A**. We selected sublethal concentration of SOR to allow gradual desensitization of the cells to SOR without affecting their vital functions. This protocol was adopted to simulate the real situation in human patients, where prolonged treatment with SOR together with the low tumor accumulation of the drug eventually result in the emergence of the acquired chemoresistance.

Cell viability assessment confirmed the acquirement of the resistance to SOR with negligible cytotoxicity shown by usLNPs encapsulating SOR+siCntrl at an effective SOR dose. Surprisingly, MK-siRNA could dramatically reverse such resistance.

Our results suggested that the upregulation of MK gene correlates with the acquired resistance of HCC cells to SOR.

Being encouraged by the aforementioned results, we tried to extrapolate the same concept *in vivo*. Strikingly, our combination dramatically eradicated the tumor in mice, which was nearly insensitive to SOR without MK-siRNA. These results can offer a promising therapeutic option for SOR-resistant HCC that have no effective treatments so far.

Our treatment demonstrated high biosafety which was in agreement with our previous results in Chapter 2. Moreover, strong MK gene silencing could be maintained until 3 days after treatment cessation

suggesting prolonged and long-lasting action despite the low siRNA dose used.

3.5. CONCLUSIONS

We successfully established a SOR-resistant HCC cell line. We demonstrated that the overexpression of MK gene correlates with the acquired resistance to SOR. MK-siRNA could significantly reverse the resistance to SOR both *in vitro* and *in vivo*. SOR and MK-siRNA co-therapy eradicated SOR-resistant HCC in mice by 70% at low doses of SOR and siRNA. Our delivery system, usLNPs, could maintain strong MK gene silencing in the tumor tissue up to three days following treatment cessation suggesting prolonged efficacy. The data revealed in this chapter hold promise to offer a novel therapeutic approach for resistant HCC.

General conclusions

GENERAL CONCLUSIONS

In the current project, we introduced a novel combination of the cytotoxic drug, SOR, and MK-siRNA aiming at integrative therapy of HCC, allowing the reduction of SOR dose and avoiding the side effects associated with the high doses of SOR.

We designed multifunctional LNPs co-encapsulating the two agents in question. Optimizing the various formulation aspects resulted in high efficiency *in vitro* while demonstrating good biotolerability.

Modification of the LNPs with the smart SP94 peptide imparted high selectivity to both human and murine HCC while showing negligible effect on the normal hepatocytes. SP94-modified LNPs and LNPs modified with the famous cell-penetrating peptide, STR-R8, showed comparable efficiency in HCC. However, only SP94-modified LNPs could exhibit high selectivity to HCC without harming the normal hepatocytes. Selectivity was confirmed via FACS and CLSM cellular uptake studies, cytotoxicity assessments and selective MK gene silencing evaluation in a diversity of cancerous and normal cell lines.

We showed the first evidence that MK-siRNA increases the sensitivity of HCC cells to SOR *in vitro* suggesting potential synergism between them. Such phenomenon could not be seen when MK-siRNA was replaced with a control siRNA (siCntrl).

The *in vitro* optimized LNPs could not accumulate in the tumor tissue following intravenous administration to HCC-bearing mice which necessitated a comprehensive optimization strategy to overcome the harsh barriers facing the *in vivo* gene delivery to HCC. A recently-developed microfluidic device called iLiNP was used for the preparation of size-

controlled LNPs via tweaking diverse factors including the lipid composition, flow rate ratio and the buffer system used. Optimizing the pharmacokinetic performance, lipid composition and physico-chemical properties of the LNPs dramatically affected their tumor gene delivery performance and selectivity. The optimum LNPs had an average particle diameter of 60 nm and could achieve amazing MK gene silencing in the tumor with ED_{50}~0.1 mg/Kg while showing limited gene silencing in the healthy liver reflecting high selectivity. Our system may be the most powerful siRNA delivery vector to the tumor so far as to our knowledge. The optimum LNPs were referred to as ultra-small LNPs (usLNPs).

usLNPs loaded with SOR and MK-siRNA combination could efficiently eradicate HCC in mice by ~85% using very low dose of SOR and siRNA (2.5 mg/Kg and 0.5 mg/Kg, respectively). The results revealed that the aforementioned therapeutic effect of the combination was 2-fold higher than what was obtained with SOR monotherapy and 4.7-fold higher than MK-siRNA monotherapy. Moreover, the combinational effect exceeded the additive values of the individual therapeutic agents in question suggesting synergism between them. The synergism was also confirmed statistically and via the application of Chou and Talaly's model of drug-drug interaction. The combination resulted in significant downregulation of various HCC markers, namely; AFP, OSP, VEGF-1 and CD31 while showing elevated levels of the apoptosis marker, CC-3.

usLNPs showed high biosafety upon acute administration at clinically-relevant siRNA dose (30-fold higher than ED_{50}). Chronic administration of usLNPs revealed high biosafety as confirmed by the absence of elevated hepato-renal function markers in the serum or histo-pathological signs of major organ injury relative to mice treated with

HEPES buffer. No weight loss was detected in mice during the treatment unlike common chemotherapeutics.

Prolonged exposure to low concentrations of SOR resulted in acquired chemoresistance in HCC cells. The overexpression of MK gene correlates with such resistance. Concomitant treatment with MK-siRNA significantly reversed such resistance and re-sensitized the cells to SOR both *in vitro* and *in vivo*.

Potential applications

POTENTIAL APPLICATIONS

- In the current project, we introduced a novel chemotherapy/gene therapy combination of SOR and MK-siRNA. This synergistic combination enabled the eradication of HCC in mice at very low SOR dose, 2.5 mg/Kg, which to our knowledge, the lowest dose of SOR that has been ever investigated in mice model so far. Such approach will facilitate effective treatment of HCC at cost-effective dose, which is less likely to exhibit side effects.

- We reported the synergism between SOR and MK-siRNA as a new finding. Other sister drugs with similar mechanism of action may be applicable such as cabozantinib, Lenvatinib and Regorafenib.

- We created a highly-efficient and selective co-delivery system for drug and gene delivery to HCC. To our knowledge, our system may be the most powerful siRNA delivery device to tumor so far (ED_{50}~0.1 mg/Kg). We suggest the extension of its application to other siRNAs or low molecular weight drug+siRNA combinations. The high selectivity facilitates high biosafety with low chance of off-target toxicities.

- Our data suggest a new therapeutic option for SOR-resistant HCC which has no available treatment so far.

- The simple, rapid, one-step preparation method of our usLNPs will facilitate economic industrial scale-up, unlike other complicated delivery systems with multiple production steps.

- The data provided in this PhD project hold promise for potential clinical application as HCC treatment, which is nationally-demanded

in Egypt. We hope that this project will contribute to the development of health sector in Egypt as intended by the sponsors of this studentship. We hope also that we add something to the global knowledge about HCC or suggest a direction for the future research in this field.

Declaration

DECLARATION

A patent application for the intellectual property associated with the work included in this dissertation has been submitted to Japan Patent Office, Tokyo, Japan (Application number: 特願 2020-075619) on April 21st, 2020, Hokkaido University reference (P2019-170-JP01). Any reproduction of the results or the strategies revealed in this dissertation should be done in agreement with the inventors.

References

REFERENCES

(1) Rawla, P.; Sunkara, T.; Muralidharan, P.; Raj, J. P., Update in global trends and aetiology of hepatocellular carcinoma. *Contemp Oncol (Pozn)* **2018,** *22* (3), 141-150.

(2) Schutte, K.; Bornschein, J.; Malfertheiner, P., Hepatocellular carcinoma--epidemiological trends and risk factors. *Digestive diseases (Basel, Switzerland)* **2009,** *27* (2), 80-92.

(3) Saleh, D. a. A.; Amr, S.; Jillson, I. A.; Wang, J. H.-y.; Crowell, N.; Loffredo, C. A., Preventing hepatocellular carcinoma in Egypt: results of a Pilot Health Education Intervention Study. *BMC Research Notes* **2015,** *8*, 384.

(4) World Health Organization-International Agency for Research on Cancer (IARC), Some traditional herbal medicines, some mycotoxins, naphthalene and styrene. IARC press: Lyon (France), 2002; Vol. 82.

(5) Ezzat, S.; Abdel-Hamid, M ;.Eissa, S. A.; Mokhtar, N.; Labib, N. A.; El-Ghorory, L.; Mikhail, N. N.; Abdel-Hamid, A.; Hifnawy, T.; Strickland, G. T.; Loffredo, C. A., Associations of pesticides, HCV, HBV, and hepatocellular carcinoma in Egypt. *International journal of hygiene and environmental health* **2005,** *208* (5), 329-339.

(6) Blum, H. E., Hepatocellular carcinoma: therapy and prevention. *World journal of gastroenterology* **2005,** *11* (47), 7391-7400.

(7) Abou-Alfa, G. K.; Huitzil-Melendez, F.-D.; O'Reilly, E. M.; Saltz, L. B., Current Management of Advanced Hepatocellular Carcinoma. *Gastrointestinal Cancer Research : GCR* **2008,** *2* (2), 64-70.

(8) Mimeault, M.; Hauke, R.; Mehta, P. P.; Batra, S. K., Recent advances in cancer stem/progenitor cell research: therapeutic implications for overcoming resistance to the most aggressive cancers. *Journal of cellular and molecular medicine* **2007,** *11* (5), 981-1011.

(9) Ashworth, R. E.; Wu, J., Mammalian target of rapamycin inhibition in hepatocellular carcinoma. *World J Hepatol* **2014,** *6* (11), 776-78.2

(10) Clarke, M. F.; Dick, J. E.; Dirks, P. B.; Eaves, C. J.; Jamieson, C. H.; Jones, D. L.; Visvader, J.; Weissman, I. L.; Wahl, G. M., Cancer stem cells--perspectives on current status and future directions: AACR Workshop on cancer stem cells. *Cancer research* **2006,** *66* (19), 9339-9344.

(11) Elsabahy, M.; Nazarali, A.; Foldvari, M., Non-viral nucleic acid delivery: key challenges and future directions. *Current drug delivery* **2011,** *8* (3), 235-244.

(12) Hayashi, Y.; Mizuno, R.; Ikramy, K. A.; Akita, H.; Harashima, H., Pretreatment of hepatocyte growth factor gene transfer mediated by octaarginine peptide-modified nanoparticles ameliorates LPS/D-galactosamine-induced hepatitis. *Nucleic acid therapeutics* **2012,** *22* (5), 360-363.

(13) FDA, FDA approval brings first gene therapy to the United States. https://www.fda.gov/NewsEvents/Newsroom/PressAnnouncements/ucm574058.htm (accessed 9/11/2018).

(14) FDA, FDA approves novel gene therapy to treat patients with a rare form of inherited vision loss.

https://www.fda.gov/newsevents/newsroom/pressannouncements/ucm589467.htm (accessed 9/11/2018).

(15) FDA, FDA approves first-of-its kind targeted RNA-based therapy to treat a rare disease. https://www.fda.gov/NewsEvents/Newsroom/PressAnnouncements/ucm616518.htm (accessed 9/11/2018)

(16) Roberts, R. J., Restriction endonucleases. *CRC critical reviews in biochemistry* **1976,** *4* (2), 123-164.

(17) Bloom, M. V.; Freyer, G. A.; Micklos, D. A., *Laboratory DNA science: an introduction to recombinant DNA techniques and methods of genome analysis*. Benjamin/Cummings Publishing Company, Inc.: Menlo Park, 1996; p xxiii + 434 pp.

(18) Sousa, F.; Passarinha, L.; Queiroz, J. A., Biomedical application of plasmid DNA in gene therapy: A new challenge for chromatography. *Biotechnology and Genetic Engineering Reviews* **2009,** *26* (1), 83-116.

(19) Bai, H.; Lester, G. M. S.; Petishnok, L. C.; Dean, D. A., Cytoplasmic transport and nuclear import of plasmid DNA. *Biosci Rep* **2017,** *37* (6), BSR20160616.

(20) Steinle, H.; Behring, A.; Schlensak, C.; Wendel ,H. P.; Avci-Adali, M., Concise Review: Application of In Vitro Transcribed Messenger RNA for Cellular Engineering and Reprogramming: Progress and Challenges. *STEM CELLS* **2017,** *35* (1), 68-79.

(21) Kowalski, P. S.; Rudra, A.; Miao, L.; Anderson, D. G., Delivering the Messenger: Advances in Technologies for Therapeutic mRNA Delivery. *Molecular Therapy* **2019,** *27* (4), 710-728.

(22) Sazani, P.; Kole, R., Therapeutic potential of antisense oligonucleotides as modulators of alternative splicing. *Journal of Clinical Investigation* **2003,** *112* (4), 481-486.

(23) Preall, J. B.; Sontheimer, E. J., RNAi: RISC gets loaded. *Cell* **2005,** *123* (4), 543-545.

(24) Watts, J. K.; Deleavey, G. F.; Damha, M. J., Chemically modified siRNA: tools and applications. *Drug discovery today* **2008,** *13* (19-20), 842-855.

(25) Chen, J.; Zhang, W.; Lin, J.; Wang, F.; Wu, M.; Chen, C.; Zheng, Y.; Peng, X.; Li, J.; Yuan, Z., An efficient antiviral strategy for targeting hepatitis B virus genome using transcription activator-like effector nucleases. *Molecular therapy : the journal of the American Society of Gene Therapy* **2014,** *22* (2), 303-311.

(26) Weber, N. D.; Stone, D.; Sedlak, R. H.; De Silva Feelixge, H. S.; Roychoudhury, P.; Schiffer, J. T.; Aubert, M.; Jerome, K. R., AAV-Mediated Delivery of Zinc Finger Nucleases Targeting Hepatitis B Virus Inhibits Active Replication. *PLOS ONE* **2014,** *9* (5), e97579.

(27) Dash, P. K.; Kaminski, R.; Bella, R.; Su, H.; Mathews, S.; Ahooyi, T. M.; Chen, C.; Mancuso, P.; Sariyer, R.; Ferrante, P.; Donadoni, M.; Robinson, J. A.; Sillman, B.; Lin, Z.; Hilaire, J. R.; Banoub, M.; Elango, M.; Gautam, N.; Mosley, R. L.; Poluektova, L. Y.; McMillan, J.; Bade, A. N.; Gorantla, S.; Sariyer, I. K.; Burdo, T. H.; Young, W.-B.; Amini, S.; Gordon, J.; Jacobson, J. M.; Edagwa, B ;.Khalili, K.; Gendelman, H. E., Sequential LASER ART and CRISPR Treatments Eliminate HIV-1 in a Subset of Infected Humanized Mice. *Nature communications* **2019,** *10* (1), 2753.

(28) Moeini, A.; Cornellà, H.; Villanueva, A., Emerging signaling pathways in hepatocellular carcinoma. *Liver cancer* **2012,** *1* (2), 83-93.

(29) GeneCards; The Human Gene Database, CTNNB1 Gene. https://www.genecards.org/cgi-bin/carddisp.pl?gene=CTNNB1 (accessed 2020/06/02).

(30) Hoshida, Y.; Nijman, S. M. B.; Kobayashi, M.; Chan, J. A.; Brunet, J.-P.; Chiang, D. Y.; Villanueva, A.; Newell, P.; Ikeda, K.; Hashimoto, M.; Watanabe, G.; Gabriel, S.; Friedman, S. L.; Kumada, H.; Llovet, J. M.; Golub, T. R., Integrative transcriptome analysis reveals common molecular subclasses of human hepatocellular carcinoma. *Cancer research* **2009,** *69* (18), 7385-7392.

(31) Tao, J.; Calvisi, D. F.; Ranganathan, S.; Cigliano, A.; Zhou, L.; Singh, S.; Jiang, L.; Fan, B.; Terracciano, L.; Armeanu-Ebinger, S.; Ribback, S.; Dombrowski, F.; Evert, M.; Chen, X.; Monga, S. P. S., Activation of β-catenin and Yap1 in human hepatoblastoma and induction of hepatocarcinogenesis in mice. *Gastroenterology* **2014,** *147* (3), 690-701.

(32) Li, Y.; Pu, S.; Liu, Q.; Li, R.; Zhang, J.; Wu, T.; Chen, L.; Li, H.; Yang, X.; Zou, M.; Xiao, J.; Xie, W ;.He, J., An integrin-based nanoparticle that targets activated hepatic stellate cells and alleviates liver fibrosis. *Journal of Controlled Release* **2019,** *303*, 77-90.

(33) Huang, X. H.; Chen, J. S.; Wang, Q.; Chen, X. L.; Wen, L.; Chen, L. Z.; Bi, J.; Zhang ,L. J.; Su, Q.; Zeng, W. T., miR-338-3p suppresses invasion of liver cancer cell by targeting smoothened. *The Journal of pathology* **2011,** *225* (3), 463-472.

(34) Della Corte, C. M.; Viscardi, G.; Papaccio, F.; Esposito, G.; Martini, G.; Ciardiello, D.; Martinelli, E.; Ciardiello, F.; Morgillo, F., Implication of the Hedgehog pathway in hepatocellular carcinoma. *World journal of gastroenterology* **2017,** *23* (24), 4330-4340.

(35) Aoki, Y.; Niihori, T.; Narumi, Y.; Kure, S.; Matsubara, Y., The RAS/MAPK syndromes :novel roles of the RAS pathway in human genetic disorders. *Human mutation* **2008,** *29* (8), 992-1006.

(36) Guichard, C.; Amaddeo, G.; Imbeaud, S.; Ladeiro, Y.; Pelletier, L.; Maad, I. B.; Calderaro, J.; Bioulac-Sage, P.; Letexier, M.; Degos, F.; Clément, B ;.Balabaud, C.; Chevet, E.; Laurent, A.; Couchy, G.; Letouzé, E.; Calvo, F.; Zucman-Rossi, J., Integrated analysis of somatic mutations and focal copy-number changes identifies key genes and pathways in hepatocellular carcinoma. *Nature genetics* **2012,** *44*.698-694 ,(6)

(37) Weihrauch, M.; Benick, M.; Lehner, G.; Wittekind, M.; Bader, M.; Wrbitzk, R.; Tannapfel, A., High prevalence of K-ras-2 mutations in hepatocellular carcinomas in workers exposed to vinyl chloride. *International archives of occupational and environmental health* **2001,** *74* (6), 405-410.

(38) Wai Ling Khoo, T. S. R. A. O. J. K., Chapter 7: Tyrosine Kinase Inhibitors in the Treatment of Hepatocellular Carcinoma. In *Hepatocellular Carcinoma*, Tirnitz-Parker, J. E. E., Ed. Codon Publications: Brisbane (AU), 2019.

(39) Ghousein, A.; Mosca, N.; Cartier, F.; Charpentier, J.; Dupuy, J.-W.; Raymond, A.-A.; Bioulac-Sage, P.; Grosset, C. F., miR-4510 blocks hepatocellular carcinoma development through RAF1 targeting and RAS/RAF/MEK/ERK signalling inactivation. *Liver International* **2020,** *40* (1), 240-251.

(40) Liu, Y.; Tan, M.; Zhang, Y.; Huang, W.; Min, L.; Peng, S.; Yuan, K.; Qiu, L.; Min, W., Targeted Gene Silencing BRAF Synergized Photothermal Effect Inhibits Hepatoma Cell Growth Using New GAL-GNR-siBRAF Nanosystem. *Nanoscale Research Letters* **2020,** *15* (1), 116.

(41) Li, M.; Li, H.; Li, C.; Wang, S.; Jiang, W.; Liu, Z.; Zhou, S.; Liu, X.; McNutt, M. A.; Li, G., Alpha-fetoprotein: A new member of intracellular signal molecules in regulation of the PI3K/AKT signaling in human hepatoma cell lines. *International Journal of Cancer* **2011,** *128* (3), 524-532.

(42) Zhang, J.; Chen, G.; Zhang, P.; Zhang, J.; Li, X.; Gan, D. n.; Cao, X.; Han, M.; Du, H.; Ye, Y. a., The threshold of alpha-fetoprotein (AFP) for the diagnosis of hepatocellular carcinoma: A systematic review and meta-analysis. *PLOS ONE* **2020,** *15* (2), e0228857.

(43) Ohkawa, K.; Asakura, T.; Tsukada, Y.; Matsuura, T., Antibody to human α-fetoprotein inhibits cell growth of human hepatocellular carcinoma cells by resuscitating the PTEN molecule: in vitro experiments. *International journal of oncology* **2017,** *50* (6), 2180-2190.

(44) Finn, R. S. A Phase I Open Label Clinical Trial Evaluating the Safety and Anti-Tumor Activity of Autologous T Cells Expressing Enhanced TCRs Specific for Alpha Fetoprotein (AFP^{c332}T) in HLA-A2 Positive Subjects With Advanced Hepatocellular Carcinoma (HCC). https://clinicaltrials.gov/ct2/show/NCT03132792 (accessed 09/09/2019).

(45) Zhu, M.; Li, W.; Lu, Y.; Dong, X.; Chen, Y.; Lin, B ;.Xie, X.; Guo, J.; Li, M., Alpha fetoprotein antagonizes apoptosis induced by paclitaxel in hepatoma cells in vitro. *Scientific Reports* **2016,** *6* (1), 26472.

(46) Jee, Y. H.; Lebenthal, Y.; Chaemsaithong, P.; Yan, G.; Peran, I.; Wellstein, A.; Romero, R ;.Baron, J., Midkine and Pleiotrophin Concentrations in Amniotic Fluid in Healthy and Complicated Pregnancies. *PloS one* **2016,** *11* (4), e0153325-e0153325.

(47) Muramatsu, T., Midkine, a heparin-binding cytokine with multiple roles in development, repair and diseases. *Proceedings of the Japan Academy. Series B, Physical and biological sciences* **2010,** *86* (4), 410-425.

(48) Sun, B.; Hu, C.; Yang, Z.; Zhang, X.; Zhao, L.; Xiong, J.; Ma, J.; Chen, L.; Qian, H.; Luo, X.; Shi, L.; Li, J.; Cheng, X.; Yin, Z., Midkine promotes hepatocellular carcinoma metastasis by elevating anoikis resistance of circulating tumor cells. *Oncotarget* **2017,** *8* (20), 32523-32535.

(49) Zhong, J.; Huang, H. L.; Li, J.; Qian, F. C.; Li, L. Q.; Niu, P. P.; Dai, L. C., Development of hybrid-type modified chitosan derivative nanoparticles for the intracellular delivery of midkine-siRNA in hepatocellular carcinoma cells. *Hepatobiliary & pancreatic diseases international : HBPD INT* **2015,** *14* (1), 82-89.

(50) Younis, M. A.; Khalil, I. A.; Abd Elwakil, M. M.; Harashima, H., A Multifunctional Lipid-Based Nanodevice for the Highly Specific Codelivery of Sorafenib and Midkine siRNA to Hepatic Cancer Cells. *Mol Pharm* **2019,** *16* (9), 4031-4044.

(51) Ferreira, C. G.; Tolis, C.; Giaccone, G., p53 and chemosensitivity. *Annals of oncology : official journal of the European Society for Medical Oncology* **1999,** *10* (9), 1011-1021.

(52) Xu, G. W.; Sun, Z. T.; Forrester, K.; Wang, X. W.; Coursen, J.; Harris, C. C., Tissue-specific growth suppression and chemosensitivity promotion in human hepatocellular carcinoma cells by retroviral-mediated transfer of the wild-type p53 gene. *Hepatology (Baltimore, Md.)* **1996,** *24* (5), 1264-1268.

(53) Choi, J. Y.; Park, Y. M.; Byun, B. H.; Kim, B. S.; Hong, E. G.; Shin, D. Y.; Seong, Y .R.; Im, D. S., Adenovirus-mediated p53 tumor suppressor gene therapy against subcutaneous HuH7 hepatoma cell line nodule of nude mice. *Journal of Korean medical science* **1999,** *14* (3), 271-276.

(54) Anderson, S. C.; Johnson, D. E.; Harris, M. P.; Engler ,H.; Hancock, W.; Huang, W. M.; Wills, K. N.; Gregory, R. J.; Sutjipto, S.; Wen, S. F.; Lofgren, S.; Shepard, H. M.; Maneval, D. C., p53 gene therapy in a rat model of hepatocellular carcinoma: intra-arterial delivery of a recombinant adenovirus. *Clinical cancer research : an official journal of the American Association for Cancer Research* **1998,** *4* (7), 1649-1659.

(55) Ma, H.; Liu, Y.; Liu, S.; Xu, R.; Zheng, D., Oral adeno-associated virus-sTRAIL gene therapy suppresses human hepatocellular carcinoma growth in mice. *Hepatology (Baltimore, Md.)* **2005,** *42* (6), 1355-1363.

(56) Shewach, D., HSV-TK/Ganciclovir Mediated Toxicity. In *Encyclopedia of Cancer*, Schwab, M., Ed. Springer Berlin Heidelberg: Berlin, Heidelberg, 2011; pp 1748-1752.

(57) Kang, M. A.; Kim, K .Y.; Seol, J. Y.; Kim, K. C.; Nam, M. J., The growth inhibition of hepatoma by gene transfer of antisense vascular endothelial growth factor. *The journal of gene medicine* **2000,** *2* (4), 289-296.

(58) Schmitz, V.; Wang, L.; Barajas, M.; Gomar, C.; Prieto, J ;.Qian, C., Treatment of colorectal and hepatocellular carcinomas by adenoviral mediated gene transfer of endostatin and angiostatin-like molecule in mice. *Gut* **2004,** *53* (4), 561-567.

(59) Xu, R.; Sun, X.; Tse, L. Y.; Li, H.; Chan, P. C.; Xu, S.; Xiao, W ;. Kung, H. F.; Krissansen, G. W.; Fan, S. T., Long-term expression of angiostatin suppresses metastatic liver cancer in mice. *Hepatology (Baltimore, Md.)* **2003,** *37* (6), 1451-1460.

(60) Matsumoto, K.; Ishikawa, H.; Nishimura, D.; Hamasaki, K.; Nakao, K.; Eguchi, K., Antiangiogenic property of pigment epithelium-derived factor in hepatocellular carcinoma. *Hepatology (Baltimore, Md.)* **2004,** *40* (1), 252-259.

(61) Liang, C.; Xu, Y.; Li, G.; Zhao, T.; Xia, F.; Li, G.; Zhang, D.; Wu, J., Downregulation of DcR3 sensitizes hepatocellular carcinoma cells to TRAIL-induced apoptosis. *OncoTargets and therapy* **2017,** *10*, 417-428.

(62) Li, H.; Fu, X.; Chen, Y.; Hong, Y.; Tan, Y.; Cao, H.; Wu, M.; Wang, H., Use of adenovirus-delivered siRNA to target oncoprotein p28GANK in hepatocellular carcinoma. *Gastroenterology* **2005,** *128* (7), 2029-2041.

(63) Arbutus Biopharma, TKM-PLK1. http://arbutusbio.com/portfolio/tkm-plk1.php (accessed 18/10/2018).

(64) Oh, H. R.; Jo, H.-Y.; Park, J. S.; Kim, D.-E.; Cho, J.-Y.; Kim, P.-H.; Kim, K.-S., Galactosylated Liposomes for Targeted Co-Delivery of Doxorubicin/Vimentin siRNA to Hepatocellular Carcinoma. *Nanomaterials* **2016,** *6* (8), 141.

(65) Mok, W. C.; Wasser, S.; Tan, T.; Lim, S. G., Polo-like kinase 1, a new therapeutic target in hepatocellular carcinoma. *World journal of gastroenterology* **2012,** *18* (27), 3527-3536.

(66) Zhou, X. N.; Li, G. M.; Xu, Y. C.; Zhao, T. J.; Wu, J. X., Knockdown of Decoy Receptor 3 Impairs Growth and Invasiveness of Hepatocellular Carcinoma Cell Line of HepG2. *Chinese medical journal* **2016,** *129* (21), 2623-2629.

(67) Li, C.; Liao, J.; Wu, S.; Fan, J.; Peng, Z.; Wang, Z., Overexpression of DBC1, correlated with poor prognosis, is a potential therapeutic target for hepatocellular carcinoma. *Biochemical and biophysical research communications* **2017,** *494* (3-4), 511-517.

(68) Bae, J. S.; Noh, S. J.; Jang, K. Y.; Park, H. S.; Chung, M. J.; Park, C. K.; Moon, W. S., Expression and role of epithelial cell adhesion molecule in dysplastic nodule and hepatocellular carcinoma. *International journal of oncology* **2012,** *41* (6), 2150-2158.

(69) Li, Y.; Farmer, R. W.; Yang, Y.; Martin, R. C., Epithelial cell adhesion molecule in human hepatocellular carcinoma cell lines: a target of chemoresistence. *BMC cancer* **2016,** *16*, 228.

(70) Zhang, R.; Xu ,L. B.; Yue, X. J.; Yu, X. H.; Wang, J.; Liu, C., Bmi1 gene silencing inhibits the proliferation and invasiveness of human hepatocellular carcinoma cells and increases their sensitivity to 5-fluorouracil. *Oncology reports* **2013,** *29* (3), 967-974.

(71) Cavallaro, G.; Farra, R.; Craparo, E. F.; Sardo, C.; Porsio, B.; Giammona, G.; Perrone, F.; Grassi, M.; Pozzato, G.; Grassi, G.; Dapas, B., Galactosylated polyaspartamide copolymers for siRNA targeted

delivery to hepatocellular carcinoma cells. *International journal of pharmaceutics* **2017,** *525* (2), 397-406.

(72) Makita, Y.; Murata, S.; Katou, Y.; Kikuchi, K.; Uejima, H.; Teratani, M.; Hoashi, Y.; Kenjo, E.; Matsumoto, S.; Nogami, M.; Otake, K.; Kawamata, Y., Anti-tumor activity of KNTC2 siRNA in orthotopic tumor model mice of hepatocellular carcinoma. *Biochemical and biophysical research communications* **2017,** *493* (1), 800-806.

(73) Kuntzen, C.; Sonuc, N.; De Toni, E. N.; Opelz, C.; Mucha, S. R.; Gerbes, A. L.; Eichhorst, S. T., Inhibition of c-Jun-N-terminal-kinase sensitizes tumor cells to CD95-induced apoptosis and induces G2/M cell cycle arrest. *Cancer research* **2005,** *65* (15), 6780-6788.

(74) Wirth, T.; Kuhnel, F.; Fleischmann-Mundt, B.; Woller, N.; Djojosubroto, M.; Rudolph, K. L.; Manns, M.; Zender, L.; Kubicka, S., Telomerase-dependent virotherapy overcomes resistance of hepatocellular carcinomas against chemotherapy and tumor necrosis factor-related apoptosis-inducing ligand by elimination of Mcl-1. *Cancer research* **2005,** *65* (16), 7393-7402.

(75) Mazzocca ,A.; Dituri, F.; De Santis, F.; Filannino, A.; Lopane, C.; Betz, R. C.; Li, Y. Y.; Mukaida, N.; Winter, P.; Tortorella, C.; Giannelli, G.; Sabba, C., Lysophosphatidic acid receptor LPAR6 supports the tumorigenicity of hepatocellular carcinoma. *Cancer research* **2015,** *75* (3), 532-543.

(76) Carloni, V.; Lulli, M.; Madiai, S.; Mello, T.; Hall, A.; Luong, T. V.; Pinzani, M.; Rombouts, K.; Galli, A., CHK2 overexpression and mislocalisation within mitotic structures enhances chromosomal instability and hepatocellular carcinoma progression. *Gut* **2018,** *67* (2), 348-361.

(77) Turato, C.; Cannito, S.; Simonato, D.; Villano, G.; Morello, E.; Terrin, L.; Quarta, S.; Biasiolo, A.; Ruvoletto, M.; Martini, A.; Fasolato, S.; Zanus, G.; Cillo, U.; Gatta, A.; Parola, M.; Pontisso, P., SerpinB3 and Yap Interplay Increases Myc Oncogenic Activity. *Scientific Reports* **2015,** *5*, 17701.

(78) Bristol-Myers Squibb Company, Opdivo (nivolumab). https://www.opdivo.com/ (accessed 09/09/2019).

(79) Nobel Media AB 2018, The Nobel Prize in Physiology or Medicine 2018. https://www.nobelprize.org/prizes/medicine/2018/summary/ (accessed 16/10/2018).

(80) Mizukoshi, E.; Kaneko, S., Immune cell therapy for hepatocellular carcinoma. *J Hematol Oncol* **2019,** *12* (1), 52-52.

(81) Zhu, W.; Peng, Y.; Wang, L.; Hong, Y.; Jiang ,X.; Li, Q.; Liu, H.; Huang, L.; Wu, J.; Celis, E.; Merchen, T.; Kruse, E.; He, Y., Identification of alpha-fetoprotein-specific T-cell receptors for hepatocellular carcinoma immunotherapy. *Hepatology (Baltimore, Md.)* **2018,** *68* (2), 574-589.

(82) Spear, T .T.; Callender, G. G.; Roszkowski, J. J.; Moxley, K. M.; Simms, P. E.; Foley, K. C.; Murray, D. C.; Scurti, G. M.; Li, M.; Thomas, J. T.; Langerman, A.; Garrett-Mayer, E.; Zhang, Y.; Nishimura, M. I., TCR gene-modified T cells can efficiently treat established hepatitis C-associated hepatocellular carcinoma tumors. *Cancer Immunol Immunother* **2016,** *65* (3), 293-304.

(83) Gao, H.; Li, K.; Tu, H.; Pan, X.; Jiang, H.; Shi, B.; Kong, J.; Wang, H.; Yang, S.; Gu, J.; Li, Z., Development of T cells redirected to glypican-3 for the treatment of hepatocellular carcinoma. *Clinical cancer*

research : an official journal of the American Association for Cancer Research **2014,** *20* (24), 6418-6428.

(84) Li, X.-a. A Clinical Research of CAR T Cells Targeting EpCAM Positive Cancer. https://clinicaltrials.gov/ct2/show/NCT03013712 (accessed 09/09/2019).

(85) Fumoto, S., Kawakami, S., Hashida, M., Nishida, K., Targeted Gene Delivery: Importance of Administration Routes. . In *Novel Gene Therapy Approaches*, Wei, M. G., D., Ed. IntechOpen: **2013**.

(86) Hobbs, S. K.; Monsky, W. L.; Yuan, F.; Roberts, W. G.; Griffith, L.; Torchilin, V. P.; Jain, R. K., Regulation of transport pathways in tumor vessels: role of tumor type and microenvironment. *Proceedings of the National Academy of Sciences of the United States of America* **1998,** *95* (8), 4607-4612.

(87) Matsumura, Y.; Maeda, H., A new concept for macromolecular therapeutics in cancer chemotherapy: mechanism of tumoritropic accumulation of proteins and the antitumor agent smancs. *Cancer research* **198** 46 ,6(12 Pt 1), 6387-6392.

(88) Prabhakar, U.; Maeda, H.; Jain, R. K.; Sevick-Muraca, E. M.; Zamboni, W.; Farokhzad, O. C.; Barry, S. T.; Gabizon, A.; Grodzinski, P.; Blakey, D. C., Challenges and key considerations of the enhanced permeability and retention (EPR) effect for nanomedicine drug delivery in oncology. *Cancer research* **2013,** *73* (8), 2412-2417.

(89) Valkenburg, K. C.; de Groot, A. E.; Pienta, K. J., Targeting the tumour stroma to improve cancer therapy. *Nat Rev Clin Oncol* **2018,** *15* (6), 366-381.

(90) Hofheinz, R. D.; al-Batran, S. E.; Hartmann, F.; Hartung, G.; Jager, D.; Renner, C.; Tanswell, P.; Kunz, U.; Amelsberg, A.; Kuthan, H.; Stehle, G., Stromal antigen targeting by a humanised monoclonal antibody: an early phase II trial of sibrotuzumab in patients with metastatic colorectal cancer. *Onkologie* **2003,** *26* (1), 44-48.

(91) Deodhar, S.; Dash, A. K., Long circulating liposomes: challenges and opportunities. *Therapeutic Delivery* **2018,** *9* (12), 857-872.

(92) Bazak, R.; Houri, M.; Achy, S. E.; Kamel, S.; Refaat, T., Cancer active targeting by nanoparticles: a comprehensive review of literature. *Journal of cancer research and clinical oncology* **2015,** *141* (5), 769-784.

(93) Huang, K.-W.; Lai, Y.-T.; Chern, G.-J.; Huang, S.-F.; Tsai, C.-L.; Sung, Y.-C ;.Chiang, C.-C.; Hwang, P.-B.; Ho, T.-L.; Huang, R.-L.; Shiue, T.-Y.; Chen, Y.; Wang, S.-K., Galactose Derivative-Modified Nanoparticles for Efficient siRNA Delivery to Hepatocellular Carcinoma. *Biomacromolecules* **2018,** *19* (6), 2330-2339.

(94) Yang, L.; Xiao, H.; Yan, L.; Wang, R.; Huang, Y.; Xie, Z.; Jing, X., Lactose targeting oxaliplatin prodrug loaded micelles for more effective chemotherapy of hepatocellular carcinoma. *Journal of Materials Chemistry B* **2014,** *2* (15), 2097-2106.

(95) Wei, M.; Guo, X.; Tu, L.; Zou, Q.; Li, Q.; Tang, C.; Chen, B.; Xu, Y.; Wu, C., Lactoferrin-modified PEGylated liposomes loaded with doxorubicin for targeting delivery to hepatocellular carcinoma. *International journal of nanomedicine* **2015,** *10*, 5123-5137.

(96) Bansal, D.; Yadav, K.; Pandey, V.; Ganeshpurkar, A.; Agnihotri, A.; Dubey, N., Lactobionic acid coupled liposomes: an innovative

strategy for targeting hepatocellular carcinoma. *Drug Deliv* **2016,** *23* (1), 140-146.

(97) Daniels, T. R.; Bernabeu, E.; Rodriguez, J. A.; Patel, S.; Kozman, M.; Chiappetta, D. A.; Holler, E.; Ljubimova, J. Y.; Helguera, G.; Penichet, M. L., The transferrin receptor and the targeted delivery of therapeutic agents against cancer. *Biochimica et biophysica acta* **2012,** *1820* (3), 291-317.

(98) Zhang ,X.; Li, J.; Yan, M., Targeted hepatocellular carcinoma therapy: transferrin modified, self-assembled polymeric nanomedicine for co-delivery of cisplatin and doxorubicin. *Drug development and industrial pharmacy* **2016,** *42* (10), 1590-1599.

(99) Zhang, H.; Patel, N.; Ding, S.; Xiong, J.; Wu, P., Theranostics for hepatocellular carcinoma with Fe3O4@ZnO nanocomposites. *Biomaterials Science* **2016,** *4* (2), 288-298.

(100) Zhang, L.; Gong, F.; Zhang, F.; Ma, J.; Zhang, P.; Shen, J., Targeted therapy for human hepatic carcinoma cells using folate-functionalized polymeric micelles loaded with superparamagnetic iron oxide and sorafenib in vitro. *International journal of nanomedicine* **2013,** *8*, 1517-1524.

(101) Xia, Y.; Zhao, M.; Chen, Y.; Hua, L.; Xu, T.; Wang, C.; Li, Y ;. Zhu, B., Folate-targeted selenium nanoparticles deliver therapeutic siRNA to improve hepatocellular carcinoma therapy. *RSC Advances* **2018,** *8* (46), 25932-25940.

(102) Zhu, X.; Tsend-Ayush, A.; Yuan, Z.; Wen, J.; Cai, J.; Luo, S.; Yao, J.; Bian, J.; Yin, L ;.Zhou, J.; Yao, J., Glycyrrhetinic acid-modified TPGS

polymeric micelles for hepatocellular carcinoma-targeted therapy. *International journal of pharmaceutics* **2017,** *529* (1-2), 451-464.

(103) Turato, C.; Balasso, A.; Carloni, V.; Tiribelli, C.; Mastrotto ,F.; Mazzocca, A.; Pontisso, P., New molecular targets for functionalized nanosized drug delivery systems in personalized therapy for hepatocellular carcinoma. *Journal of controlled release : official journal of the Controlled Release Society* **2017,** *268*.197-184 ,

(104) Wang, K.; Kievit, F. M.; Sham, J. G.; Jeon, M.; Stephen, Z. R.; Bakthavatsalam, A.; Park, J. O.; Zhang, M., Iron oxide-based nanovector for tumor targeted siRNA delivery in an orthotopic hepatocellular carcinoma xenograft mouse model. *Small (Weinheim an der Bergstrasse, Germany)* **2016,** *12* (4), 477-487.

(105) Shapiro, J. M.; Chung, W.; Ogawa, K.; Barker, L.; Carlson, R.; Wands, J. R.; Li, J., Identification of Tumor Antigen AF20 as Glycosylated Transferrin Receptor 1 in Complex with Heat Shock Protein 90 and/or Transporting ATPase. *PLOS ONE* **2016,** *11* (11), e0165227.

(106) Mohr, L.; Schauer, J. I.; Boutin, R. H.; Moradpour, D.; Wands, J. R., Targeted gene transfer to hepatocellular carcinoma cells in vitro using a novel monoclonal antibody-based gene delivery system. *Hepatology (Baltimore, Md.)* **1999,** *29* (1), 82-89.

(107) Brazeau, P.; Vale, W.; Burgus, R.; Ling, N.; Butcher, M.; Rivier, J.; Guillemin, R., Hypothalamic polypeptide that inhibits the secretion of immunoreactive pituitary growth hormone. *Science (New York, N.Y.)* **1973,** *179* (4068), 77-79.

(108) Reynaert, H.; Rombouts, K.; Vandermonde, A.; Urbain, D.; Kumar, U.; Bioulac-Sage, P.; Pinzani, M.; Rosenbaum, J.; Geerts, A.,

Expression of somatostatin receptors in normal and cirrhotic human liver and in hepatocellular carcinoma. *Gut* **2004,** *53* (8), 1180-1189.

(109) Sun, M.; Wang, Y.; Shen, J.; Xiao, Y.; Su, Z.; Ping, Q., Octreotide-modification enhances the delivery and targeting of doxorubicin-loaded liposomes to somatostatin receptors expressing tumor in vitro and in vivo. *Nanotechnology* **2010,** *21* (47), 475101.

(110) Giancotti, F. G.; Ruoslahti, E., Integrin signaling. *Science (New York, N.Y.)* **1999,** *285* (5430), 1028-1032.

(111) Li, S.; Wei, J.; Yuan, L.; Sun, H.; Liu, Y.; Zhang, Y.; Li, J.; Liu, X., RGD-Modified Endostatin Peptide 30 Derived from Endostatin Suppresses Invasion and Migration of HepG2 Cells Through the αvβ3 Pathway. *Cancer Biotherapy and Radiopharmaceuticals* **2011,** *26* (5), 529-538.

(112) Vilaça, H.; Ferreira, P. M. T.; Micaelo ,N. M., New cyclic RGD peptides: synthesis, characterization, and theoretical activity towards αvβ3 integrin. *Tetrahedron* **2014,** *70* (35), 5420-5427.

(113) Chen, L.; Liu, Y.; Wang, W.; Liu, K. A. I., Effect of integrin receptor-targeted liposomal paclitaxel for hepatocellular carcinoma targeting and therapy. *Oncology Letters* **2015,** *10* (1), 77-84.

(114) Smith, G. P.; Petrenko, V. A., Phage Display. *Chemical reviews* **1997,** *97* (2), 391-410.

(115) Nobel Media AB 2018, The Nobel Prize in Chemistry 2018. https://www.nobelprize.org/prizes/chemistry/2018/summary/ (accessed 16/10/2018).

(116) Lo, A.; Lin, C. T.; Wu, H. C., Hepatocellular carcinoma cell-specific peptide ligand for targeted drug delivery. *Molecular cancer therapeutics* **2008,** *7* (3), 579-589.

(117) Li, Y.; Hu, Y ;.Xiao, J.; Liu, G.; Li, X.; Zhao, Y.; Tan, H.; Shi, H.; Cheng, D., Investigation of SP94 Peptide as a Specific Probe for Hepatocellular Carcinoma Imaging and Therapy. *Sci Rep* **2016,** *6*, 33511.

(118) Tuerk, C.; Gold, L., Systematic evolution of ligands by exponential enrichment: RNA ligands to bacteriophage T4 DNA polymerase. *Science (New York, N.Y.)* **1990,** *249* (4968), 505-510.

(119) Ellington, A. D.; Szostak, J. W., In vitro selection of RNA molecules that bind specific ligands. *Nature* **1990,** *346* (6287), 818.822-

(120) Kaur, H., Aptamer Conjugated Quantum Dots for Imaging Cellular Uptake in Cancer Cells. *Journal of nanoscience and nanotechnology* **2019,** *19* (7), 3798-3803.

(121) Zhou, Y.; Li, W.; Tseng, Y.; Zhang, J.; Liu, J., Developing slow-off dickkopf-1 aptamers for early-diagnosis of hepatocellular carcinoma. *Talanta* **2019,** *194*, 422-429.

(122) Xiao, S.; Liu, Z.; Deng, R.; Li, C.; Fu, S.; Chen, G.; Zhang, X.; Ke, F.; Ke, S.; Yu, X.; Wang, S.; Zhong, Z., Aptamer-mediated gene therapy enhanced antitumor activity against human hepatocellular carcinoma in vitro and in vivo. *Journal of controlled release : official journal of the Controlled Release Society* **2017,** *258*, 130-145.

(123) Liu, Y.; Wu, X.; Gao, Y.; Zhang, J.; Zhang, D.; Gu, S.; Zhu, G.; Liu, G.; Li, X ,.Aptamer-functionalized peptide H3CR5C as a novel nanovehicle for codelivery of fasudil and miRNA-195 targeting

hepatocellular carcinoma. *International journal of nanomedicine* **2016,** *11*, 3891-3905.

(124) Villaverde, G.; Baeza, A., Targeting strategies for improving the efficacy of nanomedicine in oncology. *Beilstein J Nanotechnol* **2019,** *10*, 168-181.

(125) Khalil, I. A.; Younis, M. A.; Kimura, S.; Harashima, H., Lipid Nanoparticles for Cell-Specific in Vivo Targeted Delivery of Nucleic Acids. *Biological & pharmaceutical bulletin* **2020,** *43* (4), 584-595.

(126) Zhou, K.; Nguyen, L. H.; Miller, J. B.; Yan, Y.; Kos, P.; Xiong, H.; Li, L.; Hao, J.; Minnig, J. T.; Zhu, H.; Siegwart, D. J., Modular degradable dendrimers enable small RNAs to extend survival in an aggressive liver cancer model. *Proceedings of the National Academy of Sciences* **2016,** *113* (3), 520-525.

(127) Zamboni, C. G.; Kozielski, K. L.; Vaughan, H. J.; Nakata, M. M.; Kim, J.; Higgins, L. J.; Pomper, M. G.; Green, J. J., Polymeric nanoparticles as cancer-specific DNA delivery vectors to human hepatocellular carcinoma. *Journal of controlled release : official journal of the Controlled Release Society* **2017,** *263*, 18-28.

(128) Aznar, M. A.; Tinari, N.; Rullán, A. J.; Sánchez-Paulete, A. R.; Rodriguez-Ruiz ,M. E.; Melero, I., Intratumoral Delivery of Immunotherapy-Act Locally, Think Globally. *Journal of immunology (Baltimore, Md. : 1950)* **2017,** *198* (1), 31-39.

(129) Kim, Y. I.; Ahn, B.-C.; Ronald, J. A.; Katzenberg, R.; Singh, A.; Paulmurugan, R.; Ray, S.; Gambhir, S. S.; Hofmann, L. V., Intratumoral versus intravenous gene therapy using a transcriptionally targeted viral

vector in an orthotopic hepatocellular carcinoma rat model. *J Vasc Interv Radiol* **2012,** *23* (5), 704-711.

(130) Qiu, Z.; Wang, G. S.; Gao, F ,.Whole-course management of interventional treatment in liver cancer patients with portal hypertension. *Journal of Interventional Medicine* **2019,** *2* (2), 52-54.

(131) Khan, A. A.; Vishwakarma, S. K.; Bardia, A.; Habeeb, M. A.; Dhayal, M., Chapter 59 - Repopulation of Cirrhotic Liver by Hepatic Stem/Progenitor Cells: A Promising Strategy Alternative to Liver Transplantation. In *Liver Pathophysiology*, Muriel, P., Ed. Academic Press: Boston, 2017; pp 817-836.

(132) Song, J.; Zhang, F.; Ji, J.; Chen, M.; Li, Q ;.Weng, Q.; Gu, S.; Kogut, M. J.; Yang, X., Orthotopic hepatocellular carcinoma: molecular imaging-monitored intratumoral hyperthermia-enhanced direct oncolytic virotherapy. *International Journal of Hyperthermia* **2019,** *36* (1), 343-349.

(133) National institute of health (NIH), Hepatocellular carcinoma clinical trials. https://clinicaltrials.gov/ct2/results?cond=Hepatocellular+Carcinoma&term=&cntry=&state=&city=&dist= (accessed 02/06/2020).

(134) Paul, S. B.; Sharma, H., Role of Transcatheter Intra-arterial Therapies for Hepatocellular Carcinoma. *J Clin Exp Hepatol* **2014,** *4* (Suppl 3), S112-S121.

(135) Ma, M.-C.; Chen, Y.-Y.; Li, S.-H.; Cheng, Y.-F.; Wang, C.-C.; Chiu, T.-J.; Pei, S.-N.; Liu, C.-T.; Huang, T.-L.; Huang, C.-H.; Su, Y.-L.; Chen, Y.-H.; Lu, S.-N.; Rau, K.-M., Intra-Arterial Chemotherapy with

Doxorubicin and Cisplatin Is Effective for Advanced Hepatocellular Cell Carcinoma. *The Scientific World Journal* **2014,** *2014*, 160138.

(136) Ana, C. S.; Carla, M. L.; Jose, M. S. L.; Amaral, M. H., Nucleic Acids Delivery Systems: A Challenge for Pharmaceutical Technologists. *Current Drug Metabolism* **2015,** *16* (1), 3-16.

(137) Novartis Pharmaceuticals Corporation, The KYMRIAH Experience.https://www.hcp.novartis.com/globalassets/products70/kymriah---full-site/ped-all/hcp-resources/kymriah-pall-manufacturing-brochure-digital.pdf (accessed 17/10/2018).

(138) Spark Therapeutics, Package insert-LUXTURNA https://www.fda.gov/downloads/BiologicsBloodVaccines/CellularGeneTherapyProducts/ApprovedProducts/UCM589541.pdf (accessed 17/10/2018).

(139) Li, W.; Szoka, F. C., Jr., Lipid-based nanoparticles for nucleic acid delivery. *Pharmaceutical research* **2007,** *24* (3), 438-449.

(140) Sato, Y.; Hatakeyama, H.; Sakurai, Y.; Hyodo, M.; Akita, H.; Harashima, H., A pH-sensitive cationic lipid facilitates the delivery of liposomal siRNA and gene silencing activity in vitro and in vivo. *Journal of controlled release : official journal of the Controlled Release Society* **2012,** *163* (3), 267-276.

(141) Sato, Y.; Hashiba, K.; Sasaki, K.; Maeki ,M.; Tokeshi, M.; Harashima, H., Understanding structure-activity relationships of pH-sensitive cationic lipids facilitates the rational identification of promising lipid nanoparticles for delivering siRNAs in vivo. *Journal of controlled release : official journal of the Controlled Release Society* **2019,** *295*, 140-152.

(142) Liu, C. H.; Chern, G. J.; Hsu, F. F.; Huang, K. W.; Sung, Y. C.; Huang, H. C.; Qiu, J. T.; Wang, S. K.; Lin, C. C.; Wu, C. H.; Wu, H. C.; Liu, J. Y.; Chen, Y., A multifunctional nanocarrier for efficient TRAIL-based gene therapy against hepatocellular carcinoma with desmoplasia in mice. *Hepatology (Baltimore, Md.)* **2018,** *67* (3), 899-913.

(143) Werfel, T.; Duvall, C., 7 - Polymeric nanoparticles for gene delivery. In *Polymers and Nanomaterials for Gene Therapy*, Narain, R., Ed. Woodhead Publishing: 2016; pp 147-188.

(144) Xue, W.-J.; Feng, Y.; Wang, F.; Guo, Y.-B.; Li, P.; Wang, L.; Liu, Y.-F.; Wang, Z.-W.; Yang, Y.-M.; Mao, Q.-S., Asialoglycoprotein receptor-magnetic dual targeting nanoparticles for delivery of RASSF1A to hepatocellular carcinoma. *Scientific Reports* **2016,** *6*, 22149.

(145) Sandra, F.; Khaliq, N. U.; Sunna, A.; Care, A., Developing Protein-Based Nanoparticles as Versatile Delivery Systems for Cancer Therapy and Imaging. *Nanomaterials (Basel)* **2019,** *9* (9), 1329.

(146) Ashley, C. E.; Carnes, E. C.; Phillips, G. K.; Durfee, P. N.; Buley, M. D.; Lino, C. A.; Padilla, D. P.; Phillips, B.; Carter, M. B.; Willman, C. L.; Brinker, C. J.; Caldeira, J. d. C.; Chackerian, B.; Wharton, W ;. Peabody, D. S., Cell-Specific Delivery of Diverse Cargos by Bacteriophage MS2 Virus-like Particles. *ACS Nano* **2011,** *5* (7), 5729-5745.

(147) Wang, G.; Jia, T.; Xu, X.; Chang, L.; Zhang, R.; Fu, Y.; Li, Y.; Yang, X.; Zhang, K.; Lin, G.; Han, Y.; Li, J., Novel miR-122 delivery system based on MS2 virus like particle surface displaying cell-penetrating peptide TAT for hepatocellular carcinoma. *Oncotarget* **2016,** 7(37): 59402-59416

(148) Tian, Y.; Zhou, M.; Shi, H.; Gao, S.; Xie, G.; Zhu, M.; Wu, M.; Chen, J.; Niu, Z., Integration of Cell-Penetrating Peptides with Rod-like Bionanoparticles: Virus-Inspired Gene-Silencing Technology. *Nano Letters* **2018,** *18* (9), 5453-5460.

(149) Kumar, S.; Diwan, A.; Singh, P.; Gulati, S.; Choudhary, D.; Mongia, A.; Shukla, S.; Gupta, A., Functionalized gold nanostructures: promising gene delivery vehicles in cancer treatment. *RSC Advances* **2019,** *9* (41), 23894-23907.

(150) Xia, Y.; Wang, C.; Xu, T.; Li, Y.; Guo, M.; Lin, Z.; Zhao, M.; Zhu, B., Targeted delivery of HES5-siRNA with novel polypeptide-modified nanoparticles for hepatocellular carcinoma therapy. *RSC Advances* **2018,** *8* (4), 1917-1926.

(151) Qin, L.; Yan, P.; Xie, C.; Huang, J.; Ren, Z.; Li, X.; Best, S.; Cai, X.; Han, G., Gold nanorod-assembled ZnGa2O4:Cr nanofibers for LED-amplified gene silencing in cancer cells. *Nanoscale* **2018,** *10* (28), 13432-13442.

(152) Wang, W.; Huang, S.; Yuan, J.; Xu, X.; Li, H.; Lv, Z.; Yu, W.; Duan, S.; Hu, Y., Reverse Multidrug Resistance in Human HepG2/ADR by Anti-miR-21 Combined with Hyperthermia Mediated by Functionalized Gold Nanocages. *Molecular Pharmaceutics* **2018,** *15* (9), 3767-3776.

(153) Hsu, S. H.; Yu, B.; Wang, X.; Lu, Y.; Schmidt, C. R.; Lee, R. J.; Lee, L. J.; Jacob, S. T.; Ghoshal, K., Cationic lipid nanoparticles for therapeutic delivery of siRNA and miRNA to murine liver tumor. *Nanomedicine : nanotechnology, biology, and medicine* **2013,** *9* (8), 1169-1180.

(154) Huang, X.; Magnus, J.; Kaimal, V.; Karmali, P.; Li, J.; Walls, M.; Prudente, R.; Sung, E.; Sorourian, M.; Lee, R.; Davis, S.; Yang, X ;. Estrella, H.; Lee, E. C.; Chau, B. N.; Pavlicek, A.; Zabludoff, S., Lipid Nanoparticle-Mediated Delivery of Anti-miR-17 Family Oligonucleotide Suppresses Hepatocellular Carcinoma Growth. *Molecular cancer therapeutics* **2017,** *16* (5), 905-913.

(155) Yang, Y ;.Zhang, Z.; Chen, L.; Gu, W.; Li, Y., Galactosylated Poly(2-(2-aminoethyoxy)ethoxy)phosphazene/DNA Complex Nanoparticles: In Vitro and In Vivo Evaluation for Gene Delivery. *Biomacromolecules* **2010,** *11* (4), 927-933.

(156) Opanasopit, P.; Apirakaramwong, A ;.Ngawhirunpat, T.; Rojanarata, T.; Ruktanonchai, U., Development and characterization of pectinate micro/nanoparticles for gene delivery. *AAPS PharmSciTech* **2008,** *9* (1), 67-74.

(157) Ren, Y.; Li, R.-Q.; Cai, Y.-R.; Xia, T.; Yang, M.; Xu, F.-J., Effective Codelivery of lncRNA and pDNA by Pullulan-Based Nanovectors for Promising Therapy of Hepatocellular Carcinoma. *Advanced Functional Materials* **2016,** *26* (40), 7314-7325.

(158) Li, T.; Xue, Y.; Wang, G.; Gu, T.; Li, Y.; Zhu, Y. Y.; Chen, L., Multi-target siRNA: Therapeutic Strategy for Hepatocellular Carcinoma. *Journal of Cancer* **2016,** *7* (10), 1317-1327.

(159) Zhu, Q. L.; Zhou, Y.; Guan, M.; Zhou, X. F.; Yang, S. D.; Liu, Y.; Chen, W. L.; Zhang, C. G.; Yuan, Z. Q.; Liu, C.; Zhu, A. J.; Zhang, X. N., Low-density lipoprotein-coupled N-succinyl chitosan nanoparticles co-delivering siRNA and doxorubicin for hepatocyte-targeted therapy. *Biomaterials* **2014,** *35* (22), 5965-5976.

(160) Shen, J.; Sun, H.; Meng, Q.; Yin, Q.; Zhang, Z.; Yu, H.; Li, Y., Simultaneous inhibition of tumor growth and angiogenesis for resistant hepatocellular carcinoma by co-delivery of sorafenib and survivin small hairpin RNA. *Mol Pharm* **2014,** *11* (10), 3342-3351.

(161) Devulapally, R.; Foygel, K.; Sekar, T. V.; Willmann, J. K.; Paulmurugan, R ,.Gemcitabine and Antisense-microRNA Co-encapsulated PLGA–PEG Polymer Nanoparticles for Hepatocellular Carcinoma Therapy. *ACS Applied Materials & Interfaces* **2016,** *8* (49), 33412-33422.

(162) Morgan, R. A., Live and let die: a new suicide gene therapy moves to the clinic. *Molecular therapy : the journal of the American Society of Gene Therapy* **2012,** *20* (1), 11-13.

(163) Ding, Q.; Liu, D.; Guo, D.; Yang, F.; Pang, X.; Che, R.; Zhou, N.; Xie, J.; Sun, J.; Huang, Z.; Gu, N., Shape-controlled fabrication of magnetite silver hybrid nanoparticles with high performance magnetic hyperthermia. *Biomaterials* **2017,** *124*, 35-46.

(164) Wang, Z.; Chang, Z.; Lu, M.; Shao, D.; Yue, J.; Yang, D.; Zheng, X.; Li, M.; He, K.; Zhang, M.; Chen, L.; Dong, W.-f., Shape-controlled magnetic mesoporous silica nanoparticles for magnetically-mediated suicide gene therapy of hepatocellular carcinoma. *Biomaterials* **2018,** *154*, 147-157.

(165) Vandamme, T. F., Use of rodents as models of human diseases. *J Pharm Bioallied Sci* **2014,** *6* (1), 2-9.

(166) Brown, Z. J.; Heinrich, B.; Greten, T. F., Mouse models of hepatocellular carcinoma: an overview and highlights for immunotherapy

research. *Nature reviews. Gastroenterology & hepatology* **2018,** *15* (9), 536-554.

(167) Heindryckx, F.; Colle, I.; Van Vlierberghe, H., Experimental mouse models for hepatocellular carcinoma research. *International journal of experimental pathology* **2009,** *90* (4), 367-386.

(168) Cho, K.; Ro, S. W.; Seo, S. H.; Jeon, Y.; Moon, H.; Kim, D. Y.; Kim, S. U., Genetically Engineered Mouse Models for Liver Cancer. *Cancers* **2019,** *12* (1), 14.

(169) Day, C.-P.; Merlino, G.; Van Dyke, T., Preclinical Mouse Cancer Models: A Maze of Opportunities and Challenges. *Cell* **2015,** *163* (1), 39-53.

(170) Lai, Y.; Wei, X.; Lin, S.; Qin, L.; Cheng, L.; Li ,P., Current status and perspectives of patient-derived xenograft models in cancer research. *J Hematol Oncol* **2017,** *10* (1), 106.

(171) Liu, Y.; Qi, X.; Zeng, Z.; Wang, L.; Wang, J.; Zhang, T.; Xu, Q.; Shen, C.; Zhou, G.; Yang, S.; Chen, X.; Lu, F., CRISPR/Cas9-mediated p53 and Pten dual mutation accelerates hepatocarcinogenesis in adult hepatitis B virus transgenic mice. *Sci Rep* **2017,** *7* (1), 2796.

(172) Das, D. K.; Durojaiye, V.; Ilboudo, A.; Naidoo, M. K.; Ogunwobi, O., A "Patient-Like" Orthotopic Syngeneic Mouse Model of Hepatocellular Carcinoma Metastasis. *Journal of visualized experiments : JoVE* **2015,** (105), e52858.

(173) Kang, J. H.; Mori, T.; Niidome, T.; Katayama, Y., A syngeneic hepatocellular carcinoma model rapidly and simply prepared using a hydrodynamics-based procedure. *Veterinary journal (London, England : 1997)* **2009,** *181* (3), 336-339.

(174) Uehara, T.; Pogribny, I. P.; Rusyn, I., The DEN and CCl4 -Induced Mouse Model of Fibrosis and Inflammation-Associated Hepatocellular Carcinoma. *Current protocols in pharmacology* **2014,** *66*, 14 30 11-10.

(175) Bonifant, C. L.; Jackson, H. J.; Brentjens, R. J.; Curran, K. J., Toxicity and management in CAR T-cell therapy. *Molecular therapy oncolytics* **2016,** *3*, 16011.

(176) Ramamoorth, M.; Narvekar, A., Non viral vectors in gene therapy-an overview. *J Clin Diagn Res* **2015,** *9* (1), GE01-06.

(177) Zhang, M.; Garbuzenko, O. B.; Reuhl, K. R.; Rodriguez-Rodriguez, L.; Minko, T., Two-in-one: combined targeted chemo and gene therapy for tumor suppression and prevention of metastases. *Nanomedicine (London, England)* **2012,** *7* (2), 185-197.

(178) Lazzari, C.; Karachaliou, N.; Bulotta, A.; Viganó, M.; Mirabile, A.; Brioschi, E.; Santarpia, M.; Gianni, L.; Rosell, R.; Gregorc, V., Combination of immunotherapy with chemotherapy and radiotherapy in lung cancer: is this the beginning of the end for cancer? *Therapeutic advances in medical oncology* **2018,** *10*, 1758835918762094-1758835918762094.

(179) Keating, G. M.; Santoro, A., Sorafenib: a review of its use in advanced hepatocellular carcinoma. *Drugs* **2009,** *69* (2), 223-240.

(180) Ziogas, I. A.; Tsoulfas, G., Evolving role of Sorafenib in the management of hepatocellular carcinoma. *World journal of clinical oncology* **2017,** *8* (3), 203-213.

(181) Takei, Y.; Kadomatsu, K., Midkine and Chemoresistance in Cancers. In *Midkine: From Embryogenesis to Pathogenesis and Therapy*,

Ergüven, M.; Muramatsu, T.; Bilir, A., Eds. Springer Netherlands: Dordrecht, 2012; pp 225-236.

(182) Ramamoorth, M.; Narvekar, A., Non viral vectors in gene therapy-an overview. *Journal of clinical and diagnostic research : JCDR* **2015,** *9* (1), GE01-GE06.

(183) Yin, H.; Kanasty, R. L.; Eltoukhy, A. A.; Vegas, A. J.; Dorkin, J. R.; Anderson, D. G., Non-viral vectors for gene-based therapy. *Nature Reviews Genetics* **2014,** *15*.541 ,

(184) Cullis, P. R.; Hope, M. J., Lipid Nanoparticle Systems for Enabling Gene Therapies. *Molecular Therapy* **2017,** *25* (7), 1467-1475.

(185) Sato, Y.; Hashiba, K.; Sasaki, K.; Maeki, M.; Tokeshi, M.; Harashima, H., Understanding structure-activity relationships of pH-sensitive cationic lipids facilitates the rational identification of promising lipid nanoparticles for delivering siRNAs in vivo. *Journal of Controlled Release* **2019,** *295*, 140-152.

(186) Abd Elwakil, M. M.; Khalil, I. A.; Elewa, Y. H. A ;.Kusumoto, K.; Sato, Y.; Shobaki, N.; Kon, Y.; Harashima, H., Lung-Endothelium-Targeted Nanoparticles Based on a pH-Sensitive Lipid and the GALA Peptide Enable Robust Gene Silencing and the Regression of Metastatic Lung Cancer. *Advanced Functional Materials 0* (0), 1807677.

(187) Sato, Y.; Matsui, H.; Sato, R.; Harashima, H., Neutralization of negative charges of siRNA results in improved safety and efficient gene silencing activity of lipid nanoparticles loaded with high levels of siRNA. *Journal of controlled release : official journal of the Controlled Release Society* **2018,** *284*, 179-187.

(188) Nakamura, Y.; Kogure, K.; Futaki, S.; Harashima, H., Octaarginine-modified multifunctional envelope-type nano device for siRNA. *Journal of Controlled Release* **2007**.367-360 ,(3) 119 ,

(189) Khalil, I. A.; Kogure, K.; Futaki, S.; Harashima, H., High density of octaarginine stimulates macropinocytosis leading to efficient intracellular trafficking for gene expression. *Journal of Biological Chemistry* **2006,** *281* (6), 3544.3551-

(190) Ara, M. N.; Hyodo, M.; Ohga, N.; Hida, K.; Harashima, H., Development of a novel DNA aptamer ligand targeting to primary cultured tumor endothelial cells by a cell-based SELEX method. *PloS one* **2012,** *7* (12), e50174-e50174.

(191) Li, Y.; Hu, Y ;.Xiao, J.; Liu, G.; Li, X.; Zhao, Y.; Tan, H.; Shi, H.; Cheng, D., Investigation of SP94 Peptide as a Specific Probe for Hepatocellular Carcinoma Imaging and Therapy. *Scientific Reports* **2016,** *6*, 33511.

(192) Warashina, S.; Nakamura, T.; Sato, Y.; Fujiwara, Y.; Hyodo, M.; Hatakeyama, H.; Harashima, H., A lipid nanoparticle for the efficient delivery of siRNA to dendritic cells. *Journal of Controlled Release* **2016,** *225*, 183-191.

(193) Yamada, Y.; Burger, L.; Kawamura, E.; Harashima, H., Packaging of the Coenzyme Q₁₀ into a Liposome for Mitochondrial Delivery and the Intracellular Observation in Patient Derived Mitochondrial Disease Cells. *Biological and Pharmaceutical Bulletin* **2017,** *40* (12), 2183-2190.

(194) Sakurai, Y.; Hatakeyama, H.; Sato, Y ;.Hyodo, M.; Akita, H.; Harashima, H., Gene silencing via RNAi and siRNA quantification in

tumor tissue using MEND, a liposomal siRNA delivery system. *Molecular therapy : the journal of the American Society of Gene Therapy* **2013,** *21* (6), 1195-1203.

(195) Aboutaleb, A. E., Abdel-Rahman, S. I., Ahmed, M.O., Younis, M.A., Formulation of domperidone in gastro-retentive floating tablets. *Journal of Innovations in Pharmaceuticals and Biological Sciences* **2016,** *3* (2), 81-93.

(196) Ritger, P. L.; Peppas, N. A., A simple equation for description of solute release II. Fickian and anomalous release from swellable devices. *Journal of Controlled Release* **1987,** *5* (1), 37-42.

(197) Contratto, M.; Wu, J., Targeted therapy or immunotherapy? Optimal treatment in hepatocellular carcinoma. *World journal of gastrointestinal oncology* **2018,** *10* (5), 108-114.

(198) Zhu, W.-W.; Guo, J.-J.; Guo, L.; Jia, H.-L.; Zhu, M.; Zhang, J.-B.; Loffredo, C. A.; Forgues, M.; Huang, H.; Xing, X.-J.; Ren, N.; Dong, Q.-Z.; Zhou, H.-J.; Ren, Z.-G.; Zhao, N.-Q ;.Wang, X. W.; Tang, Z.-Y.; Qin, L.-X.; Ye, Q.-H., Evaluation of Midkine as a Diagnostic Serum Biomarker in Hepatocellular Carcinoma. *Clinical Cancer Research* **2013,** *19* (14), 3944-3954.

(199) Khalil, I. A.; Harashima, H., An efficient PEGylated gene delivery system with improved targeting: Synergism between octaarginine and a fusogenic peptide. *International journal of pharmaceutics* **2018,** *538* (1), 179-187.

(200) Khalil, I. A.; Kimura, S.; Sato, Y.; Harashima, H., Synergism between a cell penetrating peptide and a pH-sensitive cationic lipid in efficient gene delivery based on double-coated nanoparticles. *Journal of*

controlled release : official journal of the Controlled Release Society **2018,** *275*, 107-116.

(201) Khalil, I. A.; Hayashi, Y.; Mizuno, R.; Harashima, H., Octaarginine- and pH sensitive fusogenic peptide-modified nanoparticles for liver gene delivery. *Journal of controlled release : official journal of the Controlled Release Society* **2011,** *156* (3), 374-380.

(202) Kauffman, K. J.; Dorkin, J. R.; Yang, J. H.; Heartlein, M. W.; DeRosa, F.; Mir, F. F.; Fenton, O. S.; Anderson, D. G., Optimization of Lipid Nanoparticle Formulations for mRNA Delivery in Vivo with Fractional Factorial and Definitive Screening Designs. *Nano Letters* **2015,** *15* (11), 7300-7306.

(203) Eetezadi, S.; Evans, J. C.; Shen, Y. T.; De Souza, R.; Piquette-Miller, M.; Allen, C., Ratio-Dependent Synergism of a Doxorubicin and Olaparib Combination in 2D and Spheroid Models of Ovarian Cancer. *Mol Pharm* **2018,** *15* (2), 472-485.

(204) Zuhorn ,I. S.; Bakowsky, U.; Polushkin, E.; Visser, W. H.; Stuart, M. C.; Engberts, J. B.; Hoekstra, D., Nonbilayer phase of lipoplex-membrane mixture determines endosomal escape of genetic cargo and transfection efficiency. *Molecular therapy : the journal of the American Society of Gene Therapy* **2005,** *11* (5), 801-810.

(205) Hong, Y.-J.; Seo, H. J.; Kim, J. D.; Shin, W. C.; Kim, J.-C., Egg phosphatidylcholine and dioleoylphosphatidylethanolamine liposomes containing acid proteinoid: Comparison of pH-sensitivity. *European Journal of Lipid Science and Technology* **2011,** *113* (2), 146-151.

(206) Cheng, X.; Lee, R. J., The role of helper lipids in lipid nanoparticles (LNPs) designed for oligonucleotide delivery. *Advanced drug delivery reviews* **2016,** *99* (Pt A), 129-137.

(207) Lang, J.; Vigo-Pelfrey, C.; Martin, F., Liposomes composed of partially hydrogenated egg phosphatidylcholines: fatty acid composition, thermal phase behavior and oxidative stability. *Chemistry and physics of lipids* **1990,** *53* (1), 91-101.

(208) Hayashi ,Y.; Yamauchi, J.; Khalil, I. A.; Kajimoto, K.; Akita, H.; Harashima, H., Cell penetrating peptide-mediated systemic siRNA delivery to the liver. *International journal of pharmaceutics* **2011,** *419* (1-2), 308-313.

(209) Hu, Y.; Haynes, M. T.; Wang, Y.; Liu ,F.; Huang, L., A highly efficient synthetic vector: nonhydrodynamic delivery of DNA to hepatocyte nuclei in vivo. *ACS nano* **2013,** *7* (6), 5376-5384.

(210) Tanaka, Y.; Tateishi, R.; Koike, K., Proteoglycans Are Attractive Biomarkers and Therapeutic Targets in Hepatocellular Carcinoma. *Int J Mol Sci* **2018,** *19* (10), 3070.

(211) Sun, W.; Wang, Y.; Cai, M.; Lin, L.; Chen, X.; Cao, Z.; Zhu, K.; Shuai, X., Codelivery of sorafenib and GPC3 siRNA with PEI-modified liposomes for hepatoma therapy. *Biomaterials Science* ,(12) 5 ,2017 .2479-2468

(212) Xiao, Y.; Liu, Y.; Yang, S.; Zhang, B.; Wang, T.; Jiang, D.; Zhang, J.; Yu, D.; Zhang, N., Sorafenib and gadolinium co-loaded liposomes for drug delivery and MRI-guided HCC treatment. *Colloids and surfaces. B, Biointerfaces*.92-83 ,141 ,2016

(213) Desai, D. S., D., Implication of Nanoparticles for Controlled Drug Delivery System. *International journal of pharmaceutical sciences and research* **2013,** *4* (7), 2478-2488.

(214) Shazly, G. A., Ciprofloxacin Controlled-Solid Lipid Nanoparticles: Characterization, In Vitro Release, and Antibacterial Activity Assessment. *Biomed Res Int* **2017,** *2017*, 2120734-2120734.

(215) Rehman, M.; Madni, A.; Ihsan, A.; Khan, W. S.; Khan, M. I.; Mahmood, M. A.; Ashfaq, M.; Bajwa, S. Z.; Shakir, I., Solid and liquid lipid-based binary solid lipid nanoparticles of diacerein: in vitro evaluation of sustained release, simultaneous loading of gold nanoparticles, and potential thermoresponsive behavior. *International journal of nanomedicine* **2015,** *10*, 2805-281.4

(216) Zhou, X.; Huang, L., DNA transfection mediated by cationic liposomes containing lipopolylysine: characterization and mechanism of action. *Biochimica et biophysica acta* **1994,** *1189* (2), 195-203.

(217) Murray, K. D.; McQuillin, A.; Stewart, L.; Etheridge, C. J.; Cooper, R. G.; Miller, A. D.; Gurling, H. M. D., Cationic liposome-mediated DNA transfection in organotypic explant cultures of the ventral mesencephalon. *Gene Therapy* **1999,** *6*, 190.

(218) Sun, Y.; Ma, W.; Yang, Y.; He, M.; Li, A.; Bai, L.; Yu, B.; Yu, Z., Cancer nanotechnology: Enhancing tumor cell response to chemotherapy for hepatocellular carcinoma therapy. *Asian Journal of Pharmaceutical Sciences* **2019,** *14* (6), 581-594.

(219) Sato, Y.; Note, Y.; Maeki, M.; Kaji, N.; Baba, Y.; Tokeshi, M ;. Harashima, H., Elucidation of the physicochemical properties and

potency of siRNA-loaded small-sized lipid nanoparticles for siRNA delivery. *Journal of Controlled Release* **2016,** *229*, 48-57.

(220) Kimura, N.; Maeki, M.; Sato, Y.; Note, Y.; Ishida, A.; Tani ,H.; Harashima, H.; Tokeshi, M., Development of the iLiNP Device: Fine Tuning the Lipid Nanoparticle Size within 10 nm for Drug Delivery. *ACS Omega* **2018,** *3* (5), 5044-5051.

(221) Fridman, R.; Benton, G.; Aranoutova, I.; Kleinman, H. K.; Bonfil, R. D., Increased initiation and growth of tumor cell lines, cancer stem cells and biopsy material in mice using basement membrane matrix protein (Cultrex or Matrigel) co-injection. *Nature protocols* **2012,** *7* (6), 1138-1144.

(222) Kimura, S.; Khalil, I. A.; Elewa, Y .H. A.; Harashima, H., Spleen selective enhancement of transfection activities of plasmid DNA driven by octaarginine and an ionizable lipid and its implications for cancer immunization. *Journal of Controlled Release* **2019,** *313*, 70-79.

(223) Zhang, Y.; Huo ,M.; Zhou, J.; Xie, S., PKSolver: An add-in program for pharmacokinetic and pharmacodynamic data analysis in Microsoft Excel. *Computer methods and programs in biomedicine* **2010,** *99* (3), 306-314.

(224) Chou, T. C.; Talalay, P., Quantitative analysis of dose-effect relationships: the combined effects of multiple drugs or enzyme inhibitors. *Advances in enzyme regulation* **1984,** *22*, 27-55.

(225) El-Naseery, N. I.; Elewa, Y. H. A.; Ichii, O.; Kon, Y., An experimental study of menopause induced by bilateral ovariectomy and mechanistic effects of mesenchymal stromal cell therapy on the parotid

gland of a rat model. *Annals of anatomy = Anatomischer Anzeiger : official organ of the Anatomische Gesellschaft* **2018,** *220*, 9-20.

(226) Yoo, J. W.; Chambers, E.; Mitragotri, S ,.Factors that control the circulation time of nanoparticles in blood: challenges, solutions and future prospects. *Current pharmaceutical design* **2010,** *16* (21), 2298-2307.

(227) Cabral, H.; Matsumoto, Y.; Mizuno, K.; Chen, Q.; Murakami, M.; Kimura, M.; Terada, Y.; Kano, M. R.; Miyazono, K.; Uesaka, M.; Nishiyama, N.; Kataoka, K., Accumulation of sub-100 nm polymeric micelles in poorly permeable tumours depends on size. *Nature nanotechnology* **2011,** *6* (12), 815-823.

(228) Hibino, M.; Yamada, Y.; Fujishita, N ;.Sato, Y.; Maeki, M.; Tokeshi, M.; Harashima, H., The Use of a Microfluidic Device to Encapsulate a Poorly Water-Soluble Drug CoQ(10) in Lipid Nanoparticles and an Attempt to Regulate Intracellular Trafficking to Reach Mitochondria. *Journal of pharmaceutical sciences* **2019,** *108* (8), 2668-2676.

(229) Tan, Z.-J.; Chen, S.-J., Nucleic acid helix stability: effects of salt concentration, cation valence and size, and chain length. *Biophys J* **2006,** *90* (4), 1175-1190.

(230) Schroeder, A.; Levins, C. G.; Cortez ,C.; Langer, R.; Anderson, D. G., Lipid-based nanotherapeutics for siRNA delivery. *J Intern Med* **2010,** *267* (1), 9-21.

(231) Zhang, Y.-R.; Lin, R.; Li, H.-J.; He, W.-l.; Du, J.-Z.; Wang, J., Strategies to improve tumor penetration of nanomedicines through

nanoparticle design. *WIREs Nanomedicine and Nanobiotechnology* **2019,** *11* (1), e1519.

(232) Khalil, I. A.; Sato, Y.; Harashima, H., Recent advances in the targeting of systemically administered non-viral gene delivery systems. *Expert opinion on drug delivery* **2**.1050-1037 ,(10) 16 ,019

(233) Kaur, J.; Kant, R., Curvature-Induced Anomalous Enhancement in the Work Function of Nanostructures. *The journal of physical chemistry letters* **2015,** *6* (15), 2870-2874.

(234) Suk, J. S.; Xu, Q.; Kim, N.; Hanes, J.; Ensign, L .M., PEGylation as a strategy for improving nanoparticle-based drug and gene delivery. *Advanced drug delivery reviews* **2016,** *99* (Pt A), 28-51.

(235) Hatakeyama, H.; Akita, H.; Harashima, H., The polyethyleneglycol dilemma: advantage and disadvantage of PEGylation of liposomes for systemic genes and nucleic acids delivery to tumors. *Biological & pharmaceutical bulletin* **2013,** *36* (6), 892-899.

(236) Hamano, N.; Böttger, R.; Lee, S. E.; Yang, Y.; Kulkarni, J. A.; Ip, S.; Cullis, P. R.; Li, S. D., Robust Microfluidic Technology and New Lipid Composition for Fabrication of Curcumin-Loaded Liposomes: Effect on the Anticancer Activity and Safety of Cisplatin. *Mol Pharm* **2019,** *16* (9), 3957-3967.

(237) Xu, J.; Zhang, S.; Machado, A.; Lecommandoux, S.; Sandre, O.; Gu ,F.; Colin, A., Controllable Microfluidic Production of Drug-Loaded PLGA Nanoparticles Using Partially Water-Miscible Mixed Solvent Microdroplets as a Precursor. *Scientific Reports* **2017,** *7* (1), 4794.

(238) Sakurai, Y.; Hatakeyama, H.; Sato, Y.; Hyodo, M ;.Akita, H.; Harashima, H., Gene silencing via RNAi and siRNA quantification in

tumor tissue using MEND, a liposomal siRNA delivery system. *Molecular therapy : the journal of the American Society of Gene Therapy* **2013,** *21* (6), 1195-1203.

(239) Wang, J.; Bai ,R.; Yang, R.; Liu, J.; Tang, J.; Liu, Y.; Li, J.; Chai, Z.; Chen, C., Size- and surface chemistry-dependent pharmacokinetics and tumor accumulation of engineered gold nanoparticles after intravenous administration. *Metallomics* **2015,** *7* (3), 516-524.

(240) Nunes, S. S.; Fernandes, R. S.; Cavalcante, C. H.; da Costa César, I.; Leite, E. A.; Lopes, S. C. A.; Ferretti, A.; Rubello, D.; Townsend, D. M.; de Oliveira, M. C.; Cardoso, V. N.; de Barros, A. L. B., Influence of PEG coating on the biodistribution and tumor accumulation of pH-sensitive liposomes. *Drug Deliv Transl Res* **2019,** *9* (1), 123-130.

(241) Yamashita, F.; Hashida, M., Pharmacokinetic considerations for targeted drug delivery. *Advanced drug delivery reviews* **2013,** *65* (1), 139-147.

(242) Shim, M. S ;.Chang, S.-S.; Kwon, Y. J., Stimuli-responsive siRNA carriers for efficient gene silencing in tumors via systemic delivery. *Biomaterials Science* **2014,** *2* (1), 35-40.

(243) Judge, A. D.; Robbins, M.; Tavakoli, I.; Levi, J.; Hu, L.; Fronda, A.; Ambegia, E ;.McClintock, K.; MacLachlan, I., Confirming the RNAi-mediated mechanism of action of siRNA-based cancer therapeutics in mice. *The Journal of clinical investigation* **2009,** *119* (3), 661-673.

(244) Lei, M.; Ma, G.; Sha, S.; Wang, X.; Feng, H.; Zhu, Y.; Du, X ,. Dual-functionalized liposome by co-delivery of paclitaxel with sorafenib for synergistic antitumor efficacy and reversion of multidrug resistance. *Drug Deliv* **2019,** *26* (1), 262-272.

(245) Navarro, G.; Sawant, R. R.; Biswas, S.; Essex, S.; Tros de Ilarduya, C.; Torchilin, V. P., P-glycoprotein silencing with siRNA delivered by DOPE-modified PEI overcomes doxorubicin resistance in breast cancer cells. *Nanomedicine (London, England)* **2012,** *7* (1), 65-78.

(246) Zhang, C.-g.; Zhu, W.-j.; Liu, Y.; Yuan, Z.-q.; Yang, S.-d.; Chen, W.-l.; Li, J.-z.; Zhou, X.-f.; Liu, C.; Zhang, X.-n., Novel polymer micelle mediated co-delivery of doxorubicin and P-glycoprotein siRNA for reversal of multidrug resistance and synergistic tumor therapy. *Scientific Reports* **2016,** *6*, 2385.9

(247) MacDiarmid, J. A.; Amaro-Mugridge, N. B.; Madrid-Weiss, J.; Sedliarou, I.; Wetzel, S.; Kochar, K.; Brahmbhatt, V. N.; Phillips, L.; Pattison, S. T.; Petti, C.; Stillman, B.; Graham, R. M.; Brahmbhatt, H., Sequential treatment of drug-resistant tumors with targeted minicells containing siRNA or a cytotoxic drug. *Nature biotechnology* **2009,** *27* (7), 643-651.

(248) Virrey, J. J.; Guan, S.; Li, W.; Schönthal, A. H.; Chen, T. C.; Hofman, F. M., Increased survivin expression confers chemoresistance to tumor-associated endothelial cells. *The American journal of pathology* **2008,** *173* (2), 575-585.

(249) Kukcinaviciute, E.; Jonusiene, V.; Sasnauskiene, A.; Dabkeviciene, D.; Eidenaite, E.; Laurinavicius, A., Significance of Notch and Wnt signaling for chemoresistance of colorectal cancer cells HCT116. *Journal of cellular biochemistry* **2018,** *119* (7), 5913-5920

Acknowledgements

ACKNOWLEDGEMENTS

- We are thankful to The Egyptian Ministry of High Education (MOHE)-Cultural Affairs and Missions Sector and Japan International Cooperation Agency (JICA) for funding this PhD scholarship through Egypt-Japan Education Partnership (EJEP) program.
- We wish also to thank The Japanese Ministry of Education, Culture, Sports, Science and Technology (MEXT) for funding The Laboratory of Innovative Nanomedicine (Mirai-Sozai) project which hosted and provided the research expenses for this study.
- We are grateful to Prof. Manabu Tokeshi, Faculty of Engineering, Hokkaido University for providing the microfluidic device used in this study.

Dedication

DEDICATION

(We bestow of our Mercy on whom we want, and We do not waste the reward of good doers)

The Holy Quran- 12:56

To my struggling wife; Mariam, who supported me during the downs of this work and shared with me the happiness of the ups,

To my little kids; Haleema and Sulaiman,

To my mother and grandmother who waited a lot for this moment,

Thank you for everything…

Mahmoud A. Younis

Sapporo, Hokkaido, Japan

Summer 2020